Moloney, Andrew Hugo Dominic (2025)
The characterization of the enzyme kinetics of lactate
dehydrogenase and its inhibition using three novel silver
organometallic compounds. Masters thesis, York St John University.

Downloaded from: https://ray.yorksj.ac.uk/id/eprint/13203/

Research at York St John (RaY) is an institutional repository. It supports the principles of open access by making the research outputs of the University available in digital form. Copyright of the items stored in RaY reside with the authors and/or other copyright owners. Users may access full text items free of charge, and may download a copy for private study or non-commercial research. For further reuse terms, see licence terms governing individual outputs. Institutional Repository Policy Statement

# RaY

Research at the University of York St John

For more information please contact RaY at ray@yorksj.ac.uk

# The characterisation of the enzyme kinetics of lactate dehydrogenase and its inhibition using three novel silver organometallic compounds

Andrew Hugo Dominic Moloney

Submitted in accordance with the requirements for the degree of Master of Science by Research

York St John University

School of Science, Technology and Health

July 2025

The candidate confirms that the work submitted is their own and that appropriate credit has been given where reference has been made to the work of others.

This copy has been supplied on the understanding that it is copyright material. Any reuse must comply with the Copyright, Designs and Patents Act 1988 and any licence under which this copy is released.

© 2025 York St John University and Andrew Hugo Dominic Moloney

The right of Andrew Hugo Dominic Moloney to be identified as Author of this work has been asserted by them in accordance with the Copyright, Designs and Patents Act 1988.

# Acknowledgements

I would like to express my deepest gratitude to those who have supported me throughout the course of this thesis.

First and foremost, my sincere thanks go to my supervisors, Adam Odell and Scott Dawson, for their unwavering guidance, constructive feedback, and encouragement throughout my research. Their expertise and patience were invaluable, and I feel incredibly fortunate to have learned under their mentorship.

To my family, thank you from the bottom of my heart. Your love patience, and belief in me have been a constant source of strength. Your support has carried me though the toughest moments and reminded me why I began this journey in the first place.

I would also like to extend my sincere appreciation to the entire biomed team, the technicians and all the PGRs. Your support and friendship was an essential part of keeping my going through this journey.

This thesis would not have been possible without the support of each of you. Thank you for everything.

# **Abstract**

Previous research by the university of Huddersfield identified a panel of silver N-heterocyclic carbine complexes (Ag-NHCs) functioning as potential inhibitors of glycolytic lactate production. Early work explored the inhibitory potential of Ag-NHCs in various cancer cell lines. Here, this is extended by analysing the impact of Ag-NHCs on pancreatic and colorectal cancer cell viability and lactate production to ascertain their potential use in chemotherapy regimens.

A standard LDH activity assay was adapted to investigate extracellular lactate utilising the high sensitivity of NADH absorbance at 340nm. The study measured the absorbance change associated with the reduction of NAD+ to NADH during lactate conversion to pyruvate. Culture media was sampled from cancer cells grown with or without various glycolytic inhibitors (including three novel Ag-NHC compounds Ag8, HA197, and HA266). Extracellular lactate released into media was assayed in vitro following the addition of reactants (LDH and NAD+), where the rate of reaction is considered proportional to the concentration of extracellular lactate. This study showed all three novel Ag-NHCs reduced extracellular lactate levels to a greater extent than two established glycolysis inhibitors (silibinin and sodium oxamate). Furthermore, in all cases cell lines were most sensitive to Ag8.

The chemotherapeutic properties of the compounds were further investigated through assessment of cell viability using the resazurin metabolic activity assay. Following exposure to the novel Ag-NHCs, IC $_{50}$  values were determined for various cancer cell lines and compared with normal human fibroblasts as a control for cancer cell specificity. Additionally, cells were co-treated with cisplatin and Ag-NHCs, where the efficacy of cisplatin was enhanced by the presence of Ag-NHC compounds. This study demonstrated that all cell lines were most sensitive to Ag8, which displayed the lowest IC $_{50}$  values. Overall, this study established three Ag-NHCs as novel inhibitors of lactate production, apoptosis inducers, and potential chemo-sensitising agents.

# Contents

Acknowledgements	3
Abstract	4
Contents	5
Abbreviations	7
List of figures	8
List of tables	8
1.Introduction	9
1.1 Current state of cancer in clinical settings	9
1.2 Cancer development	10
1.3 Hallmarks of cancer	10
1.4. Pancreatic cancer development	13
1.5. Current treatment strategies for pancreatic cancer	13
1.6. Colorectal cancer development	13
1.7. Current treatment strategies for colorectal cancer	14
1.8 Targeting glycolytic pathways in cancer – role of lactate	16
1.9. Organometallic compounds: silver N-heterocyclic complexes	17
1.10. Silver N-heterocycles	19
Project aims and objectives	24
2.Methods	25
2.1. Cell lines and media	25
2.2. Cell culture methods	26
2.3. Cell counting	26
2.4. Cytotoxicity assay	26
2.5. Chemosensitivity assay	27
2.6. Lactate release assay	27
2.6.1. Assay buffer for assessing LDH activity	28
2.6.2. LDH activity/Lactate release assay	28
2.6.3. LDH activity validation assay	28
2.6.4. Assaying LDH activity in cancer cells	28
2.7. Statistical analysis	30
3. Inhibition of lactate release by novel silver organometallic compounds	31
3.1. Introduction	31
3.2. LDH activity assay validation	31
3.3. LDH activity/Lactate Inhibition studies	34

3.3.1. Monolayer culture	34
3.3.2. Lactate Release from Cells Cultured at High Density in Round-Bottom 96-well Plates	36
3.4. Conclusion	46
4. Novel silver organometallic compounds reduce cancer cell viability.	47
4.1. Introduction to Cell Viability Assays	47
4.2. Cytotoxicity Studies	47
4.3. Chemosensitivity Studies5	51
4.4. Conclusion	53
5.Discussion	54
5.1 Inhibition of lactate release by novel organometallic compounds	54
5.1.1 Optimisation of LDH activity/lactate assay5	54
5.1.2 Lactate release study5	55
5.1.3 Conclusion5	57
5.2 Novel silver organometallic compounds reduce cancer cell viability	58
5.2.1 Cytotoxicity study5	58
5.2.2 Chemosensitivity study6	50
6. General conclusion6	53
7.Bibliography6	65
8.Appendix	77

# Abbreviations

ABBREVIATION	DEFINITION	
ADM	Acinar-to-ductal metaplasia	
AG-NHC	Silver N-heterocyclic carbine	
ATP	Adenosine triphosphate	
CRC	Colorectal cancer	
DMEM	Dulbecco's modified eagle medium	
DMSO	Dimethyl sulfoxide	
FAP	Familial adenomatous polyposis	
FBS	Foetal bovine serum	
GAPDH	Glyceraldehyde-3-phosphate dehydrogenase	
GLUT1	Glucose transporter type 1	
LDH	Lactate dehydrogenase	
MCTS	Monocarboxylate transporters	
MMPS	Matrix metalloproteinase	
NAD+	Nicotinamide adenine dinucleotide	
NADH	Nicotinamide adenine dinucleotide hydride	
NHC	N-heterocyclic carbenes	
P/S	Pen-Strep	
PANIN	Pancreatic intraepithelial neoplasia's	
PARP	Poly ADP ribose polymerase	
PBS	Phosphate buffered saline	
PDAC	Pancreatic ductal adenocarcinoma	
PHFF	Primary human foreskin fibroblast	
ROS	Reactive oxygen species	
RPMI	Roswell Park memorial institute 1640 medium	
TME	Tumour microenvironment	
VEGF	Vascular endothelial growth factor	
WHO	World health organisation	

# List of figures

Figure 1.1. The hallmarks of cancer including the emerging hallmarks and characteristics	12
Figure 1.2. The development of colorectal and pancreatic cancer	15
Figure 1.3. The pathway of cisplatin induced nephrotoxicity	18
Figure 1.4. Mechanisms of Ag <sup>+</sup> induced cell damage	20
Figure 1.5. Structural features of N-heterocyclic complexes	21
Figure 2.1. Standard method for haemocytometer	27
Figure 2.2. Target reaction for LDH activity assay	27
Figure 3.1. Results from assay optimisation and validation	33
Figure 3.2. LDH activity assay results from monolayer cultures	35
Figure 3.3. LDH activity assay results with Ag8 exposure	38
Figure 3.4. LDH activity assay results with HA197 exposure	40
Figure 3.5. LDH activity assay results with HA266 exposure	42
Figure 3.6. LDH activity assay results with silibinin exposure	44
Figure 3.7. LDH activity assay results with sodium oxamate exposure	45
Figure 4.1. Cytotoxicity data	49
Figure 4.2. Co-treatments assay	52
List of tables	
Table 1.1. Structures of novel silver organometallic complexes	23
Table 2.1. Immortalised primary cells used in the study	25
Table 2.2. Cancer cell lines used in this study	25
Table 2.3. Structures of non-novel compounds used in this study	30
Table 4.1. IC50 Data	50

# 1.Introduction

# 1.1 Current state of cancer in clinical settings

Cancer is defined by the world health organisation (WHO) as abnormal cells which divide uncontrollably, going beyond their usual boundaries to spread (World Health Organisation [WHO], 2022). This is a result of the accumulation of DNA alterations (genetic and epigenetic) and defective cellular function (Basu, 2018). The development and formation of cancer cells into a solid mass, called a tumour, is brought on by cancers unique characteristics within the body which allow it to rapidly undergo mitosis multiplying at an abnormal rate and resisting death. Tumours are categorised into being benign and malignant, (cancerous and non-cancerous), with the rate at which they can grow and invade surrounding tissues alongside metastasising to distant sites, the key characteristics of a malignant tumour (Patel, 2020). The invasion of other tissues separate from the primary tumour is called metastasis, this causes a much greater clinical challenge with metastatic cancer responsible for about 90% of cancer related deaths (Guan, 2015; Kiri and Ryba, 2024).

Despite significant advancements in cancer research with constant development in screening, identification, and treatment, cancer is still one of the leading causes of death worldwide, accounting for nearly 10 million deaths in 2020, or nearly one in six deaths (Bray et al., 2024). Breast cancer is the most common cancer in the UK, accounting for around 15% of all cancer cases in females and males combined (2017-2019). The next most common cancers in UK people are prostate (14%), lung (13%), and colorectal (11%). These four cancers alone account for more than half (53%) of all new cases in the UK (2017-2019) (Cancer incidence for common cancers | Cancer Research UK, no date). However, lung cancer is the most common cause of cancer death in the UK, accounting for around a fifth (21%) of all UK cancer deaths (2017-2019). The second most common causes of cancer death in UK people are colorectal (10%) (Cancer mortality for common cancers | Cancer Research UK, no date). Pancreatic cancer is the 10<sup>th</sup> most common cancer in the UK and the 5<sup>th</sup> most common cause of cancer related deaths, exhibiting the lowest 5-year cancer survival rate of only 8.3%.

Pancreatic cancer is known for its aggressive nature and often presents with few early symptoms, which makes early detection difficult. As a result, many people are diagnosed at later stages when the cancer has already spread (Schwingel *et al.*, 2023). Pancreatic cancer is classified into two distinct categories based on the location of origin; exocrine tumours, which accounts for most cases, and endocrine tumours, also known as pancreatic neuroendocrine tumours. The most common type, pancreatic ductal adenocarcinoma (PDAC), is an exocrine cancer that originates in the cells lining the ducts of the pancreas. PDAC is particularly aggressive and tends to grow rapidly, often spreading to other parts of the body before symptoms appear (Wood *et al.*, 2022; Halbrook *et al.*, 2023).

Colorectal cancer is the 4<sup>th</sup> most common cancer in the UK and is the second highest for mortality. Colorectal cancer defines any cancer which begins in the colon or rectum, parts of the large intestine (Matsuda, Fujimoto and Igarashi, 2025). It often develops from benign growths called polyps, which can slowly transform into cancer over time. A defining characteristic of colorectal cancer is its gradual onset. Early stages often do not present noticeable symptoms, which makes early detection crucial. As the cancer progresses, common symptoms include changes in bowel habits, blood in the stool, unexplained weight loss, fatigue, abdominal discomfort, and sometimes a feeling of incomplete bowel evacuation (De Mello *et al.*, 2020). These symptoms can easily be attributed to other, less serious conditions, which can delay diagnosis. Colorectal cancer typically develops in two main forms: sporadic and hereditary. Sporadic CRC occurs without a family history, while hereditary forms, such as Lynch syndrome and familial adenomatous polyposis (FAP), are linked to inherited genetic mutations.

The presence of these genetic conditions increases the risk of developing colorectal cancer at an earlier age (Dekker *et al.*, 2019).

Both cancers share the unfortunate trait of often going undiagnosed in their early stages which contributes to higher mortality rates. Thus, an improvement is needed in the development and design of approaches to enhance early detection of the disease, reduce exposure to known risk factors, and develop better treatments, including surgery, radiotherapy and chemotherapy options.

#### 1.2 Cancer development

While developing into a malignancy, cancer cells develop several characteristics that allow this to take place. These defining traits of a cancer cell are called its 'hallmarks'. The hallmarks of cancer were first characterised by (Hanahan and Weinberg, 2000) who aimed to better define what made an abnormal cell a cancer cell. They initially identified six key biological characteristics that all cancer cells share that are developed during carcinogenesis, the process in which normal cells become cancerous. These hallmarks were sustaining proliferative signalling, evading growth suppressors, resisting cell death, inducing angiogenesis, enabling replicative immortality, and activating invasion and metastasis (shown in Figure 1.1A).

In 2011 the same authors published a new paper, hallmarks of cancer: The next generation (Hanahan and Weinberg, 2011a), which described additional characteristics that had gained recognition in the previous decade. The paper described two emerging hallmarks: deregulating cellular energetics and avoiding immune destruction. The first of these supports neoplastic proliferation and the second allows cancer to evade cell death brought on by the body's natural immune response. Along with these two emerging hallmarks, Hanahan and Weinberg described two enabling characteristics which are only seen, due to increased complexity, at the tumour level as opposed to the cellular level. These characteristics are genomic instability and tumour promoting inflammation (Figure 1.1B). Tumours exhibit another dimension of complexity due to their ability to recruit, apparent normal cells that contribute to the acquisition of hallmark traits by creating the "tumour microenvironment" (Niu and Zhou, 2023).

#### 1.3 Hallmarks of cancer

One of the "emerging" hallmarks of cancer as described in the 2011 paper is the reprogramming of cellular metabolism falling under the category of deregulation of cellular energetics (Hanahan and Weinberg, 2011b). Due to the rapid proliferation of cancer cells and the increased energy requirements of related processes such as the upregulation of the growth of new blood vessels (i.e angiogenesis), cancer cells are required to adapt their metabolic pathways to compensate for the rapid increase of energy uptake. A key aspect of this is the Warburg effect in which malignant cells within a tumour prioritise anaerobic glycolysis despite an adequate supply of oxygen resulting in the inefficient use of glucose and high pyruvate-lactate production (Liberti and Locasale, 2016a; Spencer and Stanton, 2019; Vaupel, Schmidberger and Mayer, 2019a). As cancers upregulate glucose transporters, notably GLUT1, they can produce ATP at a significantly faster rate at the cost of glucose efficiency (Zhang, Qin and Wang, 2010a). A product of this hallmark is that pyruvate is converted into lactate instead of being fed into the citric acid cycle leading to a surplus of cellular lactate. The upregulation of monocarboxylate transporters (MCTs), such as MCT2 and MCT4 as seen in prostate cancer, allows for the transportation of the excess lactate into the tumour microenvironment (TME), contributing to the acidic environment (Xia et al., 2021).

The adaptation of the TME during the formation of solid tumours is another key phase of cancer development. The increase in extracellular lactate caused by the changing in metabolic activity leads to a drop in the pH of the TME (i.e., acidosis). Lactic acidosis has several pro-cancer effects with

studies showing that the acidic TME contains the angiogenic driver, VEGF, key invasion mediators (matrix metalloproteinases and cathepsins), along with cytokines such as transforming growth factor- $\beta$  (TGF- $\beta$ ), all of which help spread the cancer either directly or indirectly (Wei and Guan, 2012; Rastogi *et al.*, 2023).

Another key effect of lactic acidosis is contributing to the ability of a cancer cell to evade normal immune responses. Acidosis influences the ability of immune cells via several pathways including inducing leukocyte apoptosis. One mechanism is via reduced expression of the autophagy factor FIP200 in naïve T cells observed in both patients with ovarian cancer and mouse models. This resulted in suppression of cytotoxic responses mediated by CD8 $^+$ T cells and the production of IFN- $\gamma$  by Th $_1$  cells (Wei and Guan, 2012). These alterations, along with many others, can limit the ability of the immune system to effectively monitor, suppress and eliminate abnormal cells during cancer development.

12

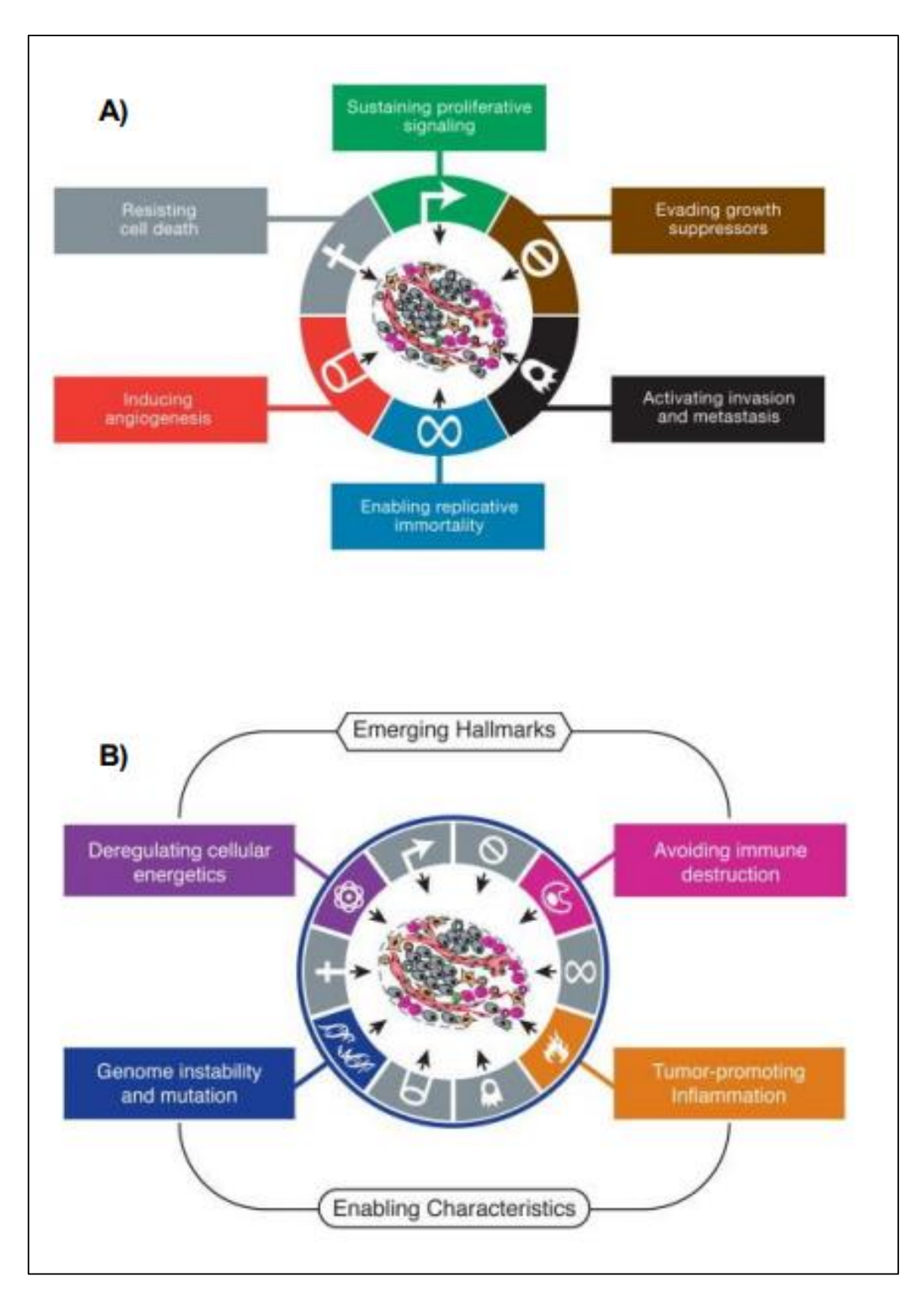


**Figure 1.1:** A) The Six originally identified hallmarks of cancer as described by Hanahan and Weinberg in 2000 and the B) Four new emerging Hallmarks/Characteristics described in the revised 2011 paper by the same authors

# 1.4. Pancreatic cancer development

PDAC most commonly develops from non-invasive precursor lesions, most typically pancreatic intraepithelial neoplasia's (PanINs), which arise through acquisition of genetic and epigenetic alterations. Pancreatic cancers can also evolve from intraductal papillary mucinous neoplasms or mucinous cystic neoplasms (Stoop *et al.*, 2025). Genetic sequencing has been used on a range of primary samples for the purpose of fully characterising the typical gene mutations seen in pancreatic cancer.

The most frequent genetic abnormalities in invasive PDAC are mutational activation of the *KRAS* oncogene, inactivation of tumour-suppressor genes including *CDKN2A*, *TP53*, *SMAD4*, and *BRCA2*, widespread chromosomal losses, gene amplifications, and telomere shortening. *KRAS* mutations and telomere shortening are seen in the earliest development of the carcinoma, even in low-grade pancreatic intraepithelial neoplasia's, with telomere shortening being responsible for further chromosomal instability. Abnormal *KRAS* signalling results in dysregulation of the mitogenic MAPK pathway, driving uncontrolled proliferation. The inactivation of TP53, SMAD4, and BRCA2 proteins typically occurs in late-stage, advanced pancreatic intraepithelial neoplasia and invasive carcinomas, exacerbating the proliferative and anti-apoptotic phenotype (Vincent *et al.*, 2011).

# 1.5. Current treatment strategies for pancreatic cancer

Surgery is the only potential curative treatment for pancreatic cancer; however, prognosis remains poor. This is primarily due to late diagnosis, with 50-60% of patients presenting with distant metastatic disease, 25-30% with regional disease, and only 10-15% of patients presenting with local disease at diagnosis (Siegel, Miller and Jemal, 2019). In metastatic cases, treatment is not considered curative and is therefore targeted at improving symptoms and quality of life. Surgical treatment of local disease is determined by the resectability of the tumour, which can be improved though radiotherapy, and the intra-pancreatic location.

Tumours in the head of the pancreases require a pancreaticoduodenectomy, often called the Whipple procedure, for complete resection (Sohn *et al.*, 2000) while less common tumours located in the distal end require a distal pancreatectomy (Vojtko *et al.*, 2024). Total pancreatectomy also occurs; however, they are rare due to the high risk of long-term complications, including significant metabolic derangements, and exocrine insufficiency, coupled with the relatively low 5-year survival rate (one study reported 34% survival after 3 years) and considerable high recurrence rates (Shtauffer *et al.*, 2009; Petrucciani *et al.*, 2020).

For any chance of patient remission, a combination of complete resection and chemotherapy is required (Strobel *et al.*, 2022). While there is no gold standard treatment regime recommended for pancreatic chemotherapy, the most common treatments include Gem-Cap, a combination of gemcitabine and capecitabine, and FOLFIRNOX, a combination of fluorouracil, leucovorin, oxaliplatin, and irinotecan (Mar Kolbeinsson *et al.*, 2023). In local and advanced metastatic pancreatic cancers these combination chemotherapies have been shown to improve the overall survival time in palliative settings by less than 6 months (Conroy *et al.*, 2011).

#### 1.6. Colorectal cancer development

Colorectal cancer has a long latent development period of around 10 years with the developments of dysplastic adenomas being the most common form of premalignant precursor lesions. One of the earliest gene mutations occurs in the *APC* gene, present in over 80% of colorectal adenomas (Zhang and Shay, 2017). Following this early stage of development, further mutations of the *KRAS* oncogene and the inactivation, via mutation, of the *TP53* tumour suppressor gene. These developments

contribute to increased chromosomal instability leading to diverse structural changes within chromosomes.

While this is the typical route of colorectal cancer development, more than 15% of sporadic colorectal cancers develop through fundamentally different pathways of molecular events. These cancers include those originating from serrated precursor lesions, which are typical premalignant precursor lesions in the proximal colon, and are often characterised by the CpG island methylator phenotype and activating *BRAF* oncogene mutations. Most cancers arising from sessile serrated adenomas display the high-level microsatellite instability (MSI-H) phenotype because of MLH1 gene promoter methylation (Brenner, Kloor and Pox, 2014).

# 1.7. Current treatment strategies for colorectal cancer

Due to increased screening procedures for colorectal cancer, more incidents are being identified at early stages where surgery only is required. In the T1 stage of colorectal cancer, endoscopic resections can be carried out with endoscopic submucosal dissection and full thickness resection only being required when there is suspicion of submucosal invasion.

For more developed tumours surgical resection is the gold standard for curative treatment. Colectomies are the most common surgery when dealing with late-stage local carcinomas in which whole sections of the colon are removed (Biller and Schrag, 2021; Morris *et al.*, 2022). Recent studies also indicate the benefits of complete mesocolon excision in which the whole mesocolon is removed along with its blood vessels and surrounding lymph nodes so as improve patient outcome and reduce the risk of recurrence (De Lange *et al.*, 2023).

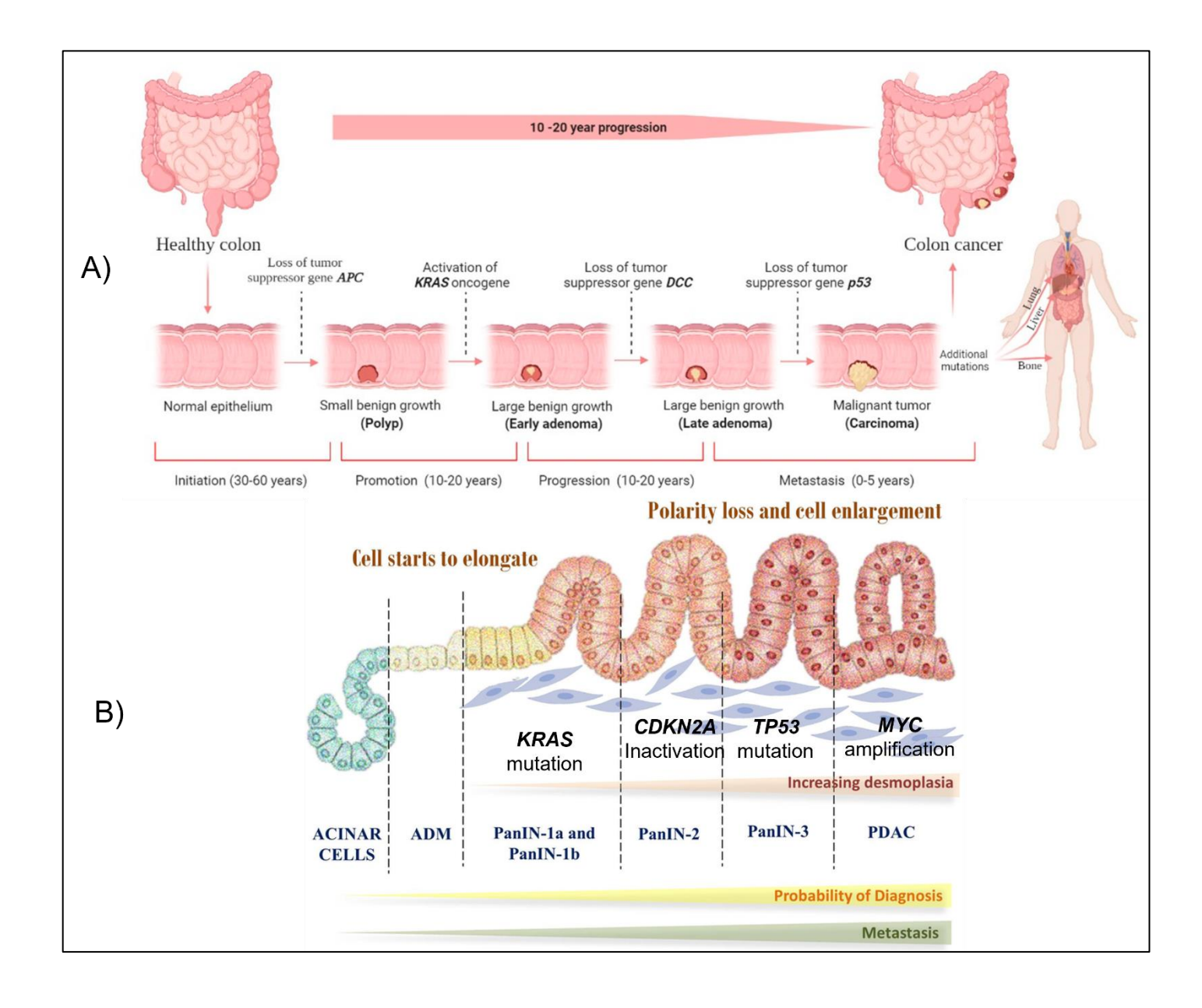


**Figure 1.2.** The development of colorectal (A) and pancreatic (B) cancers. A) Colorectal cancer (CRC) stages and development. There are four stages in the development of CRC carcinogenesis: initiation, promotion, progression, and metastasis. The liver is the most common metastatic site, followed by the lung and bone. Although it is difficult to determine the duration required for each stage, decades will likely be required to form CRC. B) The development of acinar pancreatic cells into acinar-to-ductal metaplasia (ADM) followed by the development through the pancreatic intraepithelial neoplasia (PanIN) and PDAC stages towards metastasis (Hossain *et al.*, 2022; Liu *et al.*, 2023)

# 1.8 Targeting glycolytic pathways in cancer – role of lactate

Lactate  $(C_3H_6O_3)$  is the product of glycolysis in anaerobic conditions, it allows for NAD<sup>+</sup> regeneration when complete pyruvate phosphorylation is not possible due to hypoxia. It is produced when pyruvate  $(C_3H_4O_3)$  is oxidated by NADH in the presence of lactate dehydrogenase (LDH), producing lactate and NAD+ (Valvona *et al.*, 2016). In healthy normoxic conditions lactate is converted back into pyruvate which can then be used in gluconeogenesis or the citric acid cycle. The anaerobic pathway that produces lactate requires hypoxia which is a result of an imbalance of oxygen intake/sup ply and usage. The development of malignancy in tissues has been recorded as a cause of hypoxia with a 2.7-fold decrease in partial pressure of oxygen  $(pO_2)$  in renal carcinoma tissue compared to controls (McKeown, 2014). This is a consequence of oxygen supply imbalance caused by rapid replication of the malignant cells outgrowing the established vascularisation of the neoplasm (Infantino *et al.*, 2021), as well as an increased oxygen demand for cell proliferation.

Cancer cells upregulate the HIF-1 gene in hypoxic conditions to encourage processes such as angiogenesis to return the tissue environment to normoxic conditions (Altenberg and Greulich, 2004). However, despite re-establishing normoxia, cancer cells continue to produce increased lactate, inferring that lactate production and accumulation in malignancy is not solely due to hypoxia (Yaromina *et al.*, 2009; Hirschhaeuser, Sattler and Mueller-Klieser, 2011). As mentioned previously, the preferential production of lactate despite normoxic conditions is known as the Warburg effect.

The Warburg effect was initially attributed to damage in the mitochondrial pathway preventing oxidative phosphorylation, however studies have recently suggested it to be an intentional adaptation that benefits cancer growth (Alfarouk *et al.*, 2014). One benefit of the Warburg effect is that despite being less glucose efficient, a higher ATP yield over time is achieved. Aerobic glycolysis only produces 2 moles of ATP per mole of glucose compared to up to 36 moles of ATP if complete oxidation takes place. However, aerobic glycolysis is approximately 100 times faster, due to the immediate NAD<sup>+</sup> regeneration for further glycolysis, thus, although it is less glucose efficient, it has a greater overall yield within a set period (Vazquez *et al.*, 2010; Liberti and Locasale, 2016b). This lack of efficiency is partly supported due to the upregulation of HIF-1, which also increases the transport of glucose to the malignant cells. Another potential benefit for cancer to favour production lactate is that it can be used to produce a more hospitable environment for growth. The export of lactate ions and protons, caused by the dissociation of lactic acid, to the extracellular space causes acidosis of the tumour microenvironment. This has been reported to positively affect tumour growth by providing a more favourable pH for growth and a less favourable one for the hosts immune response (Liberti and Locasale, 2016c; Vaupel, Schmidberger and Mayer, 2019b; Vaupel and Multhoff, 2021).

A key benefit of an acidic tumour microenvironment for the tumour is that it can promote metastasis. The low pH caused by lactate deprotonation promotes matrix metalloproteinase activation (MMPs). These enzymes degrade the extracellular matrix, damaging surrounding tissues and facilitating the growth and invasion of the tumour into the surrounding tissues (Dekker *et al.*, 2019). Acidosis of the tumour microenvironment also upregulates integrins which are key cell adhesion molecules against the extracellular matrix (Hamidi and Ivaska, 2018; Shie *et al.*, 2023)

In addition to acidosis, lactate has been linked to the promotion of angiogenesis which is critical for tumour growth. Lactate can bind to and activate the G-protein coupled receptor GPR81 (also known as HCA1) on cancer cells. GPR81 is highly expressed in different cancer cell lines including colon, breast, lung, hepatocellular, cervical, and pancreatic (Vrzáčková, Ruml and Zelenka, 2021). Vascular endothelial growth factor (VEGF) is also upregulated. These processes induce downstream signalling pathways that promote angiogenesis to improve blood flow, and thus nutrients and oxygen

supply, to the tumour (Porporato *et al.*, 2020). Targeting lactate production is a promising anti-tumour treatment approach, potentially modifying cancer metabolism, the TME, vascularisation, and immune responsiveness.

# 1.9. Organometallic compounds: silver N-heterocyclic complexes

The design and development of organometallic compounds is one such area of chemotherapeutic approach that has been prominent over the last few decades (Fish and Jaouen, 2003). One representative compound that has found significant clinical use is cisplatin which is used to treat several cancers including testicular and bladder (Schatzschneider and Metzler-Nolte, 2006). Due to this success there has been significant increase in the number of metal-based diagnostic agents identified (Atiyeh *et al.*, 2007; Lansdown, 2010; Brandt *et al.*, 2012; Steve D *et al.*, 2017). Furthermore, the wide variation of possible metal ions and general structures that can be used in these complexes, offers a range of drug action mechanisms compared to organic substances which are limited in their use, often constrained by specific kinetic, geometric, and atomic properties (Liang *et al.*, 2018).

One of the more common structural backbones used in organometallic compound design are electron-rich N-heterocyclic carbenes (NHC), which are capable of binding nearly every transition metal. To identify an efficient NHC complex, thousands of potential novel candidates must be designed, synthesised, investigated, and characterised. It was in 1965 that the first effective NHC complex, cisplatin, was identified by Rosenberg, Van Camp and Krigas (1965). This discovery started the ongoing development of organometallics in chemotherapeutic roles (Silver, 2003; Hindi et al., 2008, 2009; Wright et al., 2012; Gurunathan et al., 2014). Despite the significant role cisplatin has made on the clinical landscape (Siddik, 2003; Wang and Lippard, 2005), the compound itself has several significant drawbacks. Cisplatin only works on a handful of cancer phenotypes and when it does work it has the potential to cause a range of serious adverse effects such as nephrotoxicity (seen in figure 1.3), ototoxicity, and neurotoxicity (Şahin-Bölükbaşı, Cantürk-Kılıçkaya and Kılıçkaya, 2021). Another serious consequence of cisplatin treatment is the development of chemoresistance. The mechanisms that provide this drug resistance includes a decreased uptake and/or increased efflux of cisplatin, upregulation of sulphur-containing molecules such as glutathione which neutralise cisplatin, and prevention of DNA damage caused by the cisplatin via repair and defective apoptotic signal pathways (Kartalou and Essigmann, 2001; Siddik, 2002, 2003; Wernyj and Morin, 2004). Due to these deficits, there is a strong demand to further develop and synthesise new complexes which are more cancerselective and have reduced off-target effects on normal cells.

Along with cisplatin, several other platinum-based organometallic compounds are in medical use such as carboplatin, lobaplatin, nedaplatin, and oxaliplatin. All are similarly effective in their chemotherapeutic effects; however, they also display considerable adverse side effects and are susceptible to acquisition of drug resistance (Patil *et al.*, 2011; Eloy *et al.*, 2012; Browne *et al.*, 2014; Haque *et al.*, 2015).

Due to the toxicity observed with platinum-based compounds, a focus on synthesising compounds which use different metals has been seen. Over the last few decades, several alternative, less toxic, metals have been used in the synthesis of organometallic compounds, including titanium, iron, and cobalt, however gold and silver have been the most successful (Silver, 2003; Nolan, 2011; Nayak and Gaonkar, 2021).

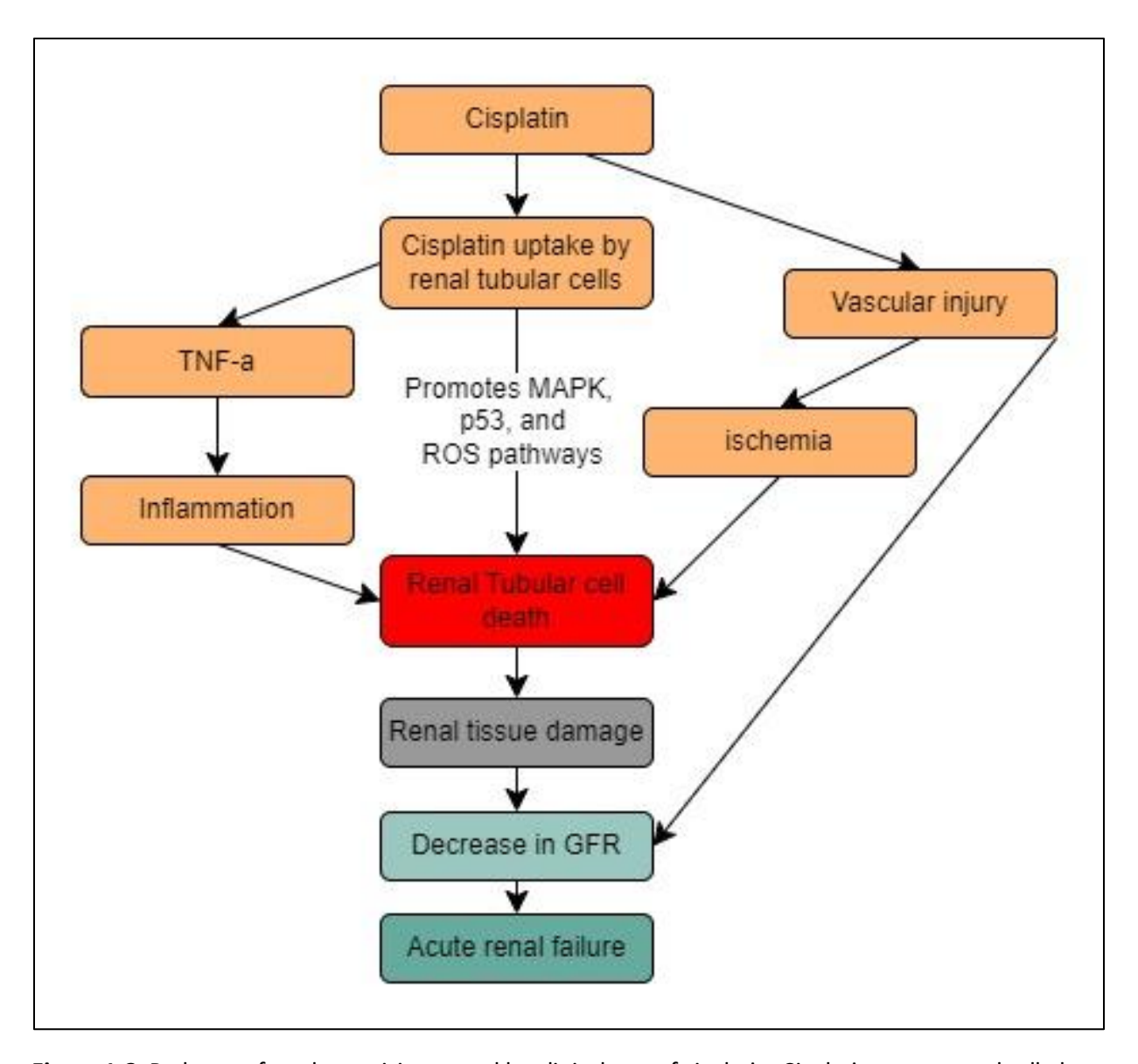


**Figure 1.3.** Pathway of nephrotoxicity caused by clinical use of cisplatin. Cisplatin enters renal cells by passive and/or facilitated mechanisms, Exposure of tubular cells to cisplatin upregulates MAPK, p53, and ROS pathways which promote cell death. Cisplatin also induces TNF- $\alpha$ , triggering an inflammatory effect which further contributes to the adverse effects. Cisplatin has also been reported to cause renal vascular damage that leads to ischemia and further cell death.

# 1.10. Silver N-heterocycles

Silver has no known role in normal biological functions but has been used in medical practice for at least six millennia as an antimicrobial agent/tool due to its high toxicity to microorganisms (Alexander, 2009; Medici *et al.*, 2019). Silver nitrate, for example, was used extensively as an antimicrobial agent prior to the development of penicillin and other more recent antibiotics (Russell and Hugo, 1994). Over the last hundred years silver has found many roles where its medical properties have been exploited, including water treatment, silverware, and in medical equipment (Lansdown, 2010).

While silver is not considered to be toxic to humans there have been some notable effects observed. In rare cases, chronic exposure can lead to bluish pigmentation of the skin (argyria) and eyes (argyrosis). Soluble silver compounds have also been observed to cause liver and kidney damage, respiratory issues, and changes in blood cells. However, metallic silver widely considered to pose minimal risk to human health providing an ideal molecule to utilise within chemotherapeutic design (Drake and Hazelwood, 2005).

The current understanding of silver-based compounds is that they affect cells via Ag(I) molecules penetrating membranes allowing them to disrupt the pathways within, as seen in figure 1.4 (Hartinger and Dyson, 2009). Due to electrostatic attraction and affinity for sulphur, Ag<sup>+</sup> adheres to the cell membrane weakening it and allowing ions pass through more easily (Khorrami *et al.*, 2018; Yin *et al.*, 2020). Following the uptake of free Ag<sup>+</sup> ions, metabolic respiratory chain enzymes are deactivated, inhibiting the release of ATP, increasing reactive oxygen species (ROS) generation, and causing ribosome denaturation (Shcherbik and Pestov, 2019). The generated ROS and intracellular Ag<sup>+</sup>, damage the cell membrane and bind to DNA to prevent replication and cell division.

Nitrogen (N)-heterocyclic carbene complexes (NHCs) are a key feature of modem organometallic chemistry. They were first synthesised and reported by Wanzlick and Schikora (1961) and then again improved by Öfele (1968) who produced the first metal-NHC. More recently, they have been developed as pivotal dative (coordinate covalent or dipolar bonds) electron doner ligands in inorganic chemistry due to their properties as strong  $\sigma$ -donors and  $\pi$ -acceptors. This allows them to form much stronger bonds with metals compared to rival ligands such as phosphates which have weaker stability (Nolan, 2006; Tialiou et~al., 2022). Additionally, the lone electron pair on the carbene carbon are stabilised by a localised nitrogen (Bourissou et~al., 2000). These properties allow NHCs to be used widely for two key reasons: they allow for strong coordination with any metal subunit, and their stability to resist destabilisation from interactions with outside sources (i.e., moisture and air), justifying the preference for NHCs compared to alternatives, such as phosphine ligands (Herrmann, 2002). Additionally, as NHCs have versatile dative bonds, they are capable of binding to both hard and soft metals (Hu et~al., 2004).

The number of synthesised metal-NHC ligands is a continuously growing with transition metals such as copper, silver, gold, platinum, palladium, and ruthenium all having hundreds of conjugated complexes which have been investigated (Johnson, Southerland and Youngs, 2017). Metal-NHCs have also found a place in several significant scientific industries since there first production. They have become important in polymeric materials, molecular switches, luminescent materials, and liquid crystalline materials (Şahin-Bölükbaşı, Cantürk-Kılıçkaya and Kılıçkaya, 2021). While NHCs do have a prominent role in catalytic chemistry, it is their potential medical application via antibacterial and anticancer mechanisms which is their most prominent role today and their focus in research.

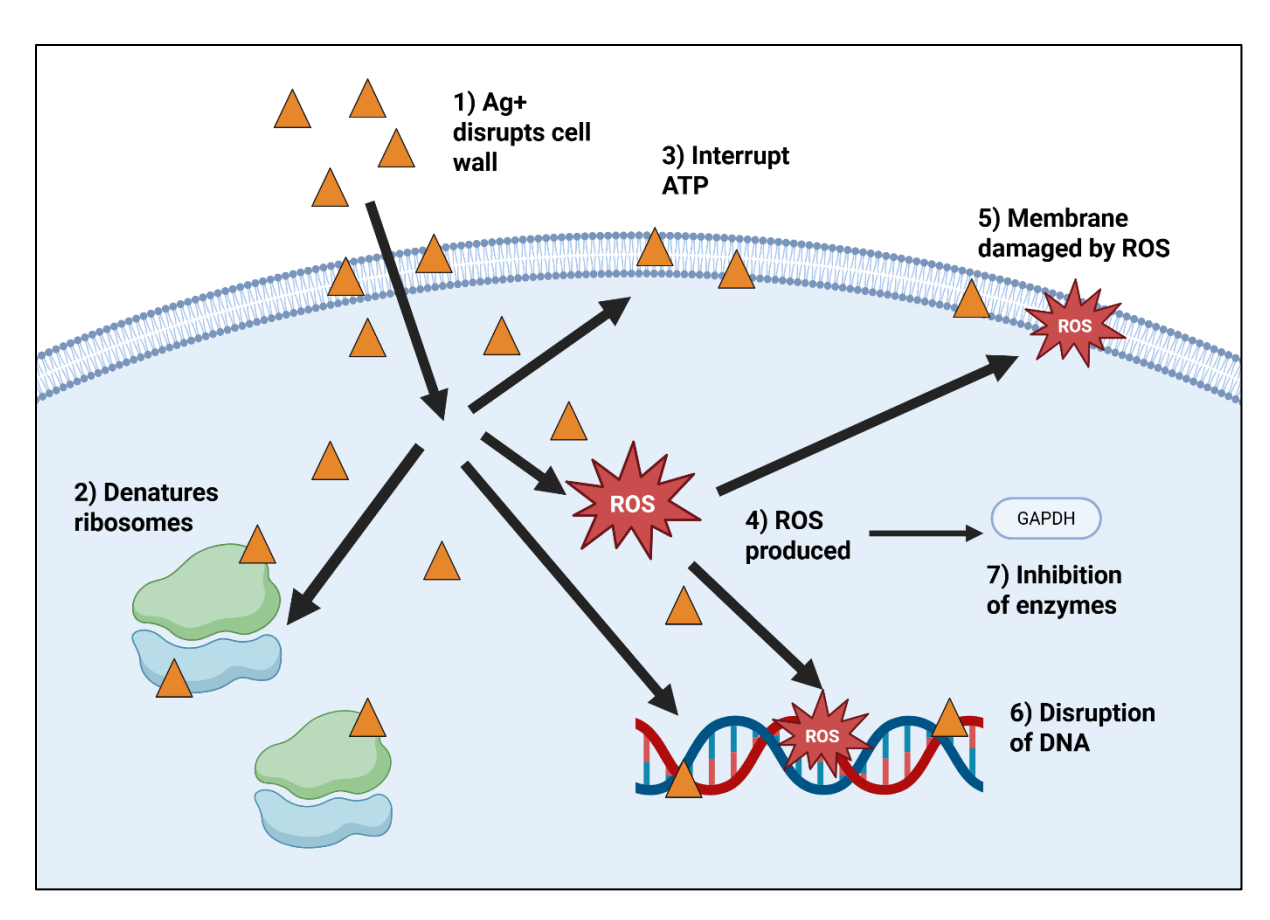


**Figure 1.4**. Ag<sup>+</sup> mechanisms of cell damage. 1) Ag<sup>+</sup> disrupts the cell membrane by adhering or passing through. 2) Ag<sup>+</sup> ions denature ribosomes and inhibit protein formation. 3) Interruption of adenosine triphosphate (ATP) production due to Ag<sup>+</sup> ions deactivating respiratory enzymes on mitochondrial membranes. 4) The damage of the cell and mitochondrial membranes releases reactive oxygen species (ROS) into the cytoplasm. 5) ROS causes membrane disruption. 6) Ag<sup>+</sup> and ROS bind to DNA and prevent its replication and cell division. 7) ROS leads to oxidative stress in key glycolytic enzymes like glyceraldehyde-3-phosphate dehydrogenase (GAPDH) reducing their activity and bottlenecking the glycolytic pathway reducing. Disruptions in key glycolytic enzymes leads to reduced lactate production

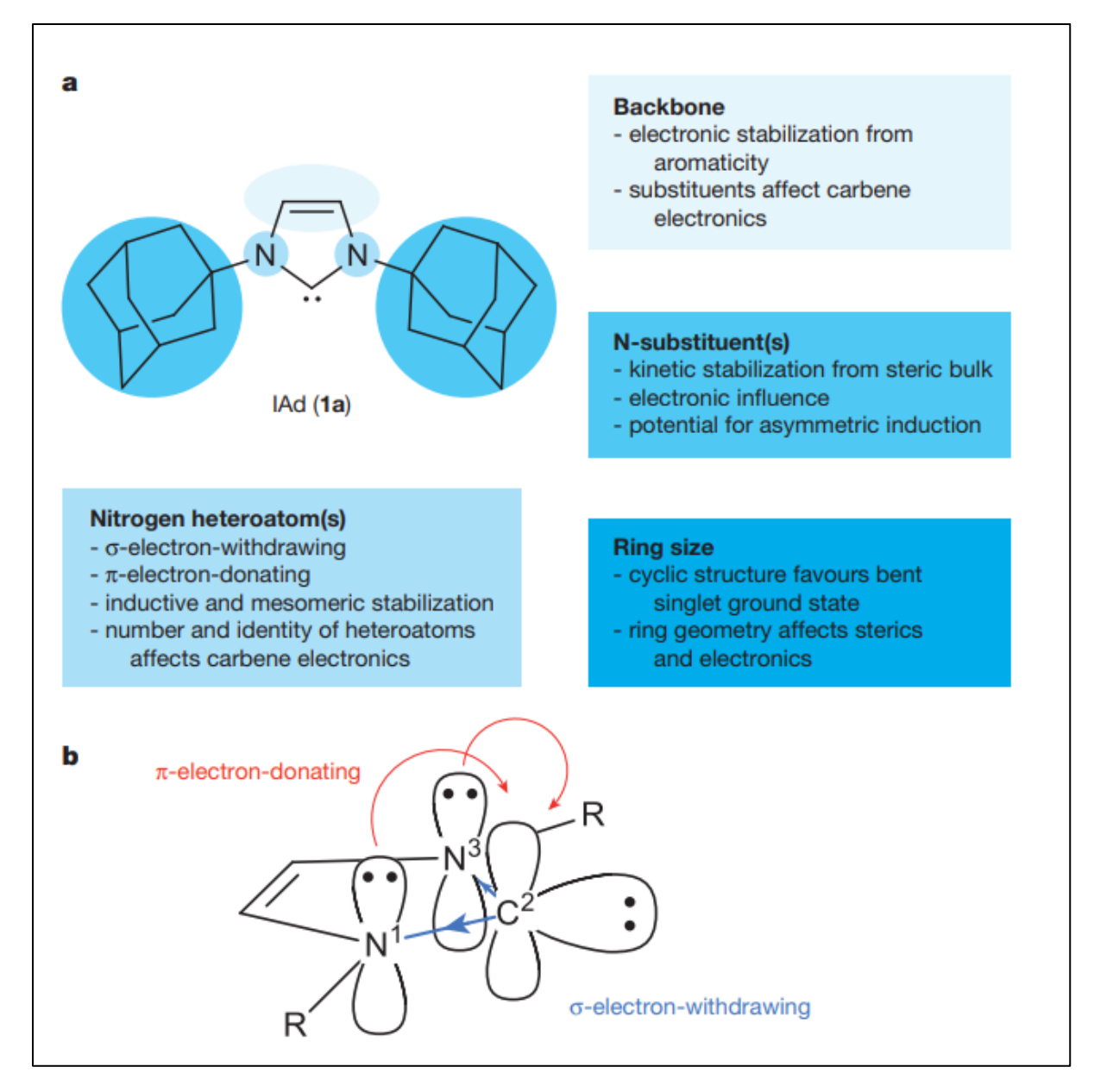


**Figure 1.5.** Structural features of 1,3-di(adamantly)imidazole-2-ylidine, the first synthesised NHC. A) General structural features IAd (1a), detailing the effects of the ring size, nitrogen heteroatoms and the ring backbone and nitrogen-substituents on the stability and reactivity of the NHC. B) Ground-state electronic structure of imidazol-2-ylidenes. The s-withdrawing and p-donating effects of the nitrogen heteroatoms help to stabilise the singlet carbene structure (Hopkinson *et al.*, 2014)

As previously discussed, silver compounds have been used throughout medical history, exploited for their antimicrobial properties in which free  $Ag^+$  ions penetrate cellular membrane allowing inhibition of intercellular processes. Due to this mechanism of action, it is important that any synthesised organometallic silver complex intended to be used pharmaceutically must be able to release  $Ag^+$  ions at a controlled rate. Many current silver compounds such as the antibiotic silver sulfadiazine release  $Ag^+$  ions too rapidly, where their effectiveness is quickly and uncontrollably lost (Brandt  $et\,al.$ , 2012; Vishwanath  $et\,al.$ , 2022). Fortunately, NHCs can be utilised here. The NHC ligand has stronger bonds and is therefore capable of producing a significantly slower, more desirable, controlled release of ions. In studies investigating silver complexes utility against bacteria, such as  $E.\,coli,\,S.\,aureus$ , and  $P.\,aeruginosa$ , the incorporation of a Ag-NHC complex enabled much lower silver content use to effectively inhibit bacterial growth (Hartinger and Dyson, 2009).

Ag-NHCs have gained significant attention as anti-cancer against in the last fewyears due to their practical nature. They are efficient for drug design, fast to optimise, have a high degree of stability, have a relatively easy development process, and their mechanisms effect multiple pathways. Silver has taken a particular interest over other metals due to its high affinity to NHC complex and its natural low toxicity (Liu and Gust, 2013; Oehninger, Rubbiani and Ott, 2013). While some of silvers apoptosis-inducing mechanisms have already been discussed, some of its alternative chemotherapeutic, cytotoxic, mechanisms are yet to be explored. A 2017 study from Steve et al. (2017) identified four key mechanisms through which Ag8, a prominent silver-NHC compound, may influence cancer cells. These were (i) the inhibition of topoisomerases I and II, causing single and double strand breaks in cellular DNA, (ii) inhibition of thioredoxin reductase, leading to an unregulated increase in thioredoxin disrupting regulation of redox reactions, (iii) inhibition of poly (ADP Ribose) polymerase (PARP), reducing the transfer of ADP-ribose to target proteins and altering apoptosis, and (iv) inhibition of glycolysis (Steve D *et al.*, 2017; Shepherd, 2018).

Ag8 is just one of many silver N-heterocyclic compounds being studied currently. A study by Shepherd (2018) investigated the properties of several potential lead Ag-NHC candidates for further study (see Table 1). Representative compounds previously investigated are shown in table 1, comparing structures and outlining the composition of the stock solutions tested. The compounds shown in Table 1 highlight some of the structural diversity evident within this family of Ag-NHCs.

NHCs can be synthesised via a wide range of protocols. The most common and simplest method to synthesis them is to produce NHCs based on 5-membered rings via the removal of a proton from a designated azolium salts such as pyrazolium, triazolium, imidazolium, benzimidazolium, oxazolium, or thiazolium via an appropriate base. The azolium precursor is first generated by alkylation of a corresponding azole. The azolium salts are then deprotonated using strong bases such as alkali metal hydrides or organolithium reagents to form free NHC. The stabilisation of this structure is accomplished via the presence of nitrogen atoms in the ring which act as electron density donors to the carbene. Once stable the NHC can be used to form a metal ligand complex due to the strong  $\sigma$ -donating and  $\pi$ -accepting properties. This synthesis can be tuned to produce a variety of NHCs with different electronic properties by varying the size of the carbene ring, the substituents on the nitrogen atoms, or the additional atoms within the heterocycle. For example, free NHCs can also be obtained by the de-chlorination of 2-chloroazolium salts using electron-rich phosphines. This method provides an alternative to the deprotonation approach and can be used to synthesize NHCs that are difficult to obtain otherwise (Garrison and Youngs, 2005; Nolan, 2006; Haque et~al., 2015; Jahnke and Ekkehardt Hahn, 2017; Böhme et~al., 2022a, 2022b)

**Table 1.1.** Silver N-Heterocyclic compounds and their molecular structures.

Compound name	Molecular weight	Structure
Ag8 (Silver xanthine derivative)	717.89	N Ag <sup>+</sup>
HA266 (Silver hydroxylated ligand)	726.15	Ag* CI*
HA197 (Silver clotrimazole based ligand)	788.76	CI Ag <sup>+</sup>

# Project aims and objectives

This project investigates the extracellular lactate inhibiting properties of three novel Ag-NHC compounds against colorectal and pancreatic cancer cell lines. Lactate production will be determined via the development and implementation of a spectrophotometry-based assay measuring the conversion of lactate to pyruvate in the presence of LDH and NAD<sup>+</sup>. These Ag-NHC compounds will then be evaluated for anti-cancer chemotherapeutic potential through resazurin-based cell viability assays. Overall, this study will expand the understanding of how Ag-NHCs influence cellular metabolism and cell survival.

# 2. Methods

# 2.1. Cell lines and media

All cell lines were obtained from collaborators at the University of Huddersfield and University of Leeds where they were regularly checked for mycoplasma contamination and authenticity. They were maintained in their associated media as monolayer cultures and incubated at  $37^{\circ}$ C in a  $CO_2$  enriched (5%) environment. Media (ThermoFisher Scientific; see Table 2.1 and 2.2) was changed regularly when discolouration could be seen or during a passage. Cancer cell lines were passaged for up to 20 passages or until a morphological change was noticed under the microscope after which they were discarded. Cryopreserved cell line stocks were stored in liquid nitrogen. Immortalised (hTERT) primary cells were maintained in culture until they showed signs of deterioration. Cells were checked daily to monitor their growth and identify any change.

**Table 2.1:** Immortalised primary cells used during this study with their culture media and additional supplementation

Cell line	Description	Media	Supplementation
HFF-1	Primary human	Roswell Park Memorial	10% foetal bovine serum (FBS)
	foreskin fibroblast	Institute 1640 medium	1% Pen-Step (P/S)
	cell	(RPMI)	

**Table 2.2:** Cancer cell lines used during this study with their culture media and additional supplementation.

Cell line	Description	Media	Supplementation
HCT116 p53*/+	P53 wildtype epithelial colonic carcinoma	Dulbecco's Modified Eagle Medium (DMEM)	10% foetal bovine serum (FBS) 1% Pen-Step (P/S)
HCT116 p53 <sup>-/-</sup>	P53 knock down epithelial colonic carcinoma	Dulbecco's Modified Eagle Medium (DMEM)	10% foetal bovine serum (FBS) 1% Pen-Step (P/S)
PSN-1	Epithelial-like pancreatic adenocarcinoma	Roswell Park Memorial Institute 1640 medium (RPMI)	10% foetal bovine serum (FBS) 1% Pen-Step (P/S)
ВхРс-3	Epithelial pancreas adenocarcinoma	Roswell Park Memorial Institute 1640 medium (RPMI)	10% foetal bovine serum (FBS) 1% Pen-Step (P/S)

#### 2.2. Cell culture methods

All cell culture was carried out in a laminar flow hood in a dedicated culture room. Only sterile equipment and reagents was used in the hoods to maintain the integrity of the cultures. All reagents where kept refrigerated (2-10°C) or frozen before being warmed to 37°C in a water bath prior to use.

Subculturing was carried out whenever a monolayer cell culture reached ≥85% confluence. Cell subculturing was used to either transfer the cells to a new culture flask/s or to seed plates for analysis. Initially, the previous media is removed, via aspirating, from the desired culture flask where the cells are attached. A PBS wash of the cells is used to neutralise any FBS from the supplemented media still present in the flask. An appropriate amount of trypsin (1-5 mL) was used depending on the size of the flask. This flask was manipulated to ensure complete contact with all cells and then incubated for 5 minutes. After this time, an equal volume of full growth media was added to the flask to neutralise the trypsin. A single cell suspension was then generated by vigorous pipetting. This suspension was then added to new labelled culture flasks in accordance with an appropriate split ratio. The cells where then left overnight in a 37°C incubator to allow the cells to settle and bind/attach. Following cell subculturing, the passage number of that culture is increased, and recorded on the flask.

### 2.3. Cell counting

Cell counting was either done via haemocytometer or automated cell counter (DeNovix BioDrop). In both cases, the culture first underwent trypsinisation, as stated above, to achieve a single cell suspension. For the automated cell counter,  $50\mu L$  of cell suspension was aliquoted into a microfuge tube and this sample was then removed from the hood. The cell counter was cleaned with 70% ethanol before use and initialised before  $10\mu L$  of sample was added to the chamber. The cell counter provided a cell/mL value for each sample. After use the cell counter was again cleaned with 70% ethanol

For cell counting using haemocytometer,  $100\mu$ l of cell suspension (culture trypsinised to single cell structure and then neutralized with media) was thoroughly mixed with  $100\mu$ l of 0.4% trypan blue stain, allowing a distinction between viable and non-viable cells. The stained sample was then used for counting on a haemocytometer. Before use, the haemocytometer and coverslip were cleaned with 70% ethanol and firmly fixed in place.  $10\mu$ l of stained cell suspension was then dispensed into the chamber and viable cells counted using a standardised method shown in Figure 2.1. The average viable cells between the 4 highlighted sections were adjusted by the dilution factor (multiply by 2 and then  $10^4$ ) giving a cell/ml value for the unstained cell suspension (Figure 2.1).

# 2.4. Cytotoxicity assay

All drugs were initial suspended in DMSO as a solvent and made up as initial stock concentrations. Any further dilution of the stock prior to investigation was prepared using sterile PBS.  $100\,\mu\text{L}$  of drugged media was added to previously seeded 96 well plates to make final concentrations of  $10\,\mu\text{M}$ ,  $50\,\mu\text{M}$ ,  $100\,\mu\text{M}$ , and  $250\,\mu\text{M}$ . These plates where then were incubated at  $37^{\circ}\text{C}$  in a  $CO_2$  rich environment for 48 hours. Following this incubation period,  $20\,\mu\text{L}$  of 0.04% resazurin. Following incubation with the resazurin, the fluorescence of each well was measured at  $555-590\,\text{nm}$ .

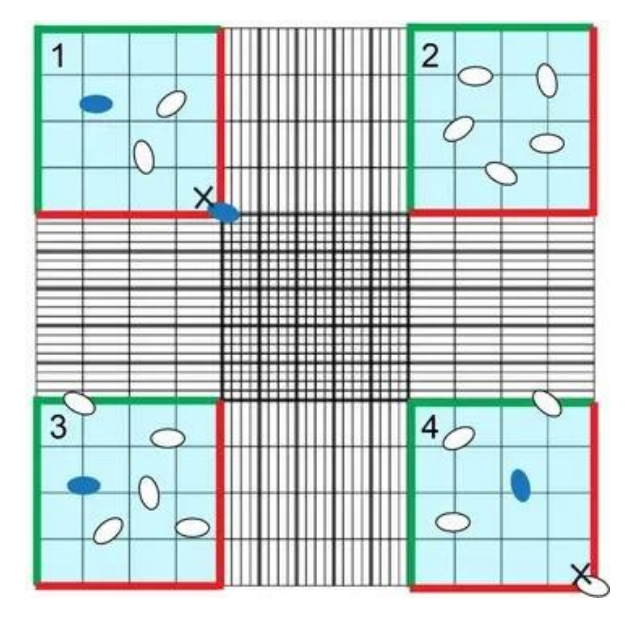


**Figure 2.1:** Standard method for counting cells on a haemocytometer grid. The four highlighted (blue) outer corner of the grid were used in the counting. All viable cells (white) and non-viable cells (blue) were tracked on separate cell counters. For each individual grid, cells on the top and left edge (indicated with green) were counted and the cells on the right and bottom (indicated with red) were not to prevent duplicate counts.

# 2.5. Chemosensitivity assay

A 96 well plate of monolayer cells was first prepared by aspirating off the growth media. Serum free media was then added to each test well to a total volume of 200  $\mu$ L including either Ag8 (10  $\mu$ M), HA266 (10  $\mu$ M), or HA197(50  $\mu$ M) and a variable concentration of Cisplatin (10  $\mu$ M, 50  $\mu$ M, 100  $\mu$ M, or 250  $\mu$ M). The drugged plate was then incubated at 37°C in 5% CO<sub>2</sub> for 48 hours. Following this incubation period, 20  $\mu$ L of 0.04% resazurin. Following incubation with the resazurin, the fluorescence of each well was measured at 555-590 nm.

### 2.6. Lactate release assay

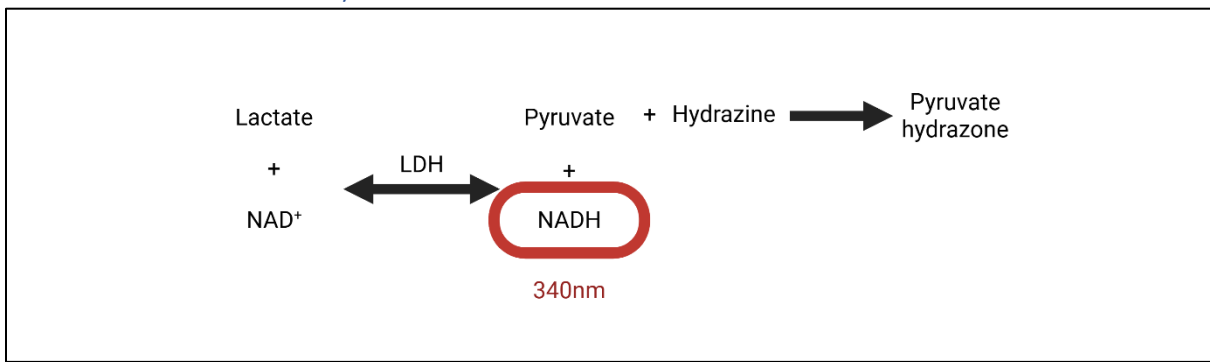


**Figure 2.2.** The base reaction on the LDH activity assay. It shows lactate's reversable reaction with NAD<sup>+</sup> in the presence of LDH to produce pyruvate and NADH, the latter of which can be measured via spectrometry at 340nm. The non reversable reaction between Pyruvate and hydrazine to produce pyruvate hydrazone can also be seen.

# 2.6.1. Assay buffer for assessing LDH activity

To investigate LDH activity following the addition of a sample, an assay buffer solution was produced. Once all the components where added, mixed by inversion until dissolved and uniformly distributed; The final assay buffer composition is 200mM glycine, 166 mM hydrazone, 2.5mM NAD $^+$ , 8U/mL lactate dehydrogenase (LDH). This solution has limited stability so for the purpose of this study a 0.6M glycine 0.5M hydrazine buffer was produced as a stock and adjusted to pH 9.2 with NaOH. The complete assay solution was then made up on the day of use by the addition of the additional components (NAD $^+$ , LDH, dH $_2$ O).

# 2.6.2. LDH activity/Lactate release assay

LDH activity and lactate release was measured via spectrometry at 340nm following the combination of  $20\mu L$  of sample media and  $180\mu L$  of complete assay buffer to a total reaction volume of  $200\mu L$  wells of a 96 well clear flatbottom plate compatible with a plate spectrophotometer. The study utilised the reaction of lactate with NAD<sup>+</sup> in the presence of LDH to produce pyruvate and NADH (Figure 2.2). The utilization of a glycine hydrazine buffer produced pyruvate-hydrazone making the reaction irreversible. As NADH has peak wavelength absorbance at 340nm, change in absorbance measured via spectrophotometry at 340nm can be used to measure the rate of reaction thus identifying enzyme activity. By controlling NAD<sup>+</sup> and LDH levels in the reaction, change of enzyme activity between samples is therefore relative to the lactate concentration of the sample.

# 2.6.3. LDH activity validation assay

Four key validations were carried out prior to the utilisation of the enzyme kinetic assay used in this study. The optimisation of sample volume was investigated by testing a range of lactate standard (1mM) volumes (5-40 $\mu$ L) and made up 200 $\mu$ L using the complete assay solution (as described above). Immediately after the addition of the buffer, the absorbance (at 340nm) of the sample was measured for an hour to calculate the rate of reaction ( $\Delta$ A/s).

To identify any potential interference caused by culture media in the assay, an investigation was carried out in which a range of stock lactate solutions concentrations were made (0.5-1000mM). These used either  $dH_2O$ , DMEM, or DMEM+ (with FBS and P/S) as the solvent.  $20\mu L$  of these stocks were added to  $190\mu L$  of the total assay buffer. After an hour, the absorbance of these samples was measured at 340nM.

To identify the stability of media samples taken from cell lines a study was carried out in which HCT116 p53 positive (+/+) and HCT116 p53 knock down (-/-) cells were grown in T25 flasks till 90% confluent. At this point the complete media was removed, a PBS wash carried out and 3mL of fresh serum free media added. At this time (T0), a sample of the media was aliquoted into a microtube. Some of this sample was used immediately to investigate enzyme activity following the addition of the assay buffer solution (spectrophotometry at 340nm). The rest of the sample was frozen. A new sample was taken from the cells every 2 hours, for a total of 6 hours, where the same procedure was repeated. 24 and 96 hours after the samples were taken, the frozen media aliquots where tested ion the same assay. The rate of reaction of these different sample ages were compared to determine the stability of the samples when frozen.

# 2.6.4. Assaying LDH activity in cancer cells

LDH activity and lactate release was measured via spectrometry at 340nm following the addition of  $20\mu\text{L}$  of sample media and  $180\mu\text{L}$  of complete assay buffer per well of a 96 well clear flatbottom plate. The study utilised the reaction of lactate with NAD<sup>+</sup> in the presence of LDH to produce pyruvate and

NADH. The utilization of a glycine hydrazine buffer produced pyruvate-hydrazone making the reaction irreversible. As NAD+ has peak wavelength absorbance at 340nm, change in absorbance measured via spectrophotometry at 340nm can be used to measure the rate of reaction thus identifying enzyme activity. By controlling NAD+ and LDH levels in the reaction, change of enzyme activity between samples is therefore relative to the lactate concentration of the sample.

In this study two methods of sample preparation where used. In the first instance media was taken from a monolayer culture. Monolayer cell cultures were seeded and grown in flat bottom 6 well plates. Cells were seeded at a concentration of  $0.3 \times 10^4$  cells/ml with each 6 well containing 5 ml of supplemented media. These cells were then incubated at 37°C in a CO<sub>2</sub> rich environment until reaching a confluence of  $\geq 80\%$  at which point they were used for testing. In testing, the samples had their growth media aspirated off and a PBS wash was carried out. The culture was then exposed to 1mL of drugged serum free media.  $10 \mu M$ ,  $50 \mu M$ ,  $100 \mu M$ , and  $250 \mu M$  of novel and control compounds (Ag8, HA197, HA266, silibinin, and sodium oxamate). Immediately after drug exposure, a  $20 \mu L$  media sample was taken for testing. Every 2 hours after exposure, another sample was taken for testing to a total of 6 hours.

The alternative method of sample collection utilised high-density cultures to increase cell concentration per well. In this method cells were suspended in 96 well round bottom plates. Cells were seeded at a concentration of  $1.0 \times 10^6$  cells/ml with each well containing  $100 \, \mu L$  of serum free media. Following the previous method, the culture was exposed to  $100 \, \mu L$  of drugged serum free media for a total well volume of  $200 \, \mu L$ .  $10 \, \mu M$ ,  $50 \, \mu M$ ,  $100 \, \mu M$ , and  $250 \, \mu M$  of novel and control compounds (Ag8, HA197, HA266, silibinin, and sodium oxamate) where used. Immediately after drug exposure, a  $20 \, \mu L$  media sample was taken for testing. Every hour after exposure, another sample was taken for testing to a total of 6 hours.

**Table 2.3.** The function and structure of non-novel compounds used in this study

Compound name	Function	Structure
Cisplatin	Platinum based chemotherapeutic - disrupts DNA repair and replication	CI — Pt — N — H
Silibinin	Inhibitor of Glycolysis  – Inhibits pyruvate kinase in glycolysis	H O H
Sodium Oxamate	Inhibitor of Glycolysis  – Inhibits the actions of the enzyme LDH	H N Na

# 2.7. Statistical analysis.

Both the Lactate inhibition data and cell viability data is presented as mean  $\pm$  Standard error (SE= $\sigma$ /Vn) of at least three biological triplicate samples unless stated otherwise. Data was analysed using Microsoft excel via the data too pack and single tailed T tests were used to ascertain statistical significance with a threshold ( $\alpha$  value) of \*p<0.05, \*\*p<0.005 unless stated otherwise.

# 3. Inhibition of lactate release by novel silver organometallic compounds

#### 3.1. Introduction

To investigate the novel silver organometallic compounds mechanisms of glycolysis inhibition, an investigation of extracellular lactate release following drug exposure was carried out. By investigating changes in lactate release we can begin to identify potential therapeutic value for these compounds within clinical cancer settings, exploiting cancers reliance on anaerobic glycolysis (i.e., the Warburg effect).

The LDH activity assay was used to examine the changes in lactate production. The assay utilises the reaction between lactate and NADH, in the presence of LDH, to produce pyruvate and NAD+, which can be reliable measured via spectrophotometry at 340nm. By controlling the concentration of all reagents but lactate, any change in NADH production occurring during the reaction (monitored as an absorbance change), are correlated to a change in lactate concentration. Thus, the rate of reaction, as measured by the loss of NAD+ and increase in NADH, is proportional to the lactate concentration of the sample.

This assay is to be utilised on extracellular media samples taken from several in vitro cancer cell lines, both pancreatic (PSN-1 and BxPc-3) and colorectal (HCT116 +/-). These cell lines will be exposed to the novel compounds and media samples taken over time to determine change in lactate concentration over time following drug exposure.

# 3.2. LDH activity assay validation

To investigate the change in extracellular lactate, a lactate dehydrogenase (LDH) activity assay was chosen from current literature (T Hass and B. Hurley, 2023). The assay was subsequently optimised and validated for the type of sample, the assay run time, and potential interference of different media types.

The general LDH activity assay utilises a reaction buffer mixed with a volume of sample. Figure 3.1A compares different sample volumes in a total reaction volume of  $200\,\mu\text{L}$  when monitoring absorbance change at 340nm over an hour. Sample volumes of  $5\,\mu\text{L}$ ,  $10\,\mu\text{L}$ ,  $20\,\mu\text{L}$ , and  $40\,\mu\text{L}$  were investigated using two different lactate-spiked solvents at a concentration of 1mM; water (control) and DMEM (media). Smaller sample volumes tended to produce a greater absorbance change ( $\Delta$ Absorbance/s), with  $5\,\mu\text{L}$  of sample producing the largest change per second for both solvent types (Figure 3.1A). At  $5\,\mu\text{L}$  the control water sample had a  $\Delta$ Absorbance/s of  $4.19\,x10^{-5}$ . As the volume increased, these values decreased to  $4.05\,x10^{-5}$ , then  $3.8\,x10^{-5}$ , and  $3.18\,x10^{-5}$  respectively. The media sample followed a similar trend, where the highest  $\Delta$ Absorbance/s of  $5.19\,x10^{-5}$  was seen with the  $5\,\mu\text{L}$  media sample, decreasing to  $5.17\,x10^{-5}$ ,  $4.94\,x10^{-5}$ , and  $3.18\,x10^{-5}$  for the  $10\,\mu\text{L}$ ,  $20\,\mu\text{L}$ , and  $40\,\mu\text{L}$  sample volumes, respectively. Comparing the control to media sample, a significant difference (p<0.005) can be seen at most volumes indicating a need for further investigation of the influence of culture media within the study.

As the kinetics assay will utilise samples derived from cell culture media, any potential interference from the media was investigated next. In Figure 3.1B the interference of two media variants (with and without 10% (v/v) foetal bovine serum; FBS) were investigated and compared to a control solvent (water) over a 1h assay period. The absorbance of these samples was measured at lactate concentrations of  $0.5 \, \text{mM}$  to  $1000 \, \text{mM}$ . The data shows that media containing FBS exhibit reduced absorbance changes across the assay period following changes to the lactate concentration.

This indicates that serum interferes with the assay and accurate determination of LDH activity. As the lactate concentration decreases, this difference in the FBS-containing samples becomes more apparent. At 1000mM lactate the difference between medias is insignificant (control= 3.3, FBS=3.0, DMEM=3.2), whereas at 80mM the difference is significant (p<0.005; control=1.7, FBS=1.9, DMEM=1.6), and at 0.5mM the FBS differs from the control at a significance level of p<0.0005 (control=0.3, FBS=1.4, DMEM=0.3).

The lactate release assay requires sequential media samples to be taken across different time periods from cells growing under standard tissue culture conditions, sometimes required storage prior to analysis. The stability of this sample is important as it determines how soon after taking the sample it must be analysed. Figure 3.1C investigates the change in LDH activity of samples from two cells lines, HCT116 p53 positive (+/+) and HCT116 p53 knock down (-/-) cells, taken from the cell lines over a 6-hour period after a media change. Samples were analysed after 0, 1, and 4 days in 0-10°C storage. The data shows that after 1 and 4 days, the rate of reaction has significantly decreased compared to the sample analysed immediately after collection (Figure 3.1C). The data shows that this change in rate becomes more prominent in the later sample time points with the T0 samples having a data range of 0 to  $2.5 \times 10^{-5}$  for the p53 positive cell lines and 0 to  $3.1 \times 10^{-5}$  for the p53 knockdown line and the T6 data ranging from  $4.8 \times 10^{-06}$  to  $1.74 \times 10^{-4}$  for the positive line and  $8.58 \times 10^{-6}$  to  $2.23 \times 10^{-4}$  for the negative line. This difference has a significance level of p<0.005 between that of the day 0 sample and the two older stored samples. This shows that lactate within the samples is not stable in storage and therefore must be analysed on the day it is taken.

In previous testing of this assay, a reaction time of 1 hour was chosen. However, to optimise this reaction there is value in comparing a range of times, as the rate of reaction is likely fastest at the start of the reaction. The data in Figure 3.1D shows the change in reaction rate based on the reaction time chosen across a range of lactate concentrations. As predicated, the shorter reactions show the greatest rates of reaction across the range of lactate concentrations. A linear trendline for each time variable was used to calculate  $R^2$  values as a measure of how linear the results obtained are. While the shorter reactions have the highest rate of reaction, they also have the lowest  $R^2$  values. The 1000s reaction has an  $R^2$  value of 0.9335, followed by 2000s with a  $R^2$  value of 0.96, and then 4000s with a  $R^2$  value of 0.9778. As the  $R^2$  value is representative of how liner the trend is, this shows that the higher the time of reaction the more linear the increase in rate over concentration with is a valuable optimisation for the study.

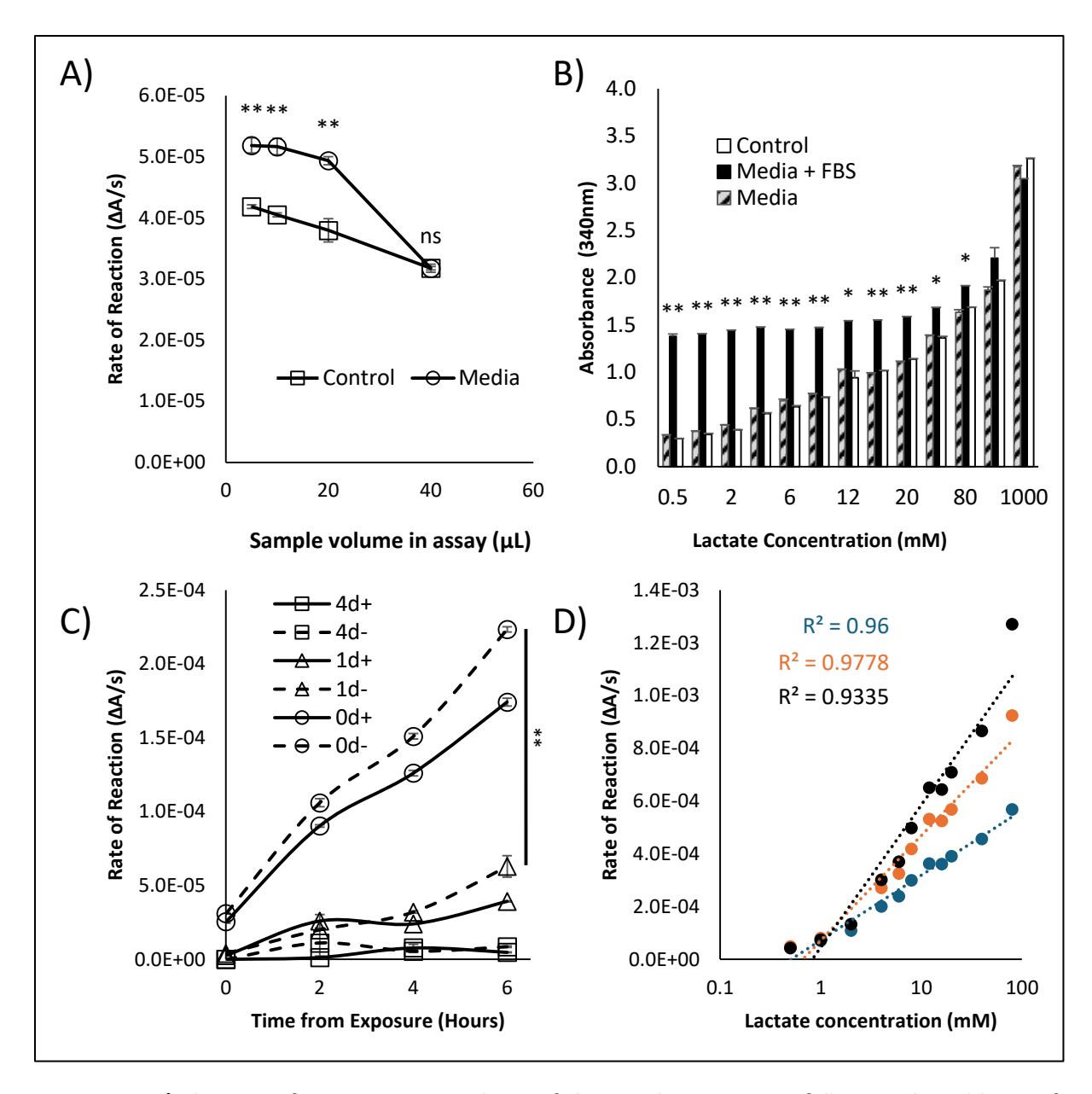


Figure 3.1: A) The rate of reaction over an hour of the LDH kinetics assay following the addition of various sample volumes (5 μL, 10 μL, 20 μL, and 50 μL). The sample was a 10 mM lactate solution of either culture media (DMEM) ( $\bigcirc$ ) or a control solvent (buffer) ( $\square$ ). Significance determined though single tailed paired T test where \*\*=P<0.005. B) A clustered column chart comparing the absorbance after 1 hour of various lactate spiked sample types in the lactate kinetics assay. The control sample (white) uses dH<sub>2</sub>O as the solvent. Both media samples use DMEM however one included 10% foetal bovine serum (black) and the other is serum free (hashed). Significance was determined via single facto ANOVA comparing the change within each lactate concentration group. \*=P<0.005 \*\*=P<0.0005 C) A comparison of the LDH activity of media samples 0, 1, and 4 days after taking the sample from a culture flask of either HCT116 p53 positive (+/+) or HCT116 p53 knock down (-/-) cells. Significance was determined via single factor ANOVA comparing the different sample ages within a single cell line. \*\*=P<0.005. Age of the sample is represented by the day number (i.e., 4d for 4 days post collection) and the cell line is represented by the +/- where HCT116 p53 positive or negative was used. D) Rate of reaction of the LDH activity assay with variable lactate concentrations (0.1 to 100mM). The graph compares  $\Delta$ Absorbance value of different assay run time 1000s (Blue), 2000s (Orange), and 3000s (Black). Each run time has a liner trendline plotted with an associated R<sup>2</sup> value. The relative R<sup>2</sup> value shows the liner nature of the results where a value of 1 is completely linear.

# 3.3. LDH activity/Lactate Inhibition studies

The investigation of changing extracellular lactate following exposure to novel drugs was carried out using the optimised LDH activity. During this study, two different methods of cell culture were investigated for the collection of media samples. The first was a monolayer culture where the media sample was taken from a confluent 6 well plate of cells and the second method utilised suspended cells in a round bottom 96 well plate.

# 3.3.1. Monolayer culture

Monolayer cultures of the colorectal cell lines HCT116 p53 positive (+/+) and HCT116 p53 knock down (-/-) where exposed to the novel silver organometallic compounds Ag8, HA197, and HA266 at a range of concentrations to investigate their effect on extracellular lactate over time investigated though the enzyme activity of LDH in a reaction buffer.

The effect of Ag8 on both colorectal cell lines is graphed in figure 3.2A and B. At initial drug exposure there was a rate of reaction of  $0\Delta A$ /min and this value then increased over time. The negative control of the HCT116 (+/+) cell line increased to 1.39x10<sup>-2</sup> at the end of the 6-hour observation while the HCT116 (-/-) line only increased to 3.60x10<sup>-3</sup>. This is over a 3-fold increase in rate of reaction in the HCT116 (+/+) line compared to the HCT116 (-/-) line. In both cell lines the increase in  $\Delta A/\min$  is greatest between the TO and T2 (A:8.06x10<sup>-3</sup> and B:2.30x10<sup>-3</sup>) time points with a notable decrease over time with a smaller change between the T4 and T6 time point (A:2.89x10<sup>-3</sup> and B:1.56x10<sup>-4</sup>). The effect of Ag8 appears dose dependant in both cell lines with an increased dose correlation to a decreased rate of reaction. In the HCT116(+/+) line a deviation from the control can be seen at the second hour following exposure to all concentrations except for 50µM, which closely follows the trend of the control. At this time point the rate of reaction following 10μM, 100μM, and 250μM of Ag8 is 4.51x10<sup>-1</sup> <sup>3</sup>, 5.02x10<sup>-3</sup>, and 3.87x10<sup>-3</sup> respectively while the control value maintains a ΔA/min of 8.06x10<sup>-3</sup>. This shows a minimum of a 1.6-fold decrease in rate of reaction caused by the addition of Ag8 at these concentrations. However, the same effect is not seen in the HCT116(-/-) line. All concentrations maintain correlation to the control value apart from 250µM, which deviates at the 2-hour point. The rate of reaction following 2 hours exposure to Ag8 on the HCT116(-/-) cell line shows a rate of reaction of 9.96x10<sup>-4</sup> compared to the control-treated value of 6.60x10<sup>-3</sup>. From this point on, this sample does not show an increase in rate of reaction, where at the 6-hour point treatment with 250μM of Ag8 produces a 8.41x10<sup>-4</sup>ΔA/min compared to the control value of 3.60x10<sup>-3</sup>ΔA/min. Overall, this demonstrates a 4.2-fold decrease in lactate production caused by exposure to Ag8.

The effect of HA197 in HCT116 p53 positive (+/+) and HCT116 p53 knock down (-/-) is seen in figure 3.2C and D. The novel silver organometallic compound has no effect on the p53 positive cell line, where no deviation is seen from the negative control sample. At the 6-hour time point, the control has a rate of reaction of  $1.39 \times 10^{-2}$  and all test samples fall within the range of  $1.29 \times 10^{-2}$  and  $1.4 \times 10^{-2}$ , falling within the standard deviation of the control replicates.

HA266 appears to have minimal influence on the rate of lactate production in HCT116 cells, where a decrease in rate of reaction within the p53 positive cell line at the 6-hour point (figure 3.2E). Only HA266 at a concentration of  $100\,\mu\text{M}$  falls below one standard deviation of the control replicates at a rate of reaction of  $1.17 \times 10^{-2}$  compared to the control samples  $1.39 \times 10^{-2}$ . All other concentration falls within the  $1.75 \times 10^{-3}$  standard deviation of the control.

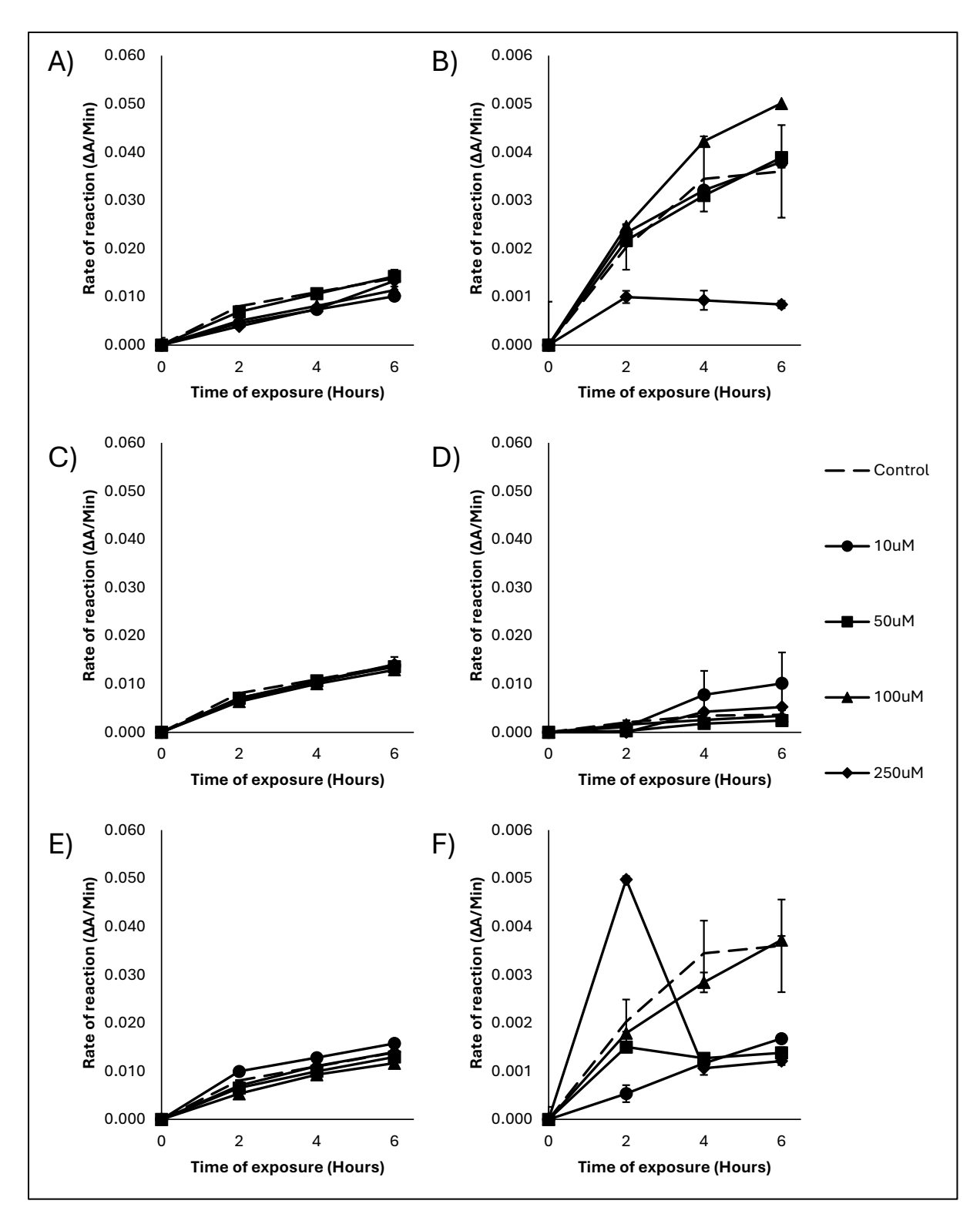


**Figure 3.2:** The rate of reaction of media samples taken from HCT116 p53 positive (+/+) (Figures 3.2A, C, and E) and HCT116 p53 knock down (-/-) cell lines, grown as a monolayer culture, (Figures 3.2B, D, and F) following exposure novel silver organometallic compounds at a range of concentrations ( $10\mu M \cdot$ ,  $100\mu M \cdot$ , and  $250\mu M \cdot$ ) compared to a negative control (Dashed Line). **A and B)** Ag8. **C and D)** HA197. **E and F)** HA266. Error bars represent standard deviation of technical triplicate replication samples.

## 3.3.2. Lactate Release from Cells Cultured at High Density in Round-Bottom 96well Plates

A high-density culture of colorectal cell lines, HCT116 p53 positive (+/+) and HCT116 p53 knock down (-/-), and pancreatic line, BxPc-3 and PSN-1, were exposed to the novel silver organometallic compounds Ag8, HA197, and HA266 and known LDH inhibitors silibilin and sodium oxamate. A range of concentrations were investigated for their effect on extracellular lactate concentration over a 4-hour period, determined using the LDH activity assay. The high-density culture consisted of cells seeded at a concentration of  $1.0 \times 10^6$  cells/ml in a 96 well plate with each well containing  $200 \mu L$  drugged serum free media for a total well volume of  $200 \mu L$ . This high-density seeding is above the recommended cell density for long term survival however due to the short length of the study this is not considered to be relevant.

The effects of the silver organometallic compound Ag8 on all cell lines is shown in Figure 3.3 for four different cell lines; A) HCT116 p53 positive (+/+) B) HCT116 p53 knock down (-/-) cell C) BxPc-3 and D) PSN-1). The data shows a dose-dependent response in which higher concentrations of treatment produced the most significant decrease in enzyme activity correlating to a reduced lactate concentration in the sample media taken from culture. Across all cell lines, a significant (\*p=<0.05 and \*\*p=<0.005) reduction in rate of reaction can be seen with Ag8 treatment at concentrations of 100  $\mu$ M and 250  $\mu$ M, with the absolute difference from controls increasing over time. Ag8 treatment also produced cell line-dependant responses at lower concentrations. For example, at 50  $\mu$ M, both pancreatic lines displayed significantly reduced lactate production, a response not evident in either HCT116 colorectal cell line.

In figures 3.3C and D,  $50\mu\text{M}$  of Ag8 reduced the rate of reaction, decreasing lactate production in the two pancreatic cell lines tested (BxPc-3 and PSN-1). In figure 3.3A the HCT116 p53 positive (+/+) cell line showed significant deviation from the control at the second hour of sampling for  $100\mu\text{M}$  and  $250\mu\text{M}$  concentrations. Control samples had a  $\Delta\text{A/s}$  of  $3.97\text{x}10^{-05}$  whereas the samples treated with high Ag8 doses decreased to  $1.17\text{x}10^{-05}$  ( $100\mu\text{M}$ ) and  $1.65\text{x}10^{-05}$  ( $250\mu\text{M}$ ), with a significance of p<0.05 compared to control treatments. At this time point,  $50\mu\text{M}$  of Ag8 also showed some difference from the control, however this did not extend to later time points. By the  $6^{th}$  hour, a greater significant difference was observed between the control and treated cells (p<0.005). The control samples  $\Delta\text{A/s}$  increased to  $9.35\text{x}10^{-05}$  whereas the treated samples remained low at  $1.90\text{x}10^{-05}$  and  $1.24\text{x}10^{-05}$ , reflective of a suppression in lactate release with Ag8.

HCT116 p53 knock down cells (-/-) showed a similar trend, however the differences compared to control treatments were evident after the first hour of drug exposure. At this time point the control displayed a  $\Delta A/s$  of  $2.9 \times 10^{-05}$ , whereas the treated samples already showed a significant reduction in lactate production, with a lower  $\Delta A/s$  of  $1.67 \times 10^{-05}$  and  $1.41 \times 10^{-05}$  observed respectively ( $100 \mu M$  and  $250 \mu M$ ). Again, the treated samples maintained a suppressed lactate production, while the control value increased to  $6.23 \times 10^{-05}$ .

As previously stated, the pancreatic lines show an increased sensitivity to Ag8 as the lower  $50\mu M$  dosage was observed to significantly impact the two lines tested. In figure 3.3C BxPc-3 is shown to differ from the control at  $50\mu M$  treatment with a significance of p<0.05 from as early as the first hour of exposure. This sample displayed a  $\Delta A/s$  of  $6.7x10^{-06}$  at this time point compared to the control values  $9.53x10^{-06}$ . As with the previous cell lines, the control gradually increases over time while the higher concentration drug treatments produce a consistently suppressed  $\Delta A/s$  which were not significantly different from each other. At T6 (6 hours) the rate of reaction in control samples increased

to  $2.0x10^{-05}$  while the 50, 100, and  $250\mu M$  treatments showed  $\Delta A/s$  of  $7.78x10^{-05}$ ,  $3.59x10^{-06}$ , and  $5.84x10^{-06}$  demonstrating a reduction of nearly 10-fold from control levels.

The PSN-1 line differs from the over pancreatic line as the low  $50\,\mu\text{M}$  treatment of Ag8 only produced a significant rate reduction after 4 hours of exposure. At this point the PSN-1 sample had a  $\Delta\text{A/s}$  of  $2.28 \times 10^{-05}$  compared to the control sample of  $4.16 \times 10^{-05}$ . While this result is shown to be significant, the higher doses of  $100\,\mu\text{M}$  and  $250\,\mu\text{M}$  produced a more significant reduction of  $4.05 \times 10^{-06}$  and  $7.04 \times 10^{-06}$ . As well as demonstrating the effect of Ag8 treatment on lactate production, Figure 3.3 also showed that lactate production in the untreated control groups of each cell line differed substantially, indicating a variable cell-dependant release of lactate during cell growth without treatment. The  $\Delta\text{A/s}$  of the controls are  $9.35 \times 10^{-05}$  (HCT116 p53 positive),  $6.23 \times 10^{-05}$  (HCT116 p53 negative),  $2.0 \times 10^{-05}$  (BxPc-3), and  $4.16 \times 10^{-05}$  (PSN-1), indicating that lactate production is highest in wild-type p53-expressing HCT116 cells.

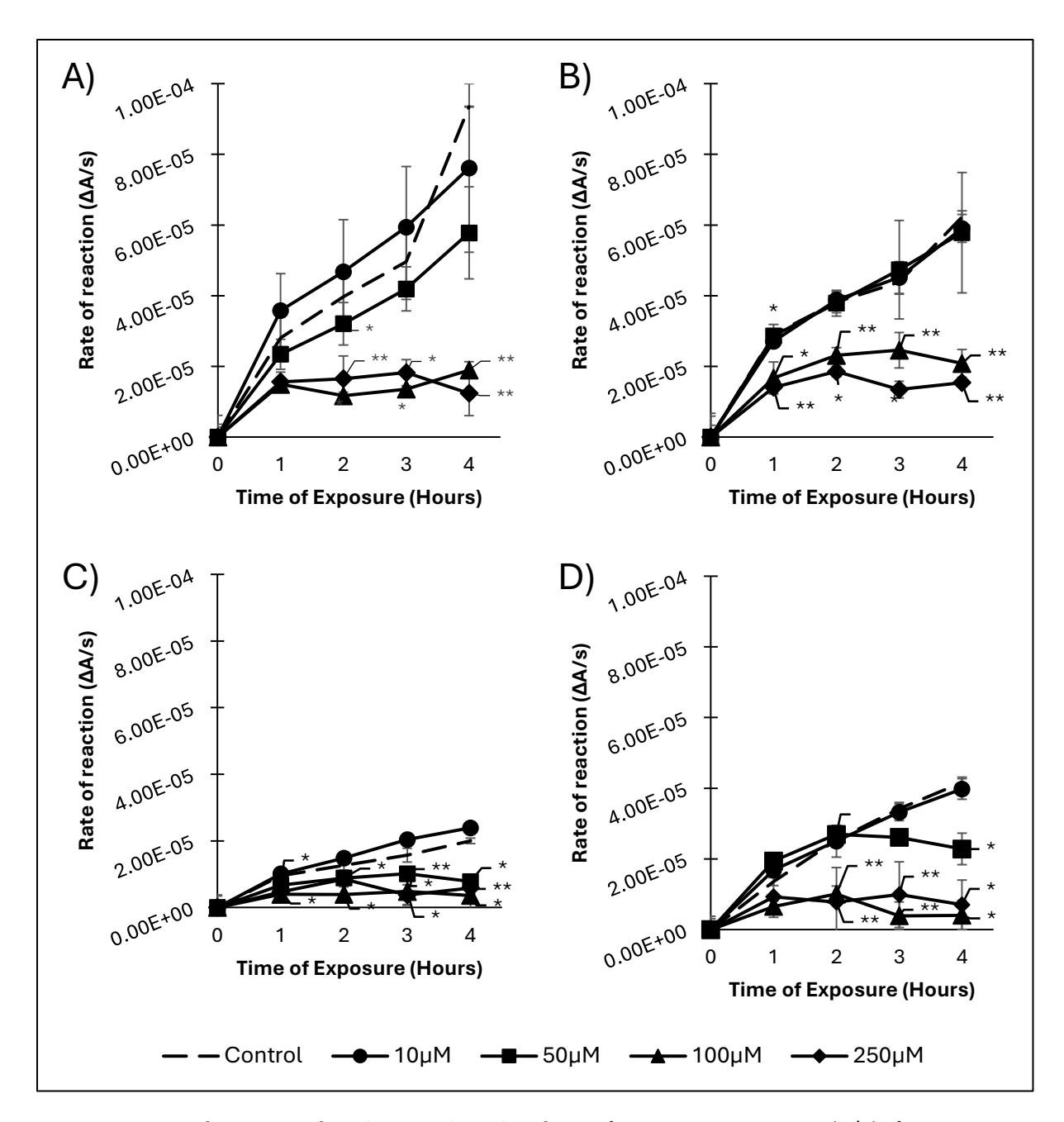


Figure 3.3 Rate of reaction of media samples taken from A) HCT116 p53 positive (+/+) B) HCT116 p53 knock down (-/-) cell C) BxPc-3 D) PSN-1cell lines over time following exposure to Ag8 at a range of concentrations ( $10\mu$ M $\bullet$ ,  $50\mu$ M $\bullet$ ,  $100\mu$ M $\bullet$ , and  $250\mu$ M $\bullet$ ) compared to a negative control. Error bars show Standard error of mean across biological triplicates (n=3). Significance difference to the control is calculated by single tail paired T test where \*=P<0.05 \*\*=P<0.005.

Figure 3.4 shows the effects HA197 treatment has on the A) HCT116 p53 positive (+/+) B) HCT116 p53 knock down (-/-) cell C) BxPc-3 and D) PSN-1 cell lines. Overall, the data shows a doseand cell line-dependant response to the novel silver organometallic compound with the colorectal cell lines only showing significant reduction in rate of reaction at high concentration and the pancreatic lines being more sensitive at lower does. Across all cell lines, a significant response can be seen after 4 hours of exposure to 250 µM of HA197 however the time it takes for this response to be seen is cell dependant. The HCT116 p53 positive cell line, as shown in figure 3.4A, showed little response to HA197 with only the 250µM treatment reducing the rate of reaction. A significant response from control production is first seen after 3 hours of exposure where the sample  $\Delta A/s$  falls from the control value,  $4.96 \times 10^{-05}$ , down to  $3.02 \times 10^{-05}$  (p<0.05). HCT116 p53 negative cells also exhibited a response at 250  $\mu$ M however this was also seen in shorter exposure times. After 1 hour of exposure to HA197, this cell line had a  $\Delta A/s$  of 1.4x10<sup>-05</sup>, which is a significant (p<0.05) reduction compared to the control sample at the same time point. This level of significance is continued over the observation period and is then increased after 4 hours to a significance of p<0.005 due to the continued increase of the control value and suppression in the HA197-treated samples. While the 250μM sample increased its ΔA/s to 2.54x10<sup>-05</sup> by the 4-hour mark, it is a significantly reduced increase compared to the increase to  $6.23x10^{-05}$  of the control. Following  $100\mu M$  treatment, a significant change can be seen after 1 hour of exposure, however this difference is lost after an additional hour of exposure. The 10 µM sample also shows some significance however there remains an increase in rate of reaction implying continued release of lactate.

The pancreatic cell lines have a different response to the novel silver organometallic compound HA197 (Figures 3.4C and D). In the BxPc-3 line a significant decrease in ΔA/s can be seen in the 250 $\mu$ M sample from the first hour of observation. At the final time point this is reduced to a  $\Delta$ A/s of 6.49x10<sup>-06</sup>. The lower concentrations of HA197 have less consistent results. 100µM of HA917 produced a significant change in rate of reaction at the T1 and T3 points however at T2 and T4 the results lose this significance. At T1 the  $\Delta A/s$  is  $5.89 \times 10^{-06}$ , this increases to  $1.15 \times 10^{-05}$  after 4-hour treatment. Following exposure to 50µM of HA197, there is a significant change in rate of reaction up until 4 hours post exposure. At all other time points examined, no significant change from the control was seen. The PSN-1 line shows a more consistent dose dependant response (Figure 3.4D). 250µM produced a significant (p<0.05) change from 2 hours (1.30x10<sup>-05</sup>) after exposure and this difference increased as time progressed, where a more significant (p<0.005) change in  $\Delta A/s$  was observed after 3  $(1.10 \times 10^{-05})$  and 4  $(7.78 \times 10^{-06})$  hours of exposure. A treatment of 100  $\mu$ M produced a similar effect but with a slightly smaller reduction in reaction rate. At the second hour this sample has a  $\Delta A/s$  of 1.53x10<sup>-05</sup> and as time progressed, it increased further to 2.06x10<sup>-05</sup>. The rate of reaction for 100µM treatment remained above that of 250µM while still causing a significant decrease in lactate production compared to the control samples. The lower HA197 concentration of 50µM also produces a significant change after 2 and 3 hours of exposure before tapering off at the 4-hour mark. While significant, these reaction rates, and hence lactate production, were higher than that of 100 µM and 250 µM treatments, consistent with a concentration-dependent suppression of lactate production with HA197 treatment.

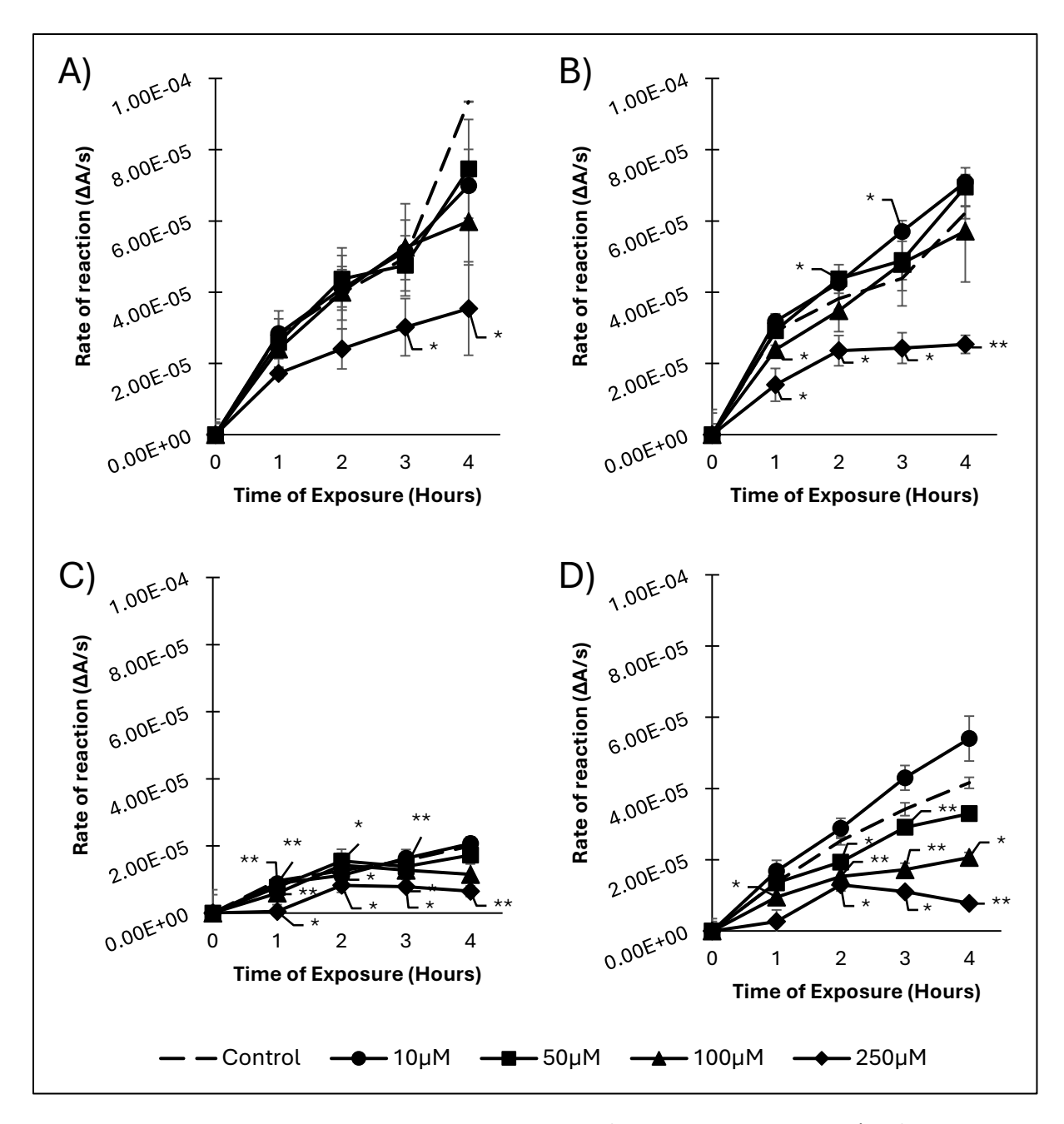


Figure 3.4 Rate of reaction of media samples taken from A) HCT116 p53 positive (+/+) B) HCT116 p53 knock down (-/-) cell C) BxPc-3 D) PSN-1cell lines over time following exposure to HA197 at a range of concentrations ( $10\mu M \bullet$ ,  $50\mu M \bullet$ ,  $100\mu M \bullet$ , and  $250\mu M \bullet$ ) compared to a negative control. Error bars show Standard error of mean across biological triplicates (N=3). Significance difference to the control is calculated by single tail paired T test where \*=P<0.05 \*\*=P<0.005.

The effect of the novel silver organometallic compound HA266 on the rate of reaction in the LDH activity assay is shown in figure 3.5. Overall, the data showed broad sensitivity to the compound, with all cell lines examined showing a consistent and significant dose-dependent suppression of lactate production. Across all cell lines a significant response was seen at HA266 concentrations of 50  $\mu$ M and above within 1 hour of exposure. Depending on the cell lines, 10  $\mu$ M of the compound also caused a significant change. The HCT116 p53 positive cell line (Figure 3.5A) showed some significant (p<0.05) changes from the first hour of exposure at the 50  $\mu$ M and 250  $\mu$ M concentrations where the  $\Delta$ A/s were 1.84x10<sup>-06</sup> and 1.22x10<sup>-05</sup> compared to the control value at 2.81x10<sup>-05</sup>. After an additional hour these concentrations result in a more significant (p<0.005) change from the control treatment. The 100  $\mu$ M also produced a significance reduction in lactate release (p<0.05).

After an additional hour (T3) of exposure, the rate of reaction for all treated samples began to plateau, remaining significantly lower than control treatments (p<0.05). By the final hour of observation, the  $\Delta A/s$  values were as follows; control =  $9.35 \times 10^{-05}$ ,  $10 \mu M = 4.53 \times 10^{-05}$  (p<0.05),  $50 \mu M = 3.80 \times 10^{-05}$  (p<0.05),  $100 \mu M = 2.79 \times 10^{-05}$  (p<0.05),  $250 \mu M = 1.42 \times 10^{-05}$  (p<0.005). This data showed a strong correlation between dose and response with all concentrations tested producing a significant reduction in lactate release by the end of 4-hour treatment period. A similar dose dependant response is seen in the HCT116 p53 negative cell line (Figure3.5B). In this line HA266 produced a significant decrease in  $\Delta A/s$  following 1 hour of exposure at concentrations  $50 \mu M$ ,  $100 \mu M$ , and  $250 \mu M$ . These samples had a  $\Delta A/s$  of  $1.87 \times 10^{-05}$ ,  $1.48 \times 10^{-05}$ , and  $4.01 \times 10^{-06}$  compared to the control value which increased by  $3.33 \times 10^{-05}$  between T1 and T4 compared to the novels, which only increased by a maximum of  $6.68 \times 10^{-06}$  across this period This difference was significant (p<0.005) for each of these three concentrations. However,  $10 \mu M$  treatment did not significantly alter rate of reaction compared to the respective controls.

Both pancreatic cell lines, BxPc-3 (Figure 3.5C) and PSN-1 (Figure 3.5D), had similar responses to treatment with HA266. Both cell lines produce a significant reduction in  $\Delta A/s$  following exposure to 50µM, 100µM, and 250µM with limited change in the 10µM samples. In the BxPc-3 line, 10µM for HA266 caused a significant decrease in  $\Delta A/s$  at 1- and 2-hours post exposure which is then lost at the later time points. The PSN-1 line differs here as it only started to show a significant change following 4 hours of exposure. The higher concentrations showed a more consistent and significant effect over the whole 4-hour observation period, where 250µM caused a significant reduction at all time points across both cell lines. 100µM of HA266 also caused a significant reduction compared to the control after a single hour of exposure in the BxPc-3 cell line, however this was not seen in PSN-1 cell until the 2-hour time point. As with the previous concentration, 50µM of HA266 produced a significant reduction after treatment at the T1 point in the BxPc-3 line but not the PSN-1 line, which became significant at T2. This potentially indicates increased sensitivity of the BxPc-3 cell line to the HA266 compound.

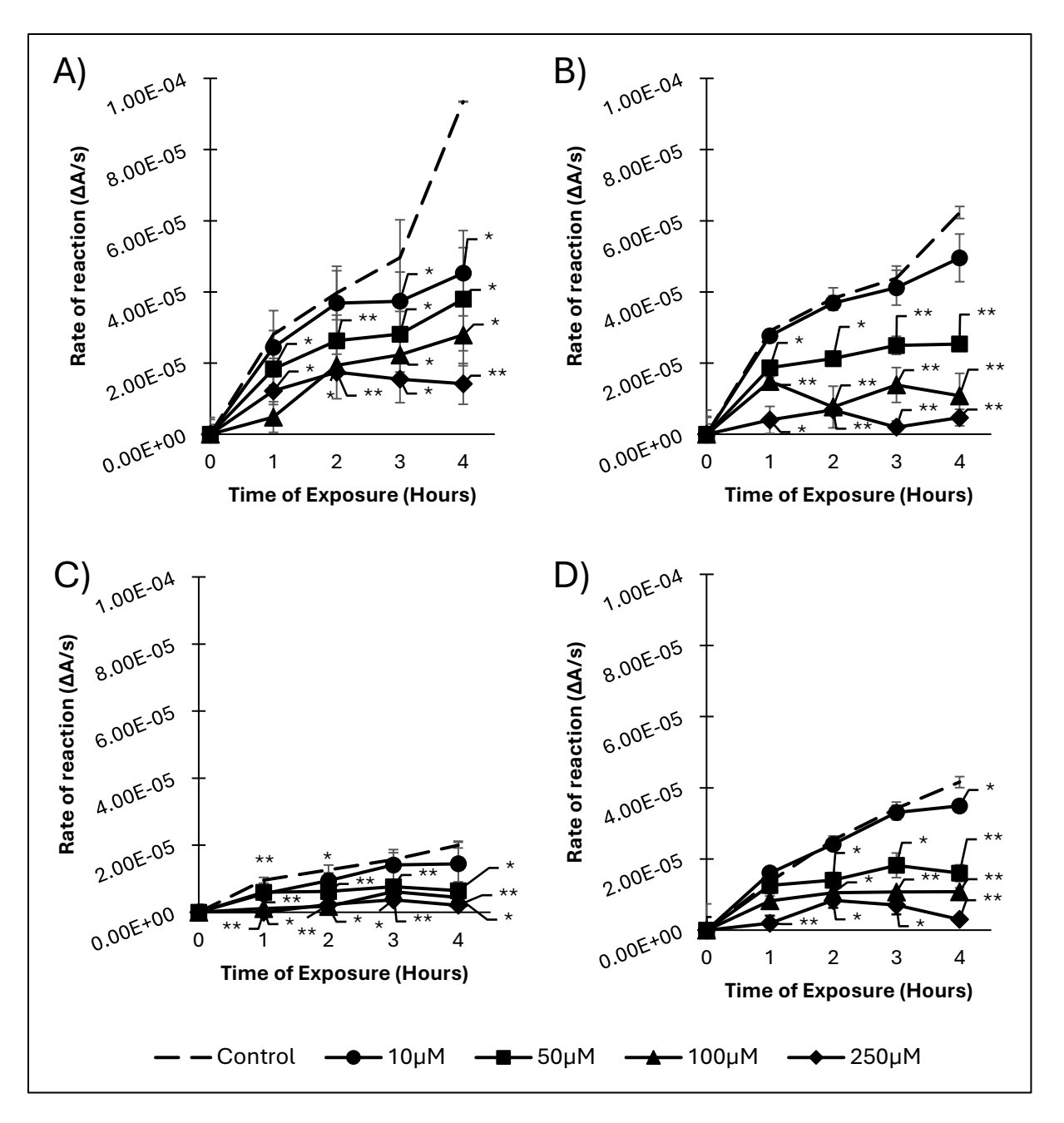


Figure 3.5 Rate of reaction of media samples taken from A) HCT116 p53 positive (+/+) B) HCT116 p53 knock down (-/-) cell C) BxPc-3 D) PSN-1cell lines over time following exposure to HA266 at a range of concentrations ( $10\mu M \bullet$ ,  $50\mu M \bullet$ ,  $100\mu M \bullet$ , and  $250\mu M \bullet$ ) compared to a negative control. Error bars show Standard error of mean across biological triplicates (n=3). Significance difference to the control is calculated by single tail paired T test where \*=P<0.05 \*\*=P<0.005.

Figures 3.6 and 3.7 show the rate of reaction from media samples in a LDH activity assay following the treatment of cells with known LDH inhibitors. This was carried out as controls to compare against the intracellular inhibition of glycolysis and extracellular lactate release of the three novel silver organometallic compounds which were identified as glycolysis inhibitors of unknown mechanisms. The LDH inhibitors silibinin (Figure 3.6) and sodium oxamate (Figure 3.7) were used to treat colorectal cells, HCT116 p53 positive (A) and negative (B), and BxPc-3 (C) and PSN-1(D) pancreatic cell lines, , at a range of concentrations ( $10\mu M \bullet$ ,  $50\mu M \bullet$ ,  $100\mu M \bullet$ , and  $250\mu M \bullet$ ). The treated cell lines had a less substantial effect on rate of reaction and lactate production than the novel silver organometallic tested previously (figures 3.3-3.5) with several lines showing no inhibition following treatment. The HCT116 p53 positive cells had no significant response when treated with sodium oxamate, although silibinin appeared to have a limited effect (figure 3.7A). 4 hours post treatment with silibinin, minor changes in  $\Delta A$ /s were evident with all concentrations tested producing a significant (p<0.05) reduction in  $\Delta A$ /s compared to the control-treated sample. The  $\Delta A$ /s observed were  $3.63 \times 10^{-05}$  to  $5.02 \times 10^{-05}$  below that of the control treatment.

The HCT116 p53 negative cells showed only a single point of significant (p<0.05) difference to the control when treated with silibinin at a concentration of 250  $\mu$ M. However, sodium oxamate induced more noticeable changes in lactate production. 250  $\mu$ M of this drug caused significant (p<0.05) changes after 3 and 4 hours of exposure, where the  $\Delta$ A/s were 4.80x10<sup>-05</sup> and 5.48x10<sup>-05</sup> compared to the control values of 4.38x10<sup>-05</sup> and 6.23x10<sup>-05</sup>. Surprisingly, this showed that at the T3 point the treated sample had a higher rate of reaction compared to the control treatments but then fell below control rates after the fourth hour. This fluctuation was seen throughout all the concentrations tested where overall minimal substantial changes were observed in lactate release following silibinin treatment.

The BxPc-3 pancreatic cell line had several points of significant change over the observation period following treatment with silibinin and sodium oxamate. The high doses (250  $\mu$ M) of each drug caused significant decreases in the mean rate of reaction at several time points. Silibinin and sodium oxamate at this concentration caused a decrease, compared to the control, after the initial hour of exposure (silibinin:5.58x10<sup>-06</sup> and sodium oxamate:7.15x10<sup>-05</sup>) and then again after 4 hours (Silibinin:1.35x10<sup>-06</sup> and sodium oxamate:1.68x10<sup>-05</sup>) compared to control treatment values of 9.53x10<sup>-06</sup> and 9.53x10<sup>-06</sup>. However, sodium oxamate also caused a drop in  $\Delta$ A/s after 3 hours of exposure (1.39x10<sup>-05</sup>). 100 $\mu$ M of silibinin was also shown to decrease  $\Delta$ A/s at T1 (4.95x10<sup>-06</sup>), T3 (1.26x10<sup>-05</sup>), and T4 (1.4x10<sup>-05</sup>) compared to control values of 9.53x10<sup>-06</sup>, 1.57x10<sup>-05</sup>, and 2.0x10<sup>-05</sup>. No other concentration of silibinin showed an effect. At T1, sodium oxamate decreased  $\Delta$ A/s at 250 $\mu$ M (7.15x10<sup>-06</sup>), 100 $\mu$ M (5.89x10<sup>-06</sup>) and 50 $\mu$ M (6.92x10<sup>-06</sup>) compared to control values of 9.53x10<sup>-06</sup> (p<0.05). 50 $\mu$ M also appeared to cause a decrease (p<0.005) at T2 (9.27x10<sup>-06</sup>) however after an additional hour (T3) it falls back within control levels.

The PSN-1 cell line (Figures 3.6D and 3.7D) showed little evidence of inhibition caused by silibinin and sodium oxamate. Silibinin had the most significant fluctuation, with some increase in rate and some decrease, from the control lactate production, with significant change at several time points across various concentrations however, only at 250  $\mu$ M after 4 hours silibinin treatment was this a reduction, where the control rate was 4.16x10 $^{-05}$  and the treated sample rate of reaction was 3.49x10 $^{-05}$ . Sodium oxamate only caused a significant decrease in reaction rate after 3-5 hours at 10  $\mu$ M treatment concentrations (p<0.05).

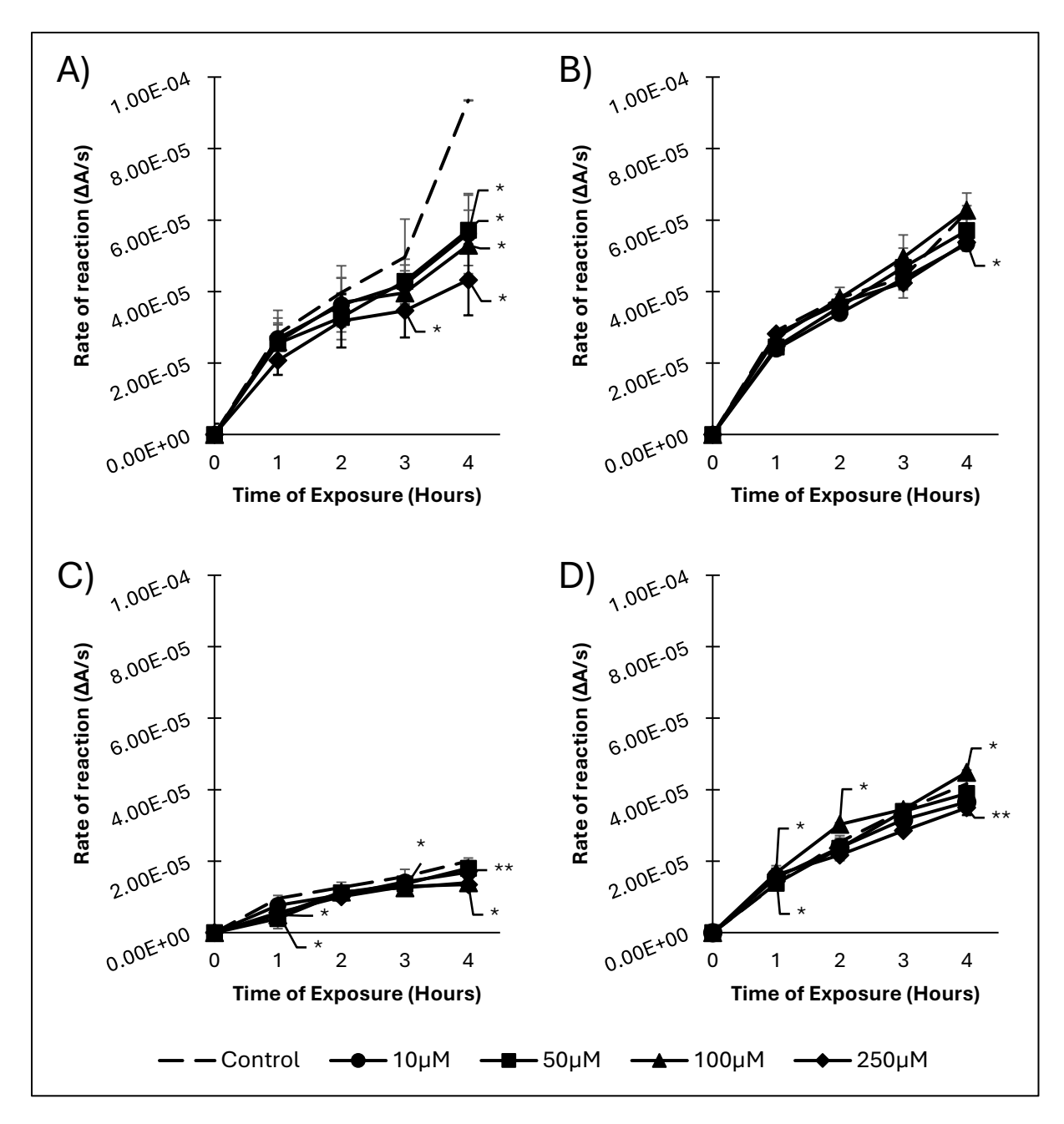


Figure 3.6 Rate of reaction of media samples taken from A) HCT116 p53 positive (+/+) B) HCT116 p53 knock down (-/-) cell C) BxPc-3 D) PSN-1cell lines over time following exposure to silibinin at a range of concentrations ( $10\mu M \bullet$ ,  $50\mu M \bullet$ ,  $100\mu M \bullet$ , and  $250\mu M \bullet$ ) compared to a negative control. Error bars show standard error of the mean across biological triplicates (n=3). Significance difference to the control is calculated by single tail paired T test where \*=P<0.05 \*\*=P<0.005.

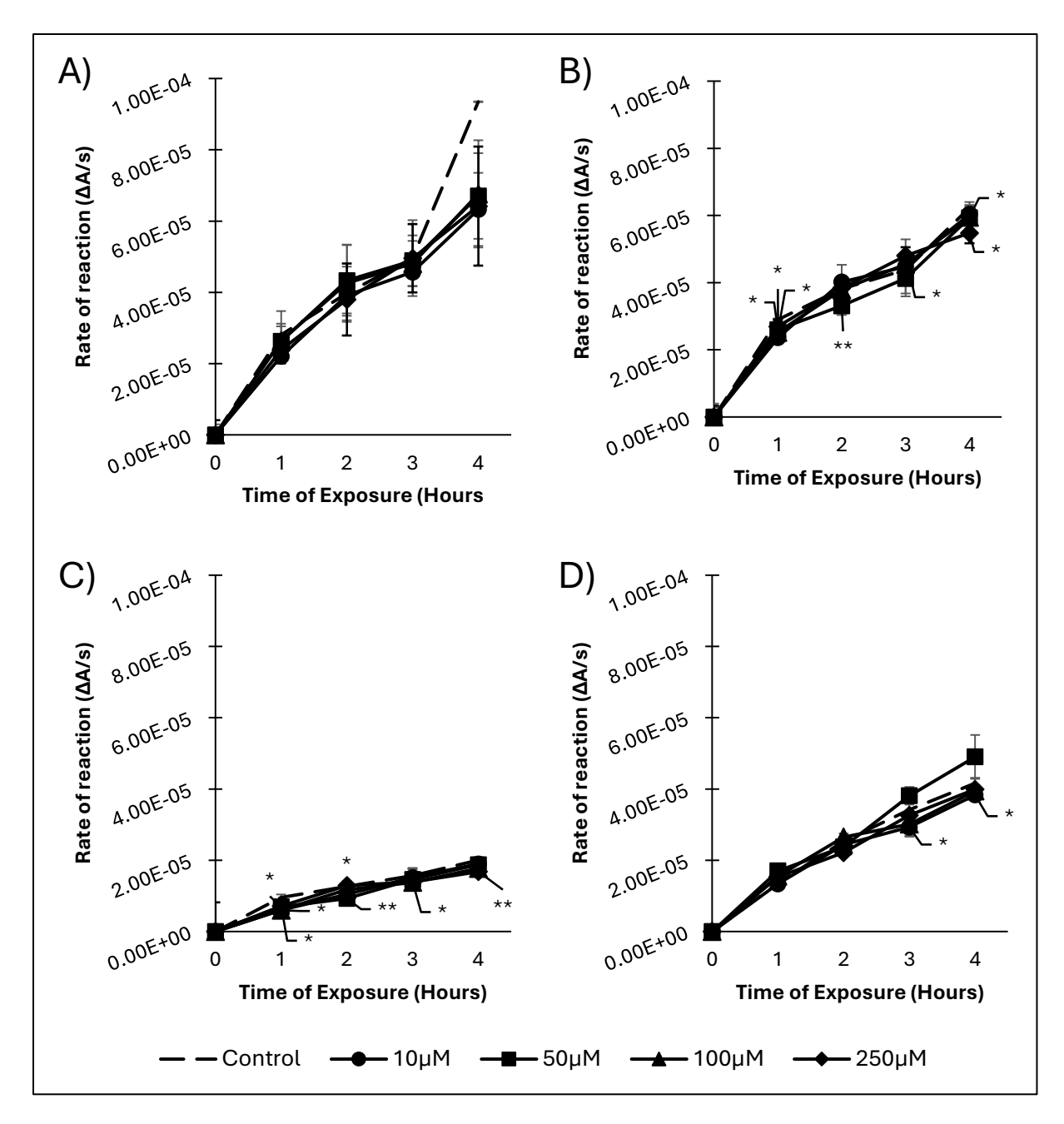


Figure 3.7 Rate of reaction of media samples taken from A) HCT116 p53 positive (+/+) B) HCT116 p53 knock down (-/-) cell C) BxPc-3 D) PSN-1cell lines over time following exposure to sodium oxamate at a range of concentrations ( $10\mu M \bullet$ ,  $50\mu M \bullet$ ,  $100\mu M \bullet$ , and  $250\mu M \bullet$ ) compared to a negative control. Error bars show Standard error of mean across biological triplicates. Significance difference to the control is calculated by single tail paired T test where \*=P<0.05 \*\*=P<0.005.

#### 3.4. Conclusion

The lactate study has identified several key features. The most prominent being that the novel silver organometallic compounds significantly reduced lactate production in a panel of cancer cells. A significant change to enzyme activity in the lactate detection assay was observed at lower drug concentrations than seen for the known glycolytic inhibitors, silibinin and sodium oxamate, indicating a strong potential for clinical use. From the three novel Ag-NHCs evaluated, the Ag8 and HA266 inhibitors were the most potent at suppressing lactate release, followed by HA197, with HA266 demonstrating a linear dose-response profile. The impact of these compounds on cell growth was investigated further.

# 4. Novel silver organometallic compounds reduce cancer cell viability.

#### 4.1. Introduction to Cell Viability Assays

To investigate the chemotherapeutic effects of these novel compounds, cell viability assays were carried out to assess their potential clinical value. The study quantifies the cell viability changes via a resazurin reaction in colorectal and pancreatic cancer cell lines following exposure to the novel silver organometallic compounds (Ag8, HA197, and HA266) and several comparative drugs (silibinin, sodium oxamate, and cisplatin). The study also investigated the effects oof the various compounds on the cell viability of a non-cancerous primary human cell line (pHFF) to assess the drugs selectivity towards cancer cell lines.

Following this viability study, the novel compounds were assessed during co-treatment with cisplatin as a form of combination therapy to determine if this approach provided a more favourable outcome compared to cisplatin alone.

#### 4.2. Cytotoxicity Studies

To investigate the cytotoxic effects of the novel silver complexes, a resazurin assay was performed on various cell lines and cell viability determined after a 48-hour treatment. Both cancerous (pancreatic and colorectal) and normal control cell lines were investigated to ascertain any increased sensitivity and selectivity of the compounds towards cancer cell lines. In addition, silibinin and sodium oxamate were again included as controls due to their role as known LDH inhibitors. Cisplatin was also included as a control organometallic chemotherapeutic.

Figure 4.1 shows the survival of cells following 48-hour exposure to variable concentrations of both novel silver organometallic compounds (Ag8, HA197, and HA266) and several controls. The controls include a chemotherapeutic control (cisplatin) and two LDH inhibitors (sodium oxamate and silibinin). Cell viability was measured via a resazurin assay and displayed as a percent survival compared to a negative control treatment. Across all cell lines, the LDH inhibitor sodium oxamate showed no cell death across all tested concentrations with all values being ≥100% of the control values. All other drugs show dose-dependent cell death/reduced cell viability.

Figure 4.1A shows the viability of HCT116 p53 positive (+/+) cells after treatment. The data showed that at the lowest concentration tested ( $50\mu M$ ) all silver organometallic compounds and silibinin caused some cell death. Cell survival observed at  $50\mu M$  were: Ag8 (15.77%), HA197 (86.76%), HA266 (63.07%), and silibinin (61.74%). Cell survival decreased in a non-linear pattern as concentration increases. At  $250\mu M$  Cisplatin also causes significant cell death with a cell survival of 36.02%. Table 4.1 shows the IC50 of these drugs calculated from the cell survival. Ag8 has the lowest IC50 of  $44.8\mu M$  followed by HA266 ( $110.8\mu M$ ), HA197 ( $128.8\mu M$ ), silibinin ( $150.5\mu M$ ), and then cisplatin ( $226.0\mu M$ ).

Figure 4.1B shows the viability of HCT116 p53 knock down (-/-) cells after treatment. Similar to the P53 positive line, this cell line showed a reduction in cell survival following treatment with all silver organometallic compounds at  $50\mu$ M (Between 42.16% and 91.35% survival) as well as silibinin (81.27% survival) and cisplatin only causing significant cell death (46.48% survival) at 250  $\mu$ M. The IC<sub>50</sub> values of these compounds (Table 4.1) were as follows: Ag8 94.8 $\mu$ M, HA197 119.2 $\mu$ M, HA266, HA197 104.7 $\mu$ M, cisplatin 277.7 $\mu$ M, and silibinin 173.6 $\mu$ M.

BxPc-3 exhibited limited cell death at  $50\mu M$  (Figure 4.1C). Treatment with Ag8 reduced cell viability to 24.88% with silibinin only reducing cell viability to 85% of control treatment values. No other

investigated compounds caused cell death at this concentration. At  $100\,\mu\text{M}$  HA266 showed significant cell death, with 31.27% cell survival observed, whereas HA197 only marginally reduced cell survival to 84.34%. At 250  $\mu$ Mall drugs, except for sodium oxamate, caused cell death with the silver organometallic compounds causing near complete cell death with a cell survival between 4.74% and 5.08%. Silibinin and cisplatin supported slightly higher cell survival of 20.92% and 28.66% respectively. The IC50 s of the compounds in BxPc-3 cells ranged from 45.9 $\mu$ M to 207.6 $\mu$ M with the silver organometallic compounds having the lowest IC50 values.

The data plotted in Figure 4.1D shows the cell survival of HFF, a non-cancerous cell line, following treatment. Similar to the pancreatic cell line, pHFF only showed a reduced cell survival following treatment with two of the three silver organometallic compounds at  $50\,\mu\text{M}$ : Ag8 (10.13%) and HA266 (58.06%). At  $100\,\mu\text{M}$  both HA197 and cisplatin started showing a reduction in cell survival, which became more significant at  $250\,\mu\text{M}$  where minimal cell survival was observed of 10.88% and 38.53%.

For all cell lines, IC $_{50}$  values of the drugs is shown in table 4.1. Overall, Ag8 had the lowest IC50 across all cell lines with an average IC50 of 53.75  $\mu$ M. This was followed by HA197 (89.75  $\mu$ M) and HA266 (107  $\mu$ M). The control compounds silibinin and cisplatin had the highest average IC $_{50}$  values of at 233.5  $\mu$ M and 188.5  $\mu$ M. This data supports exploring Ag8 further as a potential anti-cancer chemotherapeutic.

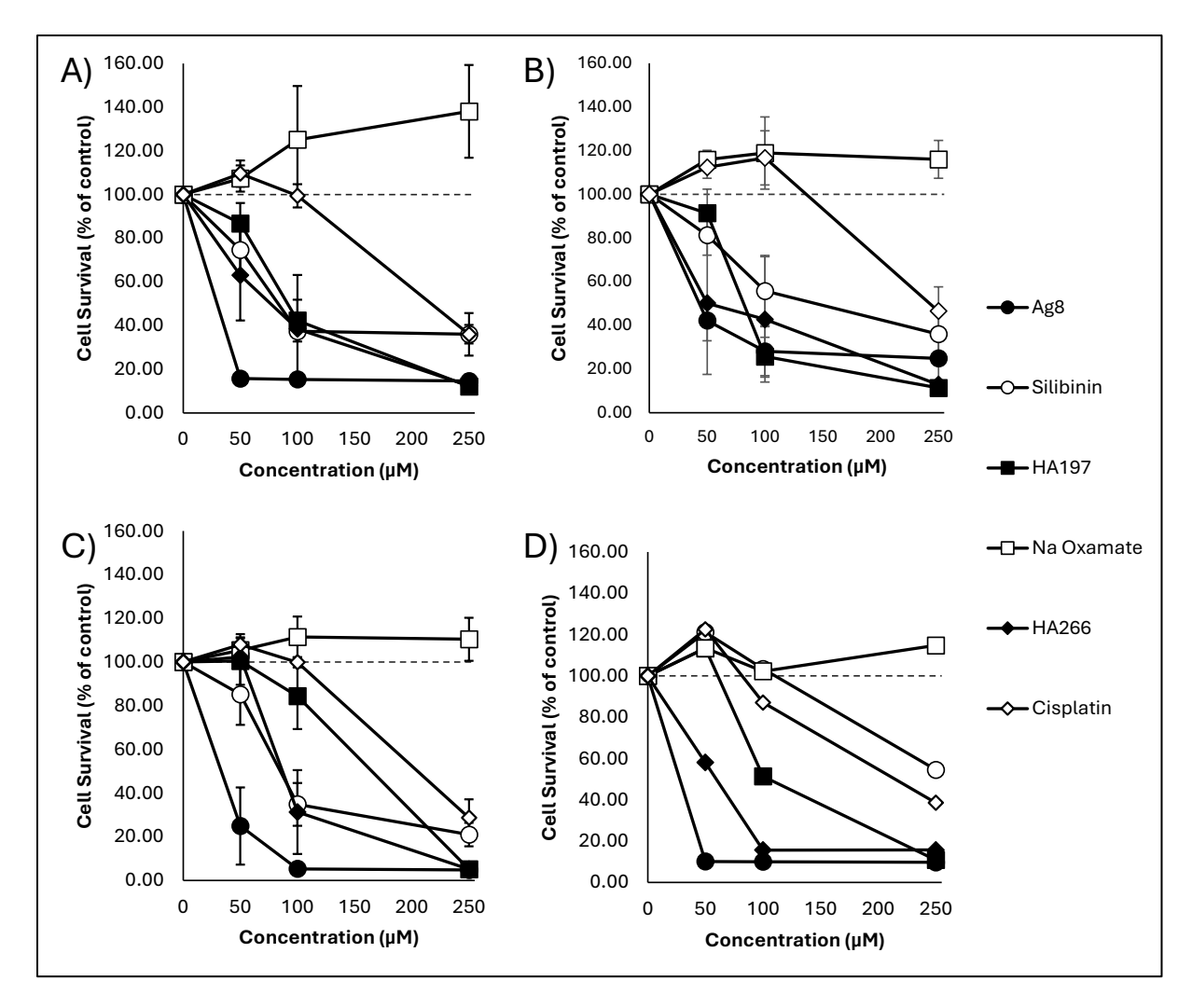


**Figure 4.1** Cell survival of **A)** HCT116 p53 positive (+/+) **B)** HCT116 p53 knock down (-/-) cell **C)** BxPc-3 **D)** HFF-1cell lines following 48 hours exposure to Ag8, HA197, HA266, silibinin, sodium (Na) oxamate, and cisplatin at a range of concentrations ( $50\mu M$ ,  $100\mu M$ , and  $250\mu M$ ) relative to a negative control. Error bars show standard error of across mean from 3 independent replicates (n=3) for all but the HFF-1 cell line which was a single biological sample (n=1).

**Table 4.1:** IC50 of investigated compounds which showed cytotoxic properties (Ag8, HA197, HA266, cisplatin, and silibinin) on a set of cell lines (HCT116 p53 positive (+/+), HCT116 p53 knock down (-/-), BxPc-3, and HFF-1). The linear equation for the line of best fit, used to calculate the IC<sub>50</sub>, and the calculated IC<sub>50</sub> values are displayed for each cell line and drug combination.

Drug/Cell line	Cytotoxicity-Trendline: Y=MX+C	IC <sub>50</sub> (μM)
Ag8		
HCT116 p53 positive (+/+)	Y=0.2456x + 38.997	44.80049
HCT116 p53 knock down (-/-)	Y=0.2395x + 27.286	94.83925
BxPc-3	Y=0.301x + 3618	45.89369
HFF-1	Y=0.2586x + 41.68	32.1732
HA197		
HCT116 p53 positive (+/+)	Y=0.3577x + 3.9284	128.7996
HCT116 p53 knock down (-/-)	Y=0.3679x + 6.1289	119.2473
BxPc-3	Y=0.4074x + 13.204	90.3191
HFF-1	Y=0.401x - 9.0033	22.4521
HA266		
HCT116 p53 positive (+/+)	Y=0.3225x + 14.256	110.8341
HCT116 p53 knock down (-/-)	Y=0.3021x + 18.37	104.7004
BxPc-3	Y=0.4101x - 0.6578	123.5255
HFF-1	Y=0.3014x + 22.51	91.2077
Cisplatin		
HCT116 p53 positive (+/+)	Y=0.2879x - 15.059	225.9778
HCT116 p53 knock down (-/-)	Y=0.347x - 18.586	277.6761
BxPc-3	Y=0.3171x - 15.815	207.5528
HFF-1	Y=0.2957x-16.26	225.316
Silibinin		
HCT116 p53 positive (+/+)	Y=0.2379x + 14.204	150.466
HCT116 p53 knock down (-/-)	Y=0.2478x + 6.9907	173.5646
BxPc-3	Y=0.3177x + 8.0146	132.1542
HFF-1	Y=0.255x - 17.299	299.107

#### 4.3. Chemosensitivity Studies

The use of the novel silver organometallic compounds as unique chemotherapeutics was investigated as single agents in the cytotoxicity studies, however there is also potential for their use in combination treatments. Next, the change in chemosensitivity of cisplatin was determined across a range of concentrations ( $10\mu M$ ,  $50\mu M$ ,  $100\mu M$ , and  $250\mu M$ ), following the addition of a single concentration of each novel silver organometallic compound (Ag8, HA197, or HA266). The concentration of the novel Ag-NHC compounds selected for use in combination with cisplatin was selected as the concentration which showed the least cytotoxic response as a monotherapy. These concentrations were well below the IC<sub>50</sub> values calculated from figure 4.1.

As seen in Figure 4.2, each cell line examined showed a concentration-dependent in chemosensitivity to cisplatin. Cell viability below the relative control value (expressed as 100%) indicated an increase in cell death caused by the co-treatment of cisplatin with the specified silver organometallic compound. Across all cell lines, Ag8 showed the most substantial effect in all but one treatment combination ( $10\mu$ M cisplatin in BxPc-3 cells). Figure 4.2A shows the change in chemosensitivity of the HCT116 p53 positive cell line. Ag8 in combination treatment with  $10\mu$ M of Ag8 reduced cell viability from 88-94% when cisplatin concentration was above  $50\mu$ M and a 49% reduction at  $10\mu$ M treatment. This response was also evident in HCT116 p53 negative (Figure 4.2B) and PSN-1 (Figure 4.2D) cells. The PSN-1 cell line appeared particularly sensitive to combination therapy, where cell viability was not seen above 5.2% at any of the cisplatin concentrations tested, consistent with chemosensitisation provided by Ag-NHCs. In the HCT116 -/- cell line, viability decreased below 40% of the respective cisplatin-only treatment values. At the higher concentrations of cisplatin (50-250 $\mu$ M), there was a strong potentiation effect with cell viability reducing to 9.7%, 8.1%, and 12.4% of monotherapy values, respectively.

Both HA197 and HA266 had a more limited effect on the colorectal and pancreatic cell lines examined. HA197 only produced a significant increase in chemosensitivity (reduction in cell viability) within the PSN-1 pancreatic cancer line. At 10μM of cisplatin a cell viability of only 19.7% of the cisplatin alone viability was seen, with the response more prominent at higher doses of cisplatin. For example, the viability dropped to only 4.6% at 50 µM, where it remained across the 50-250 µM cisplatin concentration range tested. In the same cell line, HA266 also produced a significant change but only at the higher cisplatin concentrations, where 100µM saw cell viability drop to 50.3% of cisplatin-only values and 250µM produced a decrease of 96.3% (i.e., almost complete non-viable cells remaining). These changes were highly significant achieving P<0.05 and P<0.005, respectively. The effects of HA197 and HA266 appeared less dose-dependent in the colorectal cell lines. HA197 produced a significant change in the HCT166 positive line viability at 10µM and 100µM of cisplatin whereas HA266 only showed significance at  $10\mu M$  and  $50\mu M$  on the HCT116 negative cell line. This difference may indicate a p53-dependant response to co-treatment. Similarly, the PSN-1 cell line, which has a loss of only one p53 allele, also showed an improved response to this treatment. In contrast, figure 4.2C also shows that despite some changes observed in cell viability, no significant difference in chemosensitivity to cisplatin was seen upon co-treatment with any Ag-NHC within the BxPc-3 cell line.

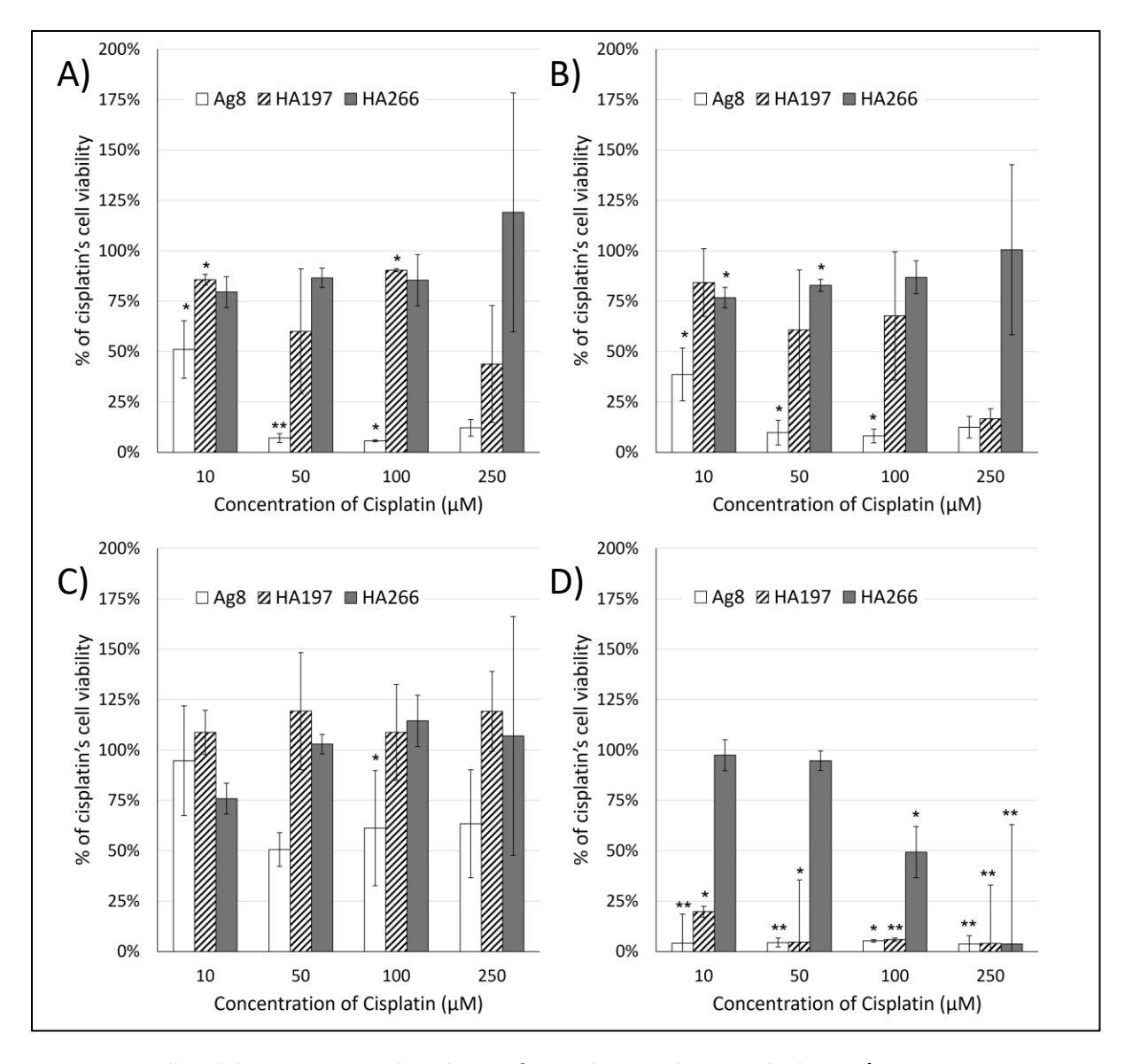


**Figure 4.2** Cell viability represented as the % of a cisplatin-only control where **A)** HCT116 p53 positive (+/+) **B)** HCT116 p53 knock down (-/-) cell **C)** BxPc-3 **D)** PSN-1 cell lines are exposed to a 48 hours cotreatment of Ag8 (10μM), HA266 (10μM), or HA197 (50μM) with cisplatin at a range of concentrations (10μM, 50μM, 100μM, and 250μM) and the control of cisplatin only at the same concentration. Error bars show the standard error of triplicate biological replicates (n=3). The columns show the mean viability of biological triplicate data of cisplatin in combination with Ag8 (white), HA197 (dashed), and HA266 (grey). Significant difference to the single-treatment cisplatin control values were calculated by performing a single tail paired T test where \*=P<0.05 \*\*=P<0.005.

#### 4.4. Conclusion

This study has shown that the novel compounds investigated produced a significant decrease in cell viability in all cell lines over the concentrations tested, with cells appearing most sensitive to Ag8. The study demonstrated that the comparative established glycolytic inhibitors had a far smaller effect on cell line viability than the novel Ag-NHC compounds. The study also established that the cellular responses to the well-characterised chemotherapeutic cisplatin were greatly enhanced by cotreatment with the novel compounds. However, this finding should be viewed with caution due to the reduced cellular sensitivity (IC<sub>50</sub>) observed for cisplatin alone compared to previously reported concentrations.

The co-treatment study indicates that for cisplatin treatment, the addition of these novel compounds, particularly Ag8 as a sensitising compound may improve clinical outcomes compared to treatment with cisplatin alone. The results also demonstrated that the novel compounds HA197 and HA266, showed greater impact on the cell lines with p53 loss of function. This suggests these compounds could be explored for clinical benefit in cancers where p53 is mutated, suppressed or lost. However, the cellular response of pHFF cells to the compounds, where they were generally more sensitive (lower IC50 values) than the cancer cells, may limit the clinical utility of the compounds in their current form and further investigation is warranted.

## 5. Discussion

## 5.1 Inhibition of lactate release by novel organometallic compounds

### 5.1.1 Optimisation of LDH activity/lactate assay

#### Determination of sample size

The LDH activity assay used in this study to determine cellular lactate release was a variation of the method published by Seidemann (1973) and then later adapted by Hass et al., (2024). The optimisation of this assay for this study identified several features in the method that needed to be adapted which have been investigated in figure 3.1. The determination of an optimised sample volume was carried out via spectrophotometry of assays with variable volumes of a 10mM lactate stock. The data identified two key features. The first, within the volume range recommended in previous studies; as sample volume increases the recorded rate of reaction at 340nm decreases. This is seen in both the PBS-based control and DMEM-based media samples. The likely cause of this is that the reactants in the assay buffer are a rate limiting factor at this concentration meaning that a relative reduction in the buffer reagents (specifically LDH and NAD\*) leads to a reduced rate of reaction when larger sample volumes and smaller reactant (assay) volumes are added. As such, one of the lower concentration volumes was chosen to be used in further investigations. 20 µL was chosen as a significant change was not seen between it and the lower volumes tested. This enabled a high rate of reaction to be generated, while still including sufficient sample to provide a representative result for the lactate within the entire culture media volume. Secondly, this investigation showed a significant (p<0.005) change between the control solvent and the media solvent.

#### Serum interference

To further investigate the effect of the sample solvent, a study was carried out comparing the absorbance of samples at a range of lactate concentrations prepared in different solvents (PBS, DMEM, and DMEM with FBS) after 1 hour of reaction. The data shows a significant increase in absorbance caused by the addition of FBS to DMEM when compared to the DMEM alone and PBS control samples. This effect is most prominent at lower concentrations of lactate as seen in figure 3.1B. The samples containing FBS exhibited a base level of absorbance which indicated a strong background signal from the serum, interfering with the assay's sensitivity. At 16mM this sample had an absorbance at 340nm of 1.5. As the concentration decreased, this value fell to 1.4 at 0.5mM within the FBS-containing DMEM samples, compared to the larger changes seen in the samples without FBS, which fell from 1 to 0.3 at the same concentration range, consistent with the changes observed within the PBS controls. Also of note, is that FBS contains LDH at a substantial concentration. ThermoFisher Scientific and MP Biomedicals FBS contains 556 IU/L of LDH. This LDH in the sample derived from FBS will increase the overall concentration within the assay and potentially altering the rate of reaction to reduce the sensitivity and accuracy of the assay (Thomas *et al.*, 2015; Nonnis *et al.*, 2016).

#### Sample stability

The stability of the lactate within the media samples used in this study was determined as this would impact the scale at which replicates could be gathered. Due to the long run time of the assay, a limited number of runs could be carried out in a single day. However, if samples displayed a high stability, then biological replicates could be taken on one day but assayed on later days. This would mean less limitations in the scale of testing which was otherwise limited by the growth rate of cells in culture. To investigate this possibility, technical replicates of a samples were taken and tested on different days; the day the sample was taken, the following day, and the fourth day post-collection. Samples were taken from cells following a media change and every subsequent 2 hours for a total of 6 hours. Samples

were stored in  $3-10^{\circ}$ C fridges to reduce degradation. The data showed a significant (p<0.005) reduction in the rate of reaction from sample day to 1 day storage post-collection as shown in figure 3.1C. This fall indicates significant degradation of the sample over time, implying that short-term sample storage at  $4^{\circ}$ C was not an option. Consequently, all testing was done on the day of sample collection.

Lactate is generally considered stable in cool conditions; however, it is possible that other components in the extracellular media could have degraded affecting the stability of the lactate. It is also possible that the trace LDH in the sample, released via damage to cell membranes (Kumar, Nagarajan and Uchil, 2018) caused the lactate to be converted to pyruvate while in storage leading to a reduced lactate concentration. In this study, freezing and thawing the samples was not investigated due to concerns of degradation caused by the thawing process. However, this could be examined in future studies, as lactate has been shown previously to be stable for several freeze-thaw cycles in media supernatant (Grist *et al.*, 2018).

#### Optimisation of run time

In determining the rate of reaction of samples taken, the change in absorbance over time must be measured. To do this consistently throughout the length of the study a set time must be used. This was investigated in figure 3.1D in which the rate of reaction of several samples of known lactate concentration were tested and the rate of reaction calculated from different data from different assay times. The data showed that while the shorter time period produced the greatest rate of reaction, the longer tests produced results that established a more linear relationship between the rate of reaction and the concentration of lactate with the samples. The linearity of this study is key in maintaining accuracy at which lactate concentrations can be determined based on the rate of reaction. Therefore, a longer timed assay of 1 hour was selected for all subsequent reactions (Kaja *et al.*, 2015).

## 5.1.2 Lactate release study

#### Mono layer vs high density suspension

To investigate the effect that the novel compounds have on extracellular lactate release, the developed LDH activity assay has been utilised. This assay quantifies the rate of production of NADH from the conversion of lactate to pyruvate in the presence of LDH as a measure of initial lactate content within extracellular media. Samples were taken at hourly time intervals following exposure to drugs at a range of concentrations. The rate of reaction at each time point was compared to a respective negative control (untreated or solvent-only treated cell media samples) to identify any change over time caused by drug exposure. In this study two methods for sample collection were investigated. Initially, monolayer cultures were used to procure the media samples during the testing. It was later decided to move toward a high-density model that did not allow for a monolayer to form. This allowed for a greater number for cells to be present in a similar media volume which improved consistency in the data generated, enhanced throughput, and improved repeatability. As growth of cancer cells is deregulated, the rate of proliferation and the glycolytic demand can be irregular leading to significant fluctuations in lactate production over time (Heiden, Cantley and Thompson, 2009; Burns et al., 2021). By increasing the cell count, and scaling down the culture size (i.e., moving from a 6-well to 96-well format), the sample size was effectively increased allowing for a more representative mean. The monolayer culture also had the substantial drawback of limited cellular metabolism at high confluence reducing lactate production at high cell confluence because of altered growth rate and contactdependent inhibition (Gal et al., 1981).

#### Reference inhibitors

The reference inhibitors used in this study, silibinin and sodium oxamate, were selected due to their glycolytic inhibiting properties. Due to the precise mechanisms of the novel compounds being unknown, compounds affecting different aspects of cellular lactate production where selected. In this study, both these compounds underperformed in comparison to the novel silver organometallic compounds. Although both compounds have been shown to reduce to reduce cellular lactate production and LDH activity in previous studies using both pancreatic and colorectal cell lines (Colturato et al., 2012; Awasthi et al., 2019; Bai et al., 2022; Malvi et al., 2022), this was not replicated in this study.

There are several possibilities for this finding. Firstly, there has not been a wide range of studies using these compounds in this culture model and therefore it is possible that their enzyme inhibition is ineffective within this high-density suspension (Gal *et al.*, 1981). Additionally, the concentrations used in this study were based on the appropriate dosage for the novel silver organometallic compounds. While studies have used similar inhibitor concentrations and demonstrated significant inhibition, it may be that in this model a higher dosage is needed to obtain similar results (Colturato *et al.*, 2012; Awasthi *et al.*, 2019). This was not investigated in this study as the aim was simply to compare their efficacy at the same concentration as the novel compounds. Regardless, this study has shown that the novel silver organometallic compounds consistently and significantly reduced extracellular lactate in the colorectal and pancreatic cell lines examined.

#### p53-dependent effects

Both wild type HCT116 and a p53 knock down cell line were investigated in this study. This allowed any p53 dependency of treatment responses to the novel silver organometallic compounds to be identified. This study has shown that the p53 negative cell line had greater variation from the control following treatment compared to the wildtype cell line. As a p53 allele has been lost in this mutated version, greater metabolic dysregulation is to be expected (Marbaniang and Kma, 2018). It is therefore possible that inhibition of metabolism had a greater impact within the p53 positive cell line, which has less severe glycolytic dysregulation caused by the p53 gene (Han *et al.*, 2015; Yeung *et al.*, 2019). Similar data has been seen in previous studies in which LDH-A was inhibited and lactate accumulation in the medium was reduced. In this LDH-A inhibition study, HCT116 p53-/- had a greater fold change in NADH/NAD+ ratio compared to the p53+/+ cell line following treatment (Allison *et al.*, 2014).

#### Pancreatic vs colorectal cell lines

Overall, the novel silver organometallic compounds inhibited lactate release in all the cell lines tested, however the dose and time point at which this was achieved varied. The most consistent trend was that the compounds inhibited lactate release at a lower Ag-NHC concentration in the pancreatic cell line than in the colorectal cell lines.

A possible cause of this decreased sensitivity of the colorectal cell lines is the cancers more robust antioxidant systems. As a key element of silver-based (indeed most organometallic-based) treatments is the promotion of ROS, where an overactive antioxidant system would support the cancers survival and limit inhibition (Narayana et al., 2024). A previous study investigated the change in antioxidant enzyme activity following treatment with capsaicin and showed that colorectal lines had a significant increase in the activity of superoxide dismutase enzyme, with the greatest observed increase in the HCT116 line specifically (Hormozi and Baharvand, 2025). This increase in antioxidant response has been identified as a compensatory defence system seen in cells with increased oxidative stress markers (Sulaiman et al., 2025).

Another potential cause of this difference in sensitivity between cancer types is membrane receptor expression which alters the cells uptake of a given compound (Barbalinardo *et al.*, 2025). Pancreatic cell lines have been shown to have an increased transferrin receptor expression which has been shown to support ROS production in PDAC cells (Jeong, Hwang and Seong, 2016).

#### 5.1.3 Conclusion

The investigated lactate studies have shown that the novel Ag-NHCs have some potential as glycolytic inhibitors in both pancreatic and colorectal cancers, particularly in p53-compromised cell lines. The study has shown that concentrations as low as  $10\,\mu\text{M}$  of the compounds produce a significant decrease in the rate of reaction indicating a reduction in extracellular lactate release. The variance in results obtained by the different silver compounds indicates the influence of the compound structures (Table 1.1) in regulating the uptake, retention, and cellular sensitivity of the silver compounds and their intracellular mechanisms of action. One such structurally significant factor may be the inclusion of hydroxyl groups on the compound structures. Ag8 has no hydroxyl subunit, HA197 has a single hydroxyl group, and HA266 has two. This structural subunit has been identified as changing a compounds membrane permeability (Nakamura *et al.*, 2018). To investigate this further, it will be critical to analyse other markers of glycolytic activity and cellular proliferation for an impact on lactate release following Ag-NHC treatment. Cellular glucose and oxygen consumption processes would be likely candidates for further study. Furthermore, the effect of Ag-NHC compounds on cell viability and proliferation will be explored below.

# 5.2 Novel silver organometallic compounds reduce cancer cell viability

## 5.2.1 Cytotoxicity study

#### Summary of findings

Investigation of the novel silver organometallic compounds efficacy in the reduction of cancer cell viability was carried out via a resazurin assay. Cell viability was determined following cell exposure to the novel compounds or relevant controls for 48 hours. The data clearly showed that the novel silver organometallic compounds investigated all caused a reduction in cell viability following 48 hours exposure in all cell lines investigated. The  $IC_{50}$  values of the novel silver organometallic compounds were lower than all control drugs investigated, with Ag8 having the lowest half-maximal inhibitory concentration across all cell lines investigated (as seen in table 4.1). Of the three known compounds investigated, sodium oxamate was the only one to show no reduction in the viability of the investigated cell lines. This compound has been shown to be a competitive LDH-A inhibitor which leads to the suppression of cell viability and energy metabolism in nasopharyngeal, breast, and hepatocellular cancer (Fiume  $et\ al.$ , 2010; Zhai  $et\ al.$ , 2013). However, the  $IC_{50}$  values of sodium oxamate in CNE-1 and CNE-2 human nasopharyngeal carcinoma cells were reported as 3.6 and 4.8 mM (Altinoz and Ozpinar, 2022), a concentration far greater than that of this study. Overall, this data is supportive of the novel silver organometallic compounds having an increased efficacy compared to several currently accepted inhibitors of glycolysis.

Silibinin, another widely accepted glycolysis inhibitor, was also investigated. Previously, it has been shown to cause a reduction in cell viability of several tumour types including hepatic, pancreatic, and colorectal cancer. This is consistent with the findings of this study, where silibinin produced similar IC<sub>50</sub> values in related cell lines (Raina *et al.*, 2015; Shukla *et al.*, 2015; Vakili Zahir *et al.*, 2018). Silibinin functions as a non-specific enzyme inhibitor, affecting key glycolytic enzymes such as hexokinase II, 6-phosphofructokinases, and pyruvate kinase (Iqbal *et al.*, 2021).

Cisplatin, a widely used chemotherapeutic was also compared in this study. Cisplatin binds to DNA forming a monoadduct resulting in the inhibition of replication and transcription, impairing the cell cycle and inducing cell death (Belmonte-Fernández et al., 2022). Cisplatin is known to have a low IC<sub>50</sub> in most cancers, including the BxPc-3 cell line, where it was reported to have an IC50 of  $5.96\pm2.32\mu$ M (Muscella et al., 2024), which is significantly lower than the 207.55  $\mu$ M seen in this study. One reason for the high IC<sub>50</sub> seen in this study, could be due to cisplatin interaction with DMSO, which was used as the solvent to resuspend the drug in. Cisplatin can bind with DMSO to form a DMSO adduct, where the resulting compound has been shown to have a reduced affinity to DNA in vitro, reducing its efficacy in causing cell death (Fischer et al., 2008; Raghavan, Cheriyamundath and Madassery, 2015).

#### Colorectal vs pancreatic sensitivity

This study explored the impact of these drugs on both pancreatic and colorectal cell lines. Due to the varied nature of these cells, having different source tissues, genetic mutations, and development processes, the cell lines were shown to have different sensitivities to the treatments. Here, the pancreatic cell line BcPc-3 was the most sensitive to Ag8 and HA197, but not HA266, displaying their lowest  $IC_{50}$  values in this cell line. This suggests that these novel glycolytic and lactate inhibiting compounds are more efficient at causing cell death against BxPc-3 specifically.

BxPc-3 cells have a unique genetic makeup compared to most other pancreatic cell lines, as it contains a wildtype *KRAS* gene and not a more commonly occurring mutated form, such as G12C or G12D mutation. This unmutated gene variant is relatively unique to BxPc-3 cells compared to other pancreatic cells lines and other cancers, such as the colorectal cancer cell line, HCT116 (Metildi *et al.*, 2013). The *KRAS* gene product is the signalling protein K-ras, which plays a major role in the mitogenactivated protein kinase (MAPK) pathway. This signalling cascade uses an activated from of the Ras protein, following extracellular signalling, to activate Raf which is then used in a phosphorylation cascade to activate MEK and then the MAPK, ERK1/2, which subsequently translocates to the nucleus and activates transcription factors controlling cellular proliferation (Bonni *et al.*, 1999; Bahar, Kim and Kim, 2023). Mutations in the *KRAS* oncogene dysregulate this process often resulting in overactivation of the cascade, leading to rapid uncontrolled proliferation and enhancement of cellular survival (De Roock *et al.*, 2010).

As mentioned above, the colorectal cell line HCT116 investigated in this study, has a mutation in its *KRAS* gene - the G13D (c.38D>A) mutation (Alves *et al.*, 2015). Studied have shown that this mutation leads to increased proliferation with only partial sensitivity to investigated chemotherapeutics, such as cetuximab, noted in the study by De Roock et al. (2010). From this it could be assumed that this dysregulation may contribute to the reduced sensitivity of HCT166 cells to the novel silver organometallic compounds Ag8 and HA197 shown in this study. As this reduced sensitivity cannot be seen in the HA266 cell lines, it is possible that this compound is able to avoid this KRAS gained resistance though a mechanism that likely involves the MAPK pathway.

#### P53 sensitivity

Two variants of the colorectal carcinoma HCT116 cell line were investigated in this study in which the p53 gene was either wildtype (p53 positive) or a truncated version (p53 negative). This difference in p53 status enabled the impact of p53 expression and functionality to be assessed on the therapeutic potential of the novel compounds. The p53 protein is a critical component in cancer development as it is a key tumour suppressor gene responding to DNA damage to promote cell cycle arrest or apoptosis. It has a wide variety of functional mechanisms which allow it to carry out this role, including as a transcriptional *trans*activator and regulator of mitochondrial function. In glycolysis, p53 is capable to both inhibit and promote the process depending on cellular need. In cancer, when functioning properly, p53 can downregulate glycolysis and promote oxidative phosphorylation acting against the Warburg effect preventing the rapid production of ATP as seen in cancer (Zhang, Qin and Wang, 2010b; Puzio-Kuter, 2011; Liang, Liu and Feng, 2013).

The down regulation of glycolysis caused by functional p53 genes in cancer allows cells to resist/limit the effect of the deregulated metabolism hallmark mechanism. This "head start" in inhibiting glycolysis supports the findings of this study, where p53 positive cell lines were generally more sensitive to several drug treatments (Figures 3.3 to 3.7). Ag8, cisplatin, and silibinin all have lower IC $_{50}$ s in the p53 positive cell lines with Ag8 having the most significant change with a 52.7% reduction of IC $_{50}$ s in the positive line compared to the p53 negative variant. In each case, both the drugs and the p53 mechanisms appear to be working in tandem to provide a more substantial decrease in viability. However, the novel HA197 and HA266 compounds did not fit into this trend. Following treatment with these compounds the p53 knockdown cell lines had the lower IC $_{50}$ , although this change was smaller than most other compounds. This suggests that the activity of these compounds may be less p53-dependant, and the drugs may function more effectively in tumours where p53 gene is inactivated or mutated.

#### Cancerous vs non-cancerous sensitivity

In this study, the cell viability of HFF-1 cells following treatment was also investigated. These cells were used to compare the sensitivity of cancerous and non-cancerous cells to the novel compounds. This data showed significant cell death in the non-cancerous cell line caused by the novel compounds. This high sensitivity can be seen in the calculated IC50 values in table 3.1 where Ag8 had a IC $_{50}$  of 32.17µM, HA197 had 22.45µM, and HA266 was 91.21µM. In contrast pHFF-1 were less sensitive to the comparative compounds, cisplatin and silibinin, which are an established chemotherapeutic and glycolysis inhibitor, respectively. This high sensitivity of the HFF-1 cell line indicated a poor selective toxicity in which normal cells would likely be damaged alongside, or at a faster rate, than the expected target cancer cells (Berrouet *et al.*, 2020; González-Larraza *et al.*, 2020). Improving the cell selectivity or enhancing the targeting of the novel Ag-NHCs to tumours (i.e., through encapsulation or conjugation to antibodies) will be required to translate the compounds into the clinic.

### 5.2.2 Chemosensitivity study

#### Summary of findings

This study showed the change in cell viability of the colorectal cell lines, HCT116+/+ and -/-, and the pancreatic cell lines, PSN-1 and BxPc-3, following co-treatment with cisplatin at a range of concentrations (10-250 $\mu$ M) in combination with each novel silver organometallic compound; Ag8 (10 $\mu$ M), HA197 (50 $\mu$ M), and HA266 (10 $\mu$ M). The study aimed to investigate the potential clinical benefits of combining a DNA damage-inducing chemotherapeutic, cisplatin, with a glycolytic interfering compound. By simultaneously targeting these different proliferation and survival pathways, a reduction in the chemotherapeutic resistance due to upregulation of anaerobic glycolysis (i.e., the Warburg effect) may be mitigated. The concentration of the novel silver compounds was selected as the concentration at which they caused minimal cell death as a monotherapy (see figure 4.1). This allowed any observed increase in cytotoxicity when combined with cisplatin, compared to cisplatin alone, to be attributed to an enhancement of cisplatin's activity, rather than independent effects of the individual silver compound.

The main trend observed was as the concentration of cisplatin increased, the adjuvant cotreatment produced a greater decrease in cell viability compared to cisplatin monotherapy.

- Ag8 proved to be the most effective adjunct, notably in HCT116 (both p53+ and p53-) and PSN-1 cells. In HCT116 p53+ cells, the inclusion of Ag8 caused a reduction in cell viability by 49% when co-administered with 10μM cisplatin, with further decreases to below 13% of the control observed at higher concentrations. The HCT116 p53-/- cell line followed a similar trend, but with an even greater change at 10μM cisplatin, were a decrease from the control of 61.4% was evident. PSN-1 cells showed exceptional sensitivity, maintaining viability below 5.2% of the control, across all cisplatin doses when co-treated with Ag8.
- HA197 showed significant but selective enhancement, primarily in PSN-1 cells. It lowered cell viability to 19.7% at  $10\mu$ M cisplatin co-treatment and 4.6% at  $50\mu$ M cisplatin, with minimal further decreases in viability observed at higher doses primarily due to most cells having died (<5% viability). This suggests that a lower dose of cisplatin could be used and should be investigated in further studies.
- HA266 had more modest effects at lower concentrations of cisplatin, showing statistically significant differences in PSN-1 viability in the co-treatments only at 100μM and 250μM cisplatin concentrations, with reductions in cell viability of 50.3% and 96.3%, respectively. Interestingly, BxPc-3 cells exhibited minimal response to any combination, underscoring cell-type variability.

Overall, these findings support Ag8 as a strong candidate for use as an adjunct to chemotherapy, while HA197 and HA266 may offer selective benefits dependent on tumour profile and p53 status.

#### Significance of data

The statistical analysis used in this study was a single-tailed paired T test to identify if the co-treatment arm showed a significant change compared to cisplatin on its own. Some data in which had a visibly large difference in mean viability, did not reach significance of p<0.05, which makes it harder to say with confidence what trends can be identified from this study. This is most likely due to the small sample size of the study with only triplicate data being obtained. A larger sample size may help to improve the reproducibility and reliability of the data, reduce the variance impact, and enable significance to be determined with greater confidence.

#### PSN-1 KRAS mutation

Within this study, the PSN-1 cell line was shown to be the most sensitive to the co-treatment, exhibiting the greatest change in cell viability from the cisplatin only and negative control treatments across most inhibitor combinations and cisplatin concentrations. PSN-1 is a pancreatic cell line with a key characteristic of having a loss of function p53 allele, with a K132R point mutation in the remaining allele (Hobbs et al., 2019; Maki et al., 2025). The significance of this being in p53's role in the regulation of cellular proliferation. When one allele is lost and the only remaining gene has been mutated, such as in PSN-1, it significantly limits the cells' ability to regulate growth leading to rapid proliferation increasing the cellular energy demand and thus increasing cellular lactate release from glycolysis. In contrast to the BxPc-3 pancreatic cell line, the PSN-1 line also has the G12R KRAS mutation, whereas the BxPc-3 cell line is wild-type for KRAS. The KRAS mutation seen in the PSN-1 cell line is often attributed to increased cell survival due to its role in driving uncontrolled cell proliferation (Zhang et al., 2023). This increase in cell proliferation requires an increased rate of energy production in cancer cells often caused by an increase in anaerobic glycolysis (Ying et al., 2012). It can be assumed that the role of the novel silver organometallics as an inhibitor/limiter of this process assists in the co-treatment of this cell lines, where it limits the cells growth rate. This may reduce the resistance to cell death and increase the chemosensitivity to cisplatin.

#### p53 dependency

When comparing the data within each cancer type, it becomes clear that for each cancer, the cell lines with the greatest inhibition of the p53 gene were the most sensitive to the treatments performed in this study. This is the HCT116 -/- cell line which expresses a substantially truncated, functionally inactive, p53 gene, and the PSN-1 cell line which has a loss of a p53 allele and a mutation in the other rendering it inactive (Rivlin et al., 2011; Dsouza, Jain and Khattar, 2024). Due to p53's key role in tumour suppression, the loss of p53 functionality will often increase a cancers survival. However, in this study we have shown an increase in the sensitivity of these normally resistant cells to cisplatin with cotreatment (Lew et al., 2023; Miciak et al., 2025). This data suggests that treatment of novel silver glycolytic inhibitor compounds improves the chemotherapeutic potential of cisplatin against p53 mutated cancer cell lines which would otherwise have an increased chance of resistance. This data supports the earlier findings from the single drug cell viability studies (figures 3.3 to 3.7), that the novel Ag-NHC compounds tended to have a greater effect on the cell lines with inactive p53, and thus may be beneficial in clinical settings where the p53 pathway is inactivated in many human cancers.

#### Ag8 in cisplatin co-treatment

Throughout this study, the co-treatment of cisplatin with the silver organometallic compound Ag8 outperformed all other drug combinations at all but one cisplatin concentration (10 µM in the BxPc-3

cell line where HA226 had the greatest decrease in viability). The high sensitivity to the cisplatin and Ag8 combination treatment is a strong indicator for its potential clinical use.

## 6. General conclusion

This study explored the effectiveness of three novel silver organometallic compounds on cancer cell viability and lactate production in a selection of pancreatic and colorectal cancer cell lines. Several key findings were identified: all three Ag-NHCs are able to suppress lactate release, efficacy is cell-line dependant, the novel compounds do not display an increased selectivity for cancer cells, and Ag8 improves the sensitivity and cytotoxic effect of cisplatin upon co-treatment.

In the investigation of lactate inhibition, it was found that the novel silver organometallic compounds reduced the concentration of extracellular lactate to a greater significance at lower dosage than the known glycolytic inhibitors, silibinin and sodium oxamate. The study has shown that at concentrations as low as  $10\mu M$ , a reduction in the rate of reaction, equating to extracellular lactate, can be significantly reduced over a 4-hour period with particular sensitivity of pancreatic cell lines. While colorectal cancer cells lines were also affected, the change observed was not as substantive. This is likely due to the more robust antioxidant defence system of colorectal cancer cells. This strongly supports ROS upregulation as a key mechanism of the Ag-NHC in lactate inhibition — a mechanism of action that will be explored in future studies. This project also identified p53 as a key regulator in this process, influencing the efficacy of the treatment, where cells with a compromised p53 pathway were more sensitive to Ag-NHCs. The structure of the novel compounds was also shown to impact their effect, as demonstrated by the variation in lactate inhibition and viability changes observed between the three different novel Ag-NHC compounds. A factor in this is the different number of hydroxyl groups in each structure likely effecting cell membrane permeability.

In the investigation of cytotoxicity, there was significant variance between cell lines responses, both within and between cell lines, dependent on tissue origins. Generally, the pancreatic cell lines were more sensitive than the colorectal cell lines with lower IC $_{50}$  values exhibited. Within the colorectal cell line studies, the p53 positive cell line was more sensitive to activation of cell death. Unfortunately, the cytotoxicity studies also showed that cell death was not cancer cell specific, with the pHFF-1 cell line being the most sensitive to the novel Ag-NHCs, overall. This indicates poor selectivity of these compounds for cancer cells, potentially limiting their therapeutic potential in their current forms. However, this interpretation is partially limited by the origin of the pHFF-1 cell line. As these cells are fibroblasts, they may be more sensitive to the particular mechanisms of the silver compounds. Fibroblasts are actively involved in extracellular matrix production and wound healing, which often requires higher metabolic activity making them more vulnerable to drugs impairing ATP production (Lemons *et al.*, 2010). Fibroblasts also have been identified as more susceptible to ROS-induced apoptosis (Balin, Allen and Reimer, 1988). An investigation of further non-cancerous cell lines may support this work.

When investigated as a co-treatment with cisplatin, the novel silver compounds were shown to significantly increase the cellular sensitivity to the cisplatin. All cell lines investigated were shown to have the greatest change in sensitivity when treated with Ag8. Combination therapy with Ag8 consistently reduced cancer cell viability when compared to cisplatin treatment monotherapy, at a Ag8 concentration that did not produce significant cell death. These results imply Ag8 potentially acts as a chemosensitiser for cisplatin therapy, where the combination approach dramatically improved the cellular anti-cancer outcomes.

Overall, this study has shown that Ag-NHCs are strong inhibitors of extracellular lactate in the investigated cell lines. They lead to significant cell death in vitro and they improved the sensitivity of cancer cells to chemotherapeutics. The investigation showed a clear reduction in LDH activity through

the lactate detection assay and produced significant cell death in both single and co-treatment settings. The data may support ROS upregulation via release of Ag<sup>+</sup> ions into the cell as the key mechanism of action leading to these results. Further investigation into clarifying the mechanisms of action, improving the selectivity, enhancing the efficacy, and exploring other glycolytic markers is warranted to determine the full clinical potential for these novel silver organometallic compounds.

## 7.Bibliography

Alexander, J. W. (2009) 'History of the medical use of silver', *Surgical infections*, 10(3), pp. 289–292. doi: 10.1089/SUR.2008.9941.

Alfarouk, K. O. *et al.* (2014) 'Glycolysis, tumor metabolism, cancer growth and dissemination. A new pH-based etiopathogenic perspective and therapeutic approach to an old cancer question', *Oncoscience*, 1(12), p. 777. doi: 10.18632/ONCOSCIENCE.109.

Allison, S. J. *et al.* (2014) 'Identification of LDH-A as a therapeutic target for cancer cell killing via (i) p53/NAD(H)-dependent and (ii) p53-independent pathways', 3, p. 102. doi: 10.1038/oncsis.2014.16.

Altenberg, B. and Greulich, K. O. (2004) 'Genes of glycolysis are ubiquitously overexpressed in 24 cancer classes', *Genomics*, 84(6), pp. 1014–1020. doi: 10.1016/J.YGENO.2004.08.010.

Altinoz, M. A. and Ozpinar, A. (2022) 'Oxamate targeting aggressive cancers with special emphasis to brain tumors', *Biomedicine and Pharmacotherapy*, 147. doi: 10.1016/j.biopha.2022.112686.

Alves, S. et al. (2015) 'Colorectal cancer-related mutant KRAS alleles function as positive regulators of autophagy', Oncotarget, 6(31), p. 30787. doi: 10.18632/ONCOTARGET.5021.

Atiyeh, B. S. *et al.* (2007) 'Effect of silver on burn wound infection control and healing: review of the literature', *Burns : journal of the International Society for Burn Injuries*, 33(2), pp. 139–148. doi: 10.1016/J.BURNS.2006.06.010.

Awasthi, D. et al. (2019) 'Glycolysis dependent lactate formation in neutrophils: A metabolic link between NOX-dependent and independent NETosis', *Biochimica et Biophysica Acta (BBA) - Molecular Basis of Disease*, 1865(12), p. 165542. doi: 10.1016/J.BBADIS.2019.165542.

Bahar, M. E., Kim, H. J. and Kim, D. R. (2023) 'Targeting the RAS/RAF/MAPK pathway for cancer therapy: from mechanism to clinical studies', *Signal Transduction and Targeted Therapy 2023 8:1*, 8(1), pp. 1–38. doi: 10.1038/s41392-023-01705-z.

Bai, Y. et al. (2022) 'Silibinin Therapy Improves Cholangiocarcinoma Outcomes by Regulating ERK/Mitochondrial Pathway', Frontiers in Pharmacology, 13. doi: 10.3389/FPHAR.2022.847905/PDF.

Balin, A. K., Allen, R. G. and Reimer, R. (1988) 'Human Fibroblast Antioxidant Defense Response to Alteration in Oxygen Tension', *Basic life sciences*, 49, pp. 707–711. doi: 10.1007/978-1-4684-5568-7\_112.

Barbalinardo, M. *et al.* (2025) 'Differential Cytotoxicity of Surface-Functionalized Silver Nanoparticles in Colorectal Cancer and Ex-Vivo Healthy Colonocyte Models', *Cancers 2025, Vol. 17, Page 1475*, 17(9), p. 1475. doi: 10.3390/CANCERS17091475.

Basu, A. K. (2018) 'DNA Damage, Mutagenesis and Cancer', *International journal of molecular sciences*, 19(4). doi: 10.3390/IJMS19040970.

Belmonte-Fernández, A. *et al.* (2022) 'Cisplatin-induced cell death increases the degradation of the MRE11-RAD50-NBS1 complex through the autophagy/lysosomal pathway', *Cell Death & Differentiation 2022 30:2*, 30(2), pp. 488–499. doi: 10.1038/s41418-022-01100-1.

Berrouet, C. *et al.* (2020) 'Comparison of Drug Inhibitory Effects (IC50) in Monolayer and Spheroid Cultures', *Bulletin of mathematical biology*, 82(6), p. 68. doi: 10.1007/S11538-020-00746-7.

Biller, L. H. and Schrag, D. (2021) 'Diagnosis and treatment of metastatic colorectal cancer: A review', JAMA - Journal of the American Medical Association, 325(7), pp. 669–685. doi: 10.1001/JAMA.2021.0106,.

Böhme, M. D. *et al.* (2022a) 'Synthesis of N-Heterocyclic Carbenes and Their Complexes by Chloronium Ion Abstraction from 2-Chloroazolium Salts Using Electron-Rich Phosphines', *Angewandte Chemie (International Ed. in English)*, 61(28). doi: 10.1002/ANIE.202202190.

Böhme, M. D. *et al.* (2022b) 'Synthesis of N-Heterocyclic Carbenes and Their Complexes by Chloronium Ion Abstraction from 2-Chloroazolium Salts Using Electron-Rich Phosphines', *Angewandte Chemie - International Edition*, 61(28). doi: 10.1002/ANIE.202202190.

Bonni, A. *et al.* (1999) 'Cell Survival Promoted by the Ras-MAPK Signaling Pathway by Transcription-Dependent and -Independent Mechanisms', *Science*, 286(5443), pp. 1358–1362. doi: 10.1126/SCIENCE.286.5443.1358.

Bourissou, D. *et al.* (2000) 'Stable Carbenes', *Chemical reviews*, 100(1), pp. 39–91. doi: 10.1021/CR940472U.

Brandt, O. et al. (2012) 'Nanoscalic silver possesses broad-spectrum antimicrobial activities and exhibits fewer toxicological side effects than silver sulfadiazine', *Nanomedicine*: nanotechnology, biology, and medicine, 8(4), pp. 478–488. doi: 10.1016/J.NANO.2011.07.005.

Bray, F. et al. (2024) 'Global cancer statistics 2022: GLOBOCAN estimates of incidence and mortality worldwide for 36 cancers in 185 countries', CA: A Cancer Journal for Clinicians, 74(3), pp. 229–263. doi: 10.3322/CAAC.21834.

Brenner, H., Kloor, M. and Pox, C. P. (2014) 'Colorectal cancer', *The Lancet*, 383(9927), pp. 1490–1502. doi: 10.1016/S0140-6736(13)61649-9.

Browne, N. et al. (2014) 'Assessment of in vivo antimicrobial activity of the carbene silver(I) acetate derivative SBC3 using Galleria mellonella larvae', Biometals: an international journal on the role of metal ions in biology, biochemistry, and medicine, 27(4), pp. 745–752. doi: 10.1007/S10534-014-9766-Z.

Burns, J. E. *et al.* (2021) 'The Warburg effect as a therapeutic target for bladder cancers and intratumoral heterogeneity in associated molecular targets', *Cancer Science*, 112(9), pp. 3822–3834. doi: 10.1111/CAS.15047,.

Cancer incidence for common cancers | Cancer Research UK (no date). Available at: https://www.cancerresearchuk.org/health-professional/cancer-statistics/incidence/common-cancers-compared#heading-Zero (Accessed: 6 March 2025).

Cancer mortality for common cancers | Cancer Research UK (no date). Available at: https://www.cancerresearchuk.org/health-professional/cancer-statistics/mortality/common-cancers-compared#heading-Zero (Accessed: 6 March 2025).

Colturato, C. P. et al. (2012) 'Metabolic effects of silibinin in the rat liver', *Chemico-Biological Interactions*, 195(2), pp. 119–132. doi: 10.1016/J.CBI.2011.11.006.

Conroy, T. et al. (2011) 'FOLFIRINOX versus Gemcitabine for Metastatic Pancreatic Cancer', New England Journal of Medicine, 364(19), pp. 1817–1825. doi: 10.1056/NEJMOA1011923/SUPPL\_FILE/NEJMOA1011923\_DISCLOSURES.PDF.

Dekker, E. *et al.* (2019) 'Colorectal cancer', *Lancet (London, England)*, 394(10207), pp. 1467–1480. doi: 10.1016/S0140-6736(19)32319-0.

Drake, P. L. and Hazelwood, K. J. (2005) 'Exposure-related health effects of silver and silver compounds: a review', *The Annals of occupational hygiene*, 49(7), pp. 575–585. doi: 10.1093/ANNHYG/MEI019.

Dsouza, R., Jain, M. and Khattar, E. (2024) 'p53-deficient cancer cells hyperactivate DNA double-strand break repair pathways to overcome chemotherapeutic damage and augment survival', *Molecular Biology Reports*, 52, p. 333. doi: 10.1007/s11033-025-10434-1.

Eloy, L. *et al.* (2012) 'Anticancer activity of silver-N-heterocyclic carbene complexes: caspase-independent induction of apoptosis via mitochondrial apoptosis-inducing factor (AIF)', *ChemMedChem*, 7(5), pp. 805–814. doi: 10.1002/CMDC.201200055.

Fischer, S. J. *et al.* (2008) 'Cisplatin and dimethyl sulfoxide react to form an adducted compound with reduced cytotoxicity and neurotoxicity', *NeuroToxicology*, 29(3), pp. 444–452. doi: 10.1016/J.NEURO.2008.02.010.

Fish, R. H. and Jaouen, G. (2003) 'Bioorganometallic chemistry: Structural diversity of organometallic complexes with bioligands and molecular recognition studies of several supramolecular hosts with biomolecules, alkali-metal ions, and organometallic pharmaceuticals', *Organometallics*, 22(11), pp. 2166–2177. doi: 10.1021/OM0300777/ASSET/IMAGES/MEDIUM/OM0300777N00001.GIF.

Fiume, L. *et al.* (2010) 'Impairment of Aerobic Glycolysis by Inhibitors of Lactic Dehydrogenase Hinders the Growth of Human Hepatocellular Carcinoma Cell Lines', *Pharmacology*, 86(3), pp. 157–162. doi: 10.1159/000317519.

Gal, D. *et al.* (1981) 'Effect of Cell Density and Confluency on Cholesterol Metabolism in Cancer Cells in Monolayer Culture1', *CANCER RESEARCH*, 41, pp. 473–477. Available at: http://aacrjournals.org/cancerres/article-pdf/41/2/473/2409564/cr0410020473.pdf (Accessed: 15 July 2025).

Garrison, J. C. and Youngs, W. J. (2005) 'Ag(I) N-heterocyclic carbene complexes: Synthesis, structure, and application', *Chemical Reviews*, 105(11), pp. 3978–4008. doi: 10.1021/CR050004S/ASSET/CR050004S.FP.PNG\_V03.

González-Larraza, P. G. *et al.* (2020) 'IC50 Evaluation of Platinum Nanocatalysts for Cancer Treatment in Fibroblast, HeLa, and DU-145 Cell Lines', *ACS Omega*, 5(39), p. 25381. doi: 10.1021/ACSOMEGA.0C03759.

Grist, J. T. et al. (2018) 'Extracellular Lactate: A Novel Measure of T Cell Proliferation', *The Journal of Immunology*, 200(3), pp. 1220–1226. doi: 10.4049/JIMMUNOL.1700886.

Guan, X. (2015) 'Cancer metastases: challenges and opportunities', *Acta Pharmaceutica Sinica B*, 5(5), pp. 402–418. doi: 10.1016/J.APSB.2015.07.005.

Gurunathan, S. *et al.* (2014) 'Enhanced antibacterial and anti-biofilm activities of silver nanoparticles against Gram-negative and Gram-positive bacteria', *Nanoscale research letters*, 9(1), pp. 1–17. doi: 10.1186/1556-276X-9-373.

Halbrook, C. J. *et al.* (2023) 'Pancreatic cancer: Advances and challenges', *Cell*, 186(8), pp. 1729–1754. doi: 10.1016/j.cell.2023.02.014.

Hamidi, H. and Ivaska, J. (2018) 'Every step of the way: integrins in cancer progression and metastasis', *Nature reviews. Cancer*, 18(9), pp. 533–548. doi: 10.1038/S41568-018-0038-Z.

Han, X. *et al.* (2015) 'Evaluation of the anti-tumor effects of lactate dehydrogenase inhibitor galloflavin in endometrial cancer cells', *Journal of Hematology and Oncology*, 8(1), pp. 1–4. doi: 10.1186/S13045-014-0097-X/FIGURES/2.

Hanahan, D. and Weinberg, R. A. (2000) 'The hallmarks of cancer', *Cell*, 100(1), pp. 57–70. doi: 10.1016/S0092-8674(00)81683-9.

Hanahan, D. and Weinberg, R. A. (2011a) 'Hallmarks of cancer: the next generation', *Cell*, 144(5), pp. 646–674. doi: 10.1016/J.CELL.2011.02.013.

Hanahan, D. and Weinberg, R. A. (2011b) 'Hallmarks of cancer: The next generation', *Cell*, 144(5), pp. 646–674. doi: 10.1016/J.CELL.2011.02.013,.

Haque, R. A. *et al.* (2015) 'Synthesis, crystal structures, characterization and biological studies of nitrile-functionalized silver(I) N-heterocyclic carbene complexes', *Inorganica Chimica Acta*, 433, pp. 35–44. doi: 10.1016/J.ICA.2015.04.023.

Hartinger, C. G. and Dyson, P. J. (2009) 'Bioorganometallic chemistry--from teaching paradigms to medicinal applications', *Chemical Society reviews*, 38(2), pp. 391–401. doi: 10.1039/B707077M.

Hass, D. T. *et al.* (2024) 'Acetyl-CoA carboxylase inhibition increases retinal pigment epithelial cell fatty acid flux and restricts apolipoprotein efflux', *Journal of Biological Chemistry*, 300(10), p. 107772. doi: 10.1016/J.JBC.2024.107772/ASSET/FD92A6CD-2617-4B27-B842-5EE1DAFC2811/MAIN.ASSETS/FIGS5.JPG.

Heiden, M. G. V., Cantley, L. C. and Thompson, C. B. (2009) 'Understanding the warburg effect: The metabolic requirements of cell proliferation', *Science*, 324(5930), pp. 1029–1033. doi: 10.1126/SCIENCE.1160809,.

Herrmann, W. A. (2002) 'N-heterocyclic carbenes: a new concept in organometallic catalysis - PubMed'. Available at: https://pubmed.ncbi.nlm.nih.gov/19750753/ (Accessed: 16 July 2024).

Hindi, K. M. *et al.* (2008) 'Synthesis, stability, and antimicrobial studies of electronically tuned silver acetate N-heterocyclic carbenes', *Journal of medicinal chemistry*, 51(6), pp. 1577–1583. doi: 10.1021/JM0708679.

Hindi, K. M. *et al.* (2009) 'The medicinal applications of imidazolium carbene-metal complexes', *Chemical reviews*, 109(8), pp. 3859–3884. doi: 10.1021/CR800500U.

Hirschhaeuser, F., Sattler, U. G. A. and Mueller-Klieser, W. (2011) 'Lactate: a metabolic key player in cancer', *Cancer research*, 71(22), pp. 6921–6925. doi: 10.1158/0008-5472.CAN-11-1457.

Hobbs, G. A. *et al.* (2019) 'Atypical KRASG12R Mutant Is Impaired in PI3K Signaling and Macropinocytosis in Pancreatic Cancer', *Cancer discovery*, 10(1), p. 104. doi: 10.1158/2159-8290.CD-19-1006.

Hopkinson, M. N. *et al.* (2014) 'An overview of N-heterocyclic carbenes', *Nature*, 510(7506), pp. 485–496. doi: 10.1038/NATURE13384.

Hormozi, M. and Baharvand, P. (2025) 'The Apoptotic and Antioxidant Effects of Capsaicin on Colorectal Cancer Cell Lines', *The Open Biochemistry Journal*, 19(1). doi: 10.2174/011874091X328840250131070747,.

Hossain, M. S. *et al.* (2022) 'Colorectal Cancer: A Review of Carcinogenesis, Global Epidemiology, Current Challenges, Risk Factors, Preventive and Treatment Strategies', *Cancers 2022, Vol. 14, Page 1732*, 14(7), p. 1732. doi: 10.3390/CANCERS14071732.

Hu, X. *et al.* (2004) 'Group 11 metal complexes of N-heterocyclic carbene ligands: Nature of the metal-carbene bond', *Organometallics*, 23(4), pp. 755–764. doi: 10.1021/OM0341855/SUPPL\_FILE/OM0341855SI20031119\_060827.CIF.

Infantino, V. et al. (2021) 'Cancer Cell Metabolism in Hypoxia: Role of HIF-1 as Key Regulator and Therapeutic Target', *International journal of molecular sciences*, 22(11). doi: 10.3390/IJMS22115703.

Iqbal, M. A. *et al.* (2021) 'Silibinin induces metabolic crisis in triple-negative breast cancer cells by modulating EGFR-MYC-TXNIP axis: potential therapeutic implications', *FEBS Journal*, 288(2), pp. 471–485. doi: 10.1111/FEBS.15353;WGROUP:STRING:PUBLICATION.

Jahnke, M. C. and Ekkehardt Hahn, F. (2017) 'CHAPTER 1: Introduction to N-Heterocyclic Carbenes: Synthesis and Stereoelectronic Parameters', *RSC Catalysis Series*, 2017-January(27), pp. 1–45. doi: 10.1039/9781782626817-00001.

Jeong, S. M., Hwang, S. and Seong, R. H. (2016) 'Transferrin receptor regulates pancreatic cancer growth by modulating mitochondrial respiration and ROS generation', *Biochemical and Biophysical Research Communications*, 471(3), pp. 373–379. doi: 10.1016/j.bbrc.2016.02.023.

Johnson, N. A., Southerland, M. R. and Youngs, W. J. (2017) 'Recent Developments in the Medicinal Applications of Silver-NHC Complexes and Imidazolium Salts', *Molecules (Basel, Switzerland)*, 22(8). doi: 10.3390/MOLECULES22081263.

Kaja, S. *et al.* (2015) 'An optimized lactate dehydrogenase release assay for screening of drug candidates in neuroscience', *Journal of pharmacological and toxicological methods*, 73, p. 1. doi: 10.1016/J.VASCN.2015.02.001.

Kartalou, M. and Essigmann, J. M. (2001) 'Mechanisms of resistance to cisplatin', *Mutation Research - Fundamental and Molecular Mechanisms of Mutagenesis*, 478(1–2), pp. 23–43. doi: 10.1016/S0027-5107(01)00141-5.

Khorrami, S. *et al.* (2018) 'Selective cytotoxicity of green synthesized silver nanoparticles against the MCF-7 tumor cell line and their enhanced antioxidant and antimicrobial properties', *International journal of nanomedicine*, 13, pp. 8013–8024. doi: 10.2147/IJN.S189295.

Kiri, S. and Ryba, T. (2024) 'Cancer, metastasis, and the epigenome', *Molecular Cancer*, 23(1). doi: 10.1186/S12943-024-02069-W,.

Kumar, P., Nagarajan, A. and Uchil, P. D. (2018) 'Analysis of cell viability by the lactate dehydrogenase assay', *Cold Spring Harbor Protocols*, 2018(6), pp. 465–468. doi: 10.1101/PDB.PROT095497,.

De Lange, G. *et al.* (2023) 'Complete mesocolic excision for right hemicolectomy: an updated systematic review and meta-analysis', *Techniques in Coloproctology*, 27(11), pp. 979–993. doi: 10.1007/S10151-023-02853-8,.

Lansdown, A. B. G. (2010) 'A pharmacological and toxicological profile of silver as an antimicrobial agent in medical devices', *Advances in pharmacological sciences*, 2010. doi: 10.1155/2010/910686.

Lemons, J. M. S. *et al.* (2010) 'Quiescent Fibroblasts Exhibit High Metabolic Activity', *PLoS Biol*, 8(10), p. 1000514. doi: 10.1371/journal.pbio.1000514.

Lew, T. E. et al. (2023) 'Treatment approaches for patients with TP53-mutated mantle cell lymphoma', The Lancet Haematology, 10(2), pp. e142–e154. doi: 10.1016/S2352-3026(22)00355-6.

Liang, X. et al. (2018) 'Recent advances in the medical use of silver complex', European journal of medicinal chemistry, 157, pp. 62–80. doi: 10.1016/J.EJMECH.2018.07.057.

Liang, Y., Liu, J. and Feng, Z. (2013) 'The regulation of cellular metabolism by tumor suppressor p53', *Cell and Bioscience*, 3(1), pp. 1–10. doi: 10.1186/2045-3701-3-9/METRICS.

Liberti, M. V. and Locasale, J. W. (2016a) 'The Warburg Effect: How Does it Benefit Cancer Cells?', *Trends in biochemical sciences*, 41(3), p. 211. doi: 10.1016/J.TIBS.2015.12.001.

Liberti, M. V. and Locasale, J. W. (2016b) 'The Warburg Effect: How Does it Benefit Cancer Cells?', *Trends in Biochemical Sciences*, 41(3), pp. 211–218. doi: 10.1016/J.TIBS.2015.12.001.

Liberti, M. V. and Locasale, J. W. (2016c) 'The Warburg Effect: How Does it Benefit Cancer Cells?', *Trends in biochemical sciences*, 41(3), p. 211. doi: 10.1016/J.TIBS.2015.12.001.

Liu, W. and Gust, R. (2013) 'Metal N-heterocyclic carbene complexes as potential antitumor metallodrugs', *Chemical Society reviews*, 42(2), pp. 755–773. doi: 10.1039/C2CS35314H.

Liu, Z. et al. (2023) 'Unravelling the enigma of siRNA and aptamer mediated therapies against pancreatic cancer', *Molecular Cancer*, 22(8). doi: 10.1186/s12943-022-01696-5.

Maki, R. et al. (2025) 'Efficacy of SOAT1 Inhibitors Against Pancreatic Cancer with TP53 Mutations', Annals of Surgical Oncology. doi: 10.1245/s10434-025-17482-8.

Malvi, P. et al. (2022) 'Transcriptional, chromatin, and metabolic landscapes of LDHA inhibitor—resistant pancreatic ductal adenocarcinoma', *Frontiers in Oncology*, 12. doi: 10.3389/FONC.2022.926437/PDF.

Mar Kolbeinsson, H. *et al.* (2023) 'Pancreatic Cancer: A Review of Current Treatment and Novel Therapies', *Journal of Investigative Surgery*, 36(1), p. 2129884. doi: 10.1080/08941939.2022.2129884.

Marbaniang, C. and Kma, L. (2018) 'Dysregulation of glucose metabolism by oncogenes and tumor suppressors in cancer cells', *Asian Pacific Journal of Cancer Prevention*, 19(9), pp. 2377–2390. doi: 10.22034/APJCP.2018.19.9.2377,.

Matsuda, T., Fujimoto, A. and Igarashi, Y. (2025) 'Colorectal Cancer: Epidemiology, Risk Factors, and Public Health Strategies', *Digestion*, 106(2), pp. 91–99. doi: 10.1159/000543921,.

McKeown, S. R. (2014) 'Defining normoxia, physoxia and hypoxia in tumours-implications for treatment response', *The British journal of radiology*, 87(1035). doi: 10.1259/BJR.20130676.

Medici, S. et al. (2019) 'Medical Uses of Silver: History, Myths, and Scientific Evidence', Journal of medicinal chemistry, 62(13), pp. 5923–5943. doi: 10.1021/ACS.JMEDCHEM.8B01439.

De Mello, M. R. S. P. *et al.* (2020) 'Clinical evaluation and pattern of symptoms in colorectal cancer patients', *Arquivos de Gastroenterologia*, 57(2), pp. 131–136. doi: 10.1590/S0004-2803.202000000-24,.

Metildi, C. A. *et al.* (2013) 'In vivo serial selection of human pancreatic cancer cells in orthotopic mouse models produces high metastatic variants irrespective of Kras status', *Journal of Surgical Research*, 184(1), pp. 290–298. doi: 10.1016/J.JSS.2013.03.049.

Miciak, J. J. *et al.* (2025) 'Robust p53 phenotypes and prospective downstream targets in telomerase-immortalized human cells', *Oncotarget*, 16, pp. 79–100. Available at: www.oncotarget.comwww.oncotarget.com (Accessed: 25 June 2025).

Morris, V. K. *et al.* (2022) 'Treatment of Metastatic Colorectal Cancer: ASCO Guideline', *J Clin Oncol*, 41, pp. 678–700. doi: 10.1200/JCO.22.

Muscella, A. *et al.* (2024) 'Different Cytotoxic Effects of Cisplatin on Pancreatic Ductal Adenocarcinoma Cell Lines', *International Journal of Molecular Sciences*, 25(24), p. 13662. doi: 10.3390/IJMS252413662/S1.

Nakamura, H. *et al.* (2018) 'Effect of number of hydroxyl groups of fullerenol C60(OH)n on its interaction with cell membrane', *Journal of the Taiwan Institute of Chemical Engineers*, 90, pp. 18–24. doi: 10.1016/J.JTICE.2017.11.016.

Narayana, S. *et al.* (2024) 'Inorganic nanoparticle-based treatment approaches for colorectal cancer: recent advancements and challenges', *Journal of Nanobiotechnology*, 22(1), pp. 1–25. doi: 10.1186/S12951-024-02701-3/TABLES/1.

Nayak, S. and Gaonkar, S. L. (2021) 'Coinage Metal N-Heterocyclic Carbene Complexes: Recent Synthetic Strategies and Medicinal Applications', *ChemMedChem*, 16(9), pp. 1360–1390. doi: 10.1002/CMDC.202000836.

Niu, T. and Zhou, F. (2023) 'Inflammation and tumor microenvironment', *Zhong nan da xue xue bao. Yi xue ban = Journal of Central South University. Medical sciences*, 48(12), pp. 1899–1913. doi: 10.11817/J.ISSN.1672-7347.2023.230231.

Nolan, S. P. (2006) 'N-Heterocyclic carbenes in synthesis', p. 304. Available at: https://books.google.com/books/about/N\_Heterocyclic\_Carbenes\_in\_Synthesis.html?id=GqIpT5qYL 94C (Accessed: 16 July 2024).

Nolan, S. P. (2011) 'The development and catalytic uses of N-heterocyclic carbene gold complexes', *Accounts of chemical research*, 44(2), pp. 91–100. doi: 10.1021/AR1000764.

Nonnis, S. et al. (2016) 'Effect of fetal bovine serum in culture media on MS analysis of mesenchymal stromal cells secretome', EuPA Open Proteomics, 10, pp. 28–30. doi: 10.1016/J.EUPROT.2016.01.005.

Oehninger, L., Rubbiani, R. and Ott, I. (2013) 'N-Heterocyclic carbene metal complexes in medicinal chemistry', *Dalton transactions (Cambridge, England : 2003)*, 42(10), pp. 3269–3284. doi: 10.1039/C2DT32617E.

Öfele, K. (1968) '1,3-Dimethyl-4-imidazolinyliden-(2)-pentacarbonylchrom ein neuer übergangsmetall-carben-komplex', *Journal of Organometallic Chemistry*, 12(3). doi: 10.1016/S0022-328X(00)88691-X.

Patel, A. (2020) 'Benign vs Malignant Tumors', *JAMA Oncology*, 6(9), p. 1488. doi: 10.1001/JAMAONCOL.2020.2592,.

Patil, S. *et al.* (2011) 'Novel benzyl-substituted N-heterocyclic carbene-silver acetate complexes: synthesis, cytotoxicity and antibacterial studies', *Metallomics : integrated biometal science*, 3(1), pp. 74–88. doi: 10.1039/C0MT00034E.

Petrucciani, N. *et al.* (2020) 'Total Pancreatectomy for Pancreatic Carcinoma: When, Why, and What Are the Outcomes? Results of a Systematic Review', *Pancreas*, 49(2), pp. 175–180. doi: 10.1097/MPA.00000000001474,.

Porporato, P. E. et al. (2020) 'Lactate Beyond a Waste Metabolite: Metabolic Affairs and Signaling in Malignancy', Frontiers in Oncology | www.frontiersin.org, 10, p. 231. doi: 10.3389/fonc.2020.00231.

Puzio-Kuter, A. M. (2011) 'The Role of p53 in Metabolic Regulation', *Genes & Cancer*, 2(4), p. 385. doi: 10.1177/1947601911409738.

Raghavan, R., Cheriyamundath, S. and Madassery, J. (2015) 'Dimethyl sulfoxide inactivates the anticancer effect of cisplatin against human myelogenous leukemia cell lines in in vitro assays', *Indian Journal of Pharmacology*, 47(3), p. 322. doi: 10.4103/0253-7613.157132.

Raina, K. *et al.* (2015) 'Silibinin and colorectal cancer chemoprevention: a comprehensive review on mechanisms and efficacy', *Journal of Biomedical Research*, 30(6), p. 452. doi: 10.7555/JBR.30.20150111.

Rastogi, S. et al. (2023) 'Lactate acidosis and simultaneous recruitment of TGF- $\beta$  leads to alter plasticity of hypoxic cancer cells in tumor microenvironment', *Pharmacology and Therapeutics*, 250. doi: 10.1016/j.pharmthera.2023.108519.

Rivlin, N. *et al.* (2011) 'Mutations in the p53 tumor suppressor gene: Important milestones at the various steps of tumorigenesis', *Genes and Cancer*, 2(4), pp. 466–474. doi: 10.1177/1947601911408889.

De Roock, W. *et al.* (2010) 'Association of KRAS p.G13D Mutation With Outcome in Patients With Chemotherapy-Refractory Metastatic Colorectal Cancer Treated With Cetuximab', *JAMA*, 304(16), pp. 1812–1820. doi: 10.1001/JAMA.2010.1535.

Rosenberg, B., Van Camp, L. and Krigas, T. (1965) 'INHIBITION OF CELL DIVISION IN ESCHERICHIA COLI BY ELECTROLYSIS PRODUCTS FROM A PLATINUM ELECTRODE', *Nature*, 205(4972), pp. 698–699. doi: 10.1038/205698A0.

Russell, A. D. and Hugo, W. B. (1994) 'Antimicrobial activity and action of silver', *Progress in medicinal chemistry*, 31(C), pp. 351–370. doi: 10.1016/S0079-6468(08)70024-9.

Şahin-Bölükbaşı, S., Cantürk-Kılıçkaya, P. and Kılıçkaya, O. (2021) 'Silver(I)-N-heterocyclic carbene complexes challenge cancer; evaluation of their anticancer properties and in silico studies', *Drug development research*, 82(7), pp. 907–926. doi: 10.1002/DDR.21822.

Schatzschneider, U. and Metzler-Nolte, N. (2006) 'New Principles in Medicinal Organometallic Chemistry', *Angewandte Chemie International Edition*, 45(10), pp. 1504–1507. doi: 10.1002/ANIE.200504604.

Schwingel, J. et al. (2023) 'Early Detection of Pancreatic Cancer', Oncology Research and Treatment, 46(6), pp. 259–267. doi: 10.1159/000530790.

Seidemann, J. (1973) 'Lowry, O. H., und J. V. Passonneau: A flexible system of enzymatic analysis. Academic Press, New York, 1972. 291 S., 32 Abb., 15 Tab., Preis \$ 14.00', *Starch - Stärke*, 25(9), pp. 322–322. doi: 10.1002/STAR.19730250914.

Shcherbik, N. and Pestov, D. G. (2019) 'The Impact of Oxidative Stress on Ribosomes: From Injury to Regulation', *Cells*, 8(11), p. 1379. doi: 10.3390/CELLS8111379.

Shepherd, S. L. (2018) 'Pre-clinical Evaluation of Novel Inorganic Compounds as Potential Anticancer Therapies'.

Shie, W. Y. *et al.* (2023) 'Acidosis promotes the metastatic colonization of lung cancer via remodeling of the extracellular matrix and vasculogenic mimicry', *International Journal of Oncology*, 63(6), p. 136. doi: 10.3892/IJO.2023.5584.

Shtauffer, J. A. *et al.* (2009) 'Patient outcomes after total pancreatectomy: a single centre contemporary experience', *HPB*: *The Official Journal of the International Hepato Pancreato Biliary Association*, 11(6), p. 483. doi: 10.1111/J.1477-2574.2009.00077.X.

Shukla, S. K. *et al.* (2015) 'Silibinin-mediated metabolic reprogramming attenuates pancreatic cancer-induced cachexia and tumor growth', *Oncotarget*, 6(38), pp. 41146–41161. doi: 10.18632/ONCOTARGET.5843,.

Siddik, Z. H. (2002) 'Biochemical and molecular mechanisms of cisplatin resistance', *Cancer treatment and research*, 112, pp. 263–284. doi: 10.1007/978-1-4615-1173-1\_13.

Siddik, Z. H. (2003) 'Cisplatin: mode of cytotoxic action and molecular basis of resistance', *Oncogene*, 22(47), pp. 7265–7279. doi: 10.1038/SJ.ONC.1206933.

Siegel, R. L., Miller, K. D. and Jemal, A. (2019) 'Cancer statistics, 2019', *CA: A Cancer Journal for Clinicians*, 69(1), pp. 7–34. doi: 10.3322/CAAC.21551;PAGE:STRING:ARTICLE/CHAPTER.

Silver, S. (2003) 'Bacterial silver resistance: molecular biology and uses and misuses of silver compounds', *FEMS microbiology reviews*, 27(2–3), pp. 341–353. doi: 10.1016/S0168-6445(03)00047-0.

Sohn, T. A. *et al.* (2000) 'Resected adenocarcinoma of the pancreas —616 patients: results, outcomes, and prognostic indicators', *Journal of Gastrointestinal Surgery*, 4(6), pp. 567–579. doi: 10.1016/S1091-255X(00)80105-5.

Spencer, N. Y. and Stanton, R. C. (2019) 'The Warburg Effect, Lactate, and Nearly a Century of Trying to Cure Cancer', *Seminars in Nephrology*, 39(4), pp. 380–393. doi: 10.1016/j.semnephrol.2019.04.007.

Steve D *et al.* (2017) 'Preclinical anti-cancer activity and multiple mechanisms of action of a cationic silver complex bearing N-heterocyclic carbene ligands Original Citation'. Available at: http://eprints.hud.ac.uk/id/eprint/31921/ (Accessed: 11 July 2024).

Stoop, T. F. *et al.* (2025) 'Pancreatic cancer', *The Lancet*, 405(10485), pp. 1182–1202. doi: 10.1016/S0140-6736(25)00261-2.

Strobel, O. *et al.* (2022) 'Actual Five-year Survival after Upfront Resection for Pancreatic Ductal Adenocarcinoma: Who Beats the Odds?', *Annals of Surgery*, 275(5), pp. 962–971. doi: 10.1097/SLA.000000000004147.

Sulaiman, S. H. *et al.* (2025) 'Biochemical Insights into Oxidative Stress in Colon Cancer Patients', *Cell Biochemistry and Biophysics 2025*, pp. 1–10. doi: 10.1007/S12013-025-01827-X.

T Hass, D. and B. Hurley, J. (2023) 'Lactate Concentration assay (LDH method) v1'. doi: 10.17504/PROTOCOLS.IO.6QPVR4733GMK/V1.

Thomas, M. G. *et al.* (2015) 'The effect of foetal bovine serum supplementation upon the lactate dehydrogenase cytotoxicity assay: Important considerations for in vitro toxicity analysis', *Toxicology in Vitro*, 30(1), pp. 300–308. doi: 10.1016/J.TIV.2015.10.007.

Tialiou, A. et al. (2022) 'Current Developments of N-Heterocyclic Carbene Au(I)/Au(III) Complexes toward Cancer Treatment', Biomedicines, 10(6). doi: 10.3390/BIOMEDICINES10061417.

Vakili Zahir, N. et al. (2018) 'Evaluation of Silibinin Effects on the Viability of HepG2 (Human hepatocellular liver carcinoma) and HUVEC (Human Umbilical Vein Endothelial) Cell Lines', Iranian Journal of Pharmaceutical Research: IJPR, 17(1), p. 261.

Valvona, C. J. *et al.* (2016) 'The Regulation and Function of Lactate Dehydrogenase A: Therapeutic Potential in Brain Tumor', *Brain pathology (Zurich, Switzerland)*, 26(1), pp. 3–17. doi: 10.1111/BPA.12299.

Vaupel, P. and Multhoff, G. (2021) 'Revisiting the Warburg effect: historical dogma versus current understanding', *The Journal of physiology*, 599(6), pp. 1745–1757. doi: 10.1113/JP278810.

Vaupel, P., Schmidberger, H. and Mayer, A. (2019a) 'The Warburg effect: essential part of metabolic reprogramming and central contributor to cancer progression', *International journal of radiation biology*, 95(7), pp. 912–919. doi: 10.1080/09553002.2019.1589653.

Vaupel, P., Schmidberger, H. and Mayer, A. (2019b) 'The Warburg effect: essential part of metabolic reprogramming and central contributor to cancer progression', *International journal of radiation biology*, 95(7), pp. 912–919. doi: 10.1080/09553002.2019.1589653.

Vazquez, A. *et al.* (2010) 'Catabolic efficiency of aerobic glycolysis: The Warburg effect revisited', *BMC Systems Biology*, 4(1), pp. 1–9. doi: 10.1186/1752-0509-4-58/COMMENTS.

Vincent, A. *et al.* (2011) 'Pancreatic cancer', *The Lancet*, 378(9791), pp. 607–620. doi: 10.1016/S0140-6736(10)62307-0.

Vishwanath, N. *et al.* (2022) 'Silver as an Antibiotic-Independent Antimicrobial: Review of Current Formulations and Clinical Relevance', *Surgical Infections*, 23(9), pp. 769–780. doi: 10.1089/SUR.2022.229.

Vojtko, Martin *et al.* (2024) 'Distal pancreatectomy', *Bratislava Medical Journal*, 125(4), pp. 239–243. doi: 10.4149/BLL\_2024\_36.

Vrzáčková, N., Ruml, T. and Zelenka, J. (2021) 'molecules Postbiotics, Metabolic Signaling, and Cancer'. doi: 10.3390/molecules26061528.

Wang, D. and Lippard, S. J. (2005) 'Cellular processing of platinum anticancer drugs', *Nature reviews*. *Drug discovery*, 4(4), pp. 307–320. doi: 10.1038/NRD1691.

Wanzlick, H. -W and Schikora, E. (1961) 'Ein nucleophiles Carben', *Chemische Berichte*, 94(9), pp. 2389–2393. doi: 10.1002/CBER.19610940905.

Wei, H. and Guan, J. L. (2012) 'Pro-tumorigenic function of autophagy in mammary oncogenesis', *Autophagy*, 8(1), pp. 129–131. doi: 10.4161/AUTO.8.1.18171,.

Wernyj, R. P. and Morin, P. J. (2004) 'Molecular mechanisms of platinum resistance: still searching for the Achilles' heel', *Drug resistance updates: reviews and commentaries in antimicrobial and anticancer chemotherapy*, 7(4–5), pp. 227–232. doi: 10.1016/J.DRUP.2004.08.002.

Wood, L. D. et al. (2022) 'Pancreatic Cancer: Pathogenesis, Screening, Diagnosis, and Treatment', Gastroenterology, 163(2), pp. 386-402.e1. doi: 10.1053/J.GASTRO.2022.03.056.

World Health Organisation [WHO] (2022) *Central Nervous System Tumours, Brain and Central Nervous Cancer System*. Edited by International Agency for Research on Cancer. Available at: https://www.iarc.who.int/news-events/publication-of-the-who-classification-of-tumours-5th-edition-volume-6-central-nervous-system-tumours/ (Accessed: 13 June 2025).

Wright, B. D. *et al.* (2012) 'Synthesis, characterization, and antimicrobial activity of silver carbene complexes derived from 4,5,6,7-tetrachlorobenzimidazole against antibiotic resistant bacteria', *Dalton transactions (Cambridge, England: 2003)*, 41(21), pp. 6500–6506. doi: 10.1039/C2DT00055E.

Xia, L. *et al.* (2021) 'The cancer metabolic reprogramming and immune response'. doi: 10.1186/s12943-021-01316-8.

Yaromina, A. *et al.* (2009) 'Co-localisation of hypoxia and perfusion markers with parameters of glucose metabolism in human squamous cell carcinoma (hSCC) xenografts', *International journal of radiation biology*, 85(11), pp. 972–980. doi: 10.3109/09553000903232868.

Yeung, C. *et al.* (2019) 'Targeting glycolysis through inhibition of lactate dehydrogenase impairs tumor growth in preclinical models of Ewing sarcoma', *Cancer Research*, 79(19), pp. 5060–5073. doi: 10.1158/0008-5472.CAN-19-0217/653817/AM/TARGETING-GLYCOLYSIS-THROUGH-INHIBITION-OF-LACTATE.

Yin, I. X. *et al.* (2020) 'The Antibacterial Mechanism of Silver Nanoparticles and Its Application in Dentistry', *International Journal of Nanomedicine*, 15, p. 2555. doi: 10.2147/IJN.S246764.

Ying, H. et al. (2012) 'Oncogenic kras maintains pancreatic tumors through regulation of anabolic glucose metabolism', Cell, 149(3), pp. 656–670. doi: 10.1016/j.cell.2012.01.058.

Zhai, X. *et al.* (2013) 'Inhibition of LDH-A by oxamate induces G2/M arrest, apoptosis and increases radiosensitivity in nasopharyngeal carcinoma cells', *Oncology Reports*, 30(6), pp. 2983–2991. doi: 10.3892/OR.2013.2735.

Zhang, L. and Shay, J. W. (2017) 'Multiple Roles of APC and its Therapeutic Implications in Colorectal Cancer', *JNCI Journal of the National Cancer Institute*, 109(8), p. djw332. doi: 10.1093/JNCI/DJW332.

Zhang, X. D., Qin, Z. H. and Wang, J. (2010a) 'The role of p53 in cell metabolism', *Acta Pharmacologica Sinica*, 31(9), pp. 1208–1212. doi: 10.1038/APS.2010.151;KWRD=BIOMEDICINE.

Zhang, X. D., Qin, Z. H. and Wang, J. (2010b) 'The role of p53 in cell metabolism', *Acta Pharmacologica Sinica*, 31(9), pp. 1208–1212. doi: 10.1038/APS.2010.151;KWRD=BIOMEDICINE.

Zhang, Z. et al. (2023) 'KRAS mutation: The booster of pancreatic ductal adenocarcinoma transformation and progression', Frontiers in Cell and Developmental Biology, 11. doi: 10.3389/FCELL.2023.1147676.

## 8.Appendix

**Table A1.1.** The average rate of reaction ( $\Delta A/s$ ) of HCT116 +/+ culture media following treatment with Ag8 over time. Table shows the mean rate of biological triplicate data (n=3) along with the standard error of the replicates. Significance to the control data at each time point was calculated via a single tailed T test to produce a p value which is shown to 2 decimal places. Significance is \*p≤0.05 \*\*p≤0.005. All data is normalised to T0=0

		0	1	2	3	4
Control	Avg	0.00E+00	2.81E-05	3.97E-05	4.96E-05	9.35E-05
	SE	1.74E-06	6.70E-06	7.54E-06	1.06E-05	1.34E-07
	P=	N/A	N/A	N/A	N/A	N/A
10μΜ	Avg	0.00E+00	3.58E-05	4.68E-05	5.94E-05	7.61E-05
	SE	6.15E-06	1.04E-05	1.47E-05	1.72E-05	2.38E-05
	P=	0.09	0.09	0.21	0.14	0.27
50μΜ	Avg	0.00E+00	2.35E-05	3.21E-05	4.19E-05	5.78E-05
	SE	1.31E-06	4.25E-06	6.03E-06	6.26E-06	1.30E-05
	P=	0.17	0.10	0.02	0.11	0.06
100μΜ	Avg	0.00E+00	1.49E-05	1.17E-05	1.36E-05	1.90E-05
	SE	2.81E-06	1.52E-07	9.89E-07	2.89E-07	2.36E-06
	P=	0.10	0.09	0.04	0.04	0.00
250μΜ	Avg	0.00E+00	1.56E-05	1.65E-05	1.83E-05	1.24E-05
	SE	3.67E-06	2.78E-06	6.46E-06	3.70E-06	6.28E-06
	P=	0.12	0.04	0.00	0.02	0.00

**Table A1.2.** The average rate of reaction ( $\Delta A/s$ ) of HCT116 -/- culture media following treatment with Ag8 over time. Table shows the mean rate of biological triplicate data (n=3) along with the standard error of the replicates. Significance to the control data at each time point was calculated via a single tailed T test to produce a p value which is shown to 2 decimal places. Significance is \*p  $\leq$  0.005 \*\*p  $\leq$  0.005. All data is normalised to T0=0

		0	1	2	3	4
Control	Avg	0.00E+00	2.90E-05	3.82E-05	4.38E-05	6.23E-05
	SE	3.63E-07	3.45E-07	2.97E-06	3.43E-06	1.72E-06
	P=	N/A	N/A	N/A	N/A	N/A
10μΜ	Avg	0.00E+00	2.71E-05	3.88E-05	4.52E-05	5.90E-05
	SE	5.85E-07	8.46E-08	1.78E-06	4.50E-06	3.93E-06
	P=	0.04	0.01	0.33	0.17	0.14
50μΜ	Avg	0.00E+00	2.87E-05	3.79E-05	4.74E-05	5.78E-05
	SE	6.72E-06	3.23E-06	3.66E-06	1.39E-05	1.70E-05
	P=	0.18	0.46	0.49	0.43	0.42
100μΜ	Avg	0.00E+00	1.67E-05	2.31E-05	2.46E-05	2.08E-05
	SE	5.92E-06	4.51E-06	2.21E-06	5.00E-06	3.95E-06
	P=	0.16	0.03	0.00	0.00	0.00
250μΜ	Avg	0.00E+00	1.41E-05	1.86E-05	1.34E-05	1.54E-05
	SE	3.30E-06	1.40E-06	1.44E-06	2.35E-06	5.20E-07
	P=	0.19	0.00	0.04	0.04	0.00

**Table A1.3.** The average rate of reaction ( $\Delta A/s$ ) of BxPc-3 culture media following treatment with Ag8 over time. Table shows the mean rate of biological triplicate data (n=3) along with the standard error of the replicates. Significance to the control data at each time point was calculated via a single tailed T test to produce a p value which is shown to 2 decimal places. Significance is \*p  $\leq$  0.05 \*\*p $\leq$ 0.005. All data is normalised to T0=0

		0	1	2	3	4
Control	Avg	0.00E+00	9.53E-06	1.26E-05	1.57E-05	2.00E-05
	SE	1.43E-07	8.34E-07	1.45E-06	2.04E-06	8.39E-07
	P=	N/A	N/A	N/A	N/A	N/A
10μΜ	Avg	0.00E+00	1.01E-05	1.48E-05	2.04E-05	2.39E-05
	SE	1.03E-06	4.82E-07	1.51E-06	4.89E-07	1.28E-06
	P=	0.28	0.36	0.27	0.10	0.10
50μΜ	Avg	0.00E+00	6.70E-06	8.81E-06	1.01E-05	7.78E-06
	SE	3.46E-06	1.50E-06	4.24E-07	9.50E-07	2.19E-06
	P=	0.22	0.03	0.03	0.02	0.01
100μΜ	Avg	0.00E+00	3.95E-06	3.88E-06	4.79E-06	3.59E-06
	SE	3.23E-06	3.30E-06	2.77E-06	3.65E-06	4.21E-06
	P=	0.10	0.08	0.01	0.01	0.02
250μΜ	Avg	0.00E+00	4.70E-06	8.48E-06	3.73E-06	5.84E-06
	SE	8.22E-07	1.93E-06	2.77E-07	3.11E-06	1.73E-06
	P=	0.02	0.02	0.07	0.00	0.00

**Table A1.4.** The average rate of reaction ( $\Delta A/s$ ) of PSN-1 culture media following treatment with Ag8 over time. Table shows the mean rate of biological triplicate data (n=3) along with the standard error of the replicates. Significance to the control data at each time point was calculated via a single tailed T test to produce a p value which is shown to 2 decimal places. Significance is \*p  $\leq$  0.005 \*\*p  $\leq$  0.005. All data is normalised to T0=0

		0	1	2	3	4
Control	Avg	0.00E+00	1.36E-05	2.54E-05	3.42E-05	4.16E-05
	SE	1.52E-06	1.10E-06	1.14E-06	1.82E-06	1.54E-06
	P=	N/A	N/A	N/A	N/A	N/A
10μΜ	Avg	0.00E+00	1.68E-05	2.50E-05	3.32E-05	3.98E-05
	SE	2.00E-06	2.09E-06	4.51E-06	2.39E-06	2.91E-06
	P=	0.01	0.04	0.48	0.42	0.16
50μΜ	Avg	0.00E+00	1.94E-05	2.70E-05	2.61E-05	2.28E-05
	SE	3.07E-06	1.29E-06	2.52E-06	9.86E-07	4.48E-06
	P=	0.08	0.11	0.00	0.00	0.01
100μΜ	Avg	0.00E+00	6.54E-06	1.00E-05	3.89E-06	4.05E-06
	SE	3.76E-06	1.56E-06	2.27E-06	3.96E-06	4.21E-06
	P=	0.08	0.06	0.00	0.00	0.01
250μΜ	Avg	0.00E+00	9.26E-06	7.75E-06	9.90E-06	7.04E-06
	SE	1.88E-06	5.83E-06	9.78E-06	9.28E-06	6.99E-06
	P=	0.07	0.17	0.45	0.27	0.04

**Table A2.1.** The average rate of reaction ( $\Delta A/s$ ) of HCT116 +/+ culture media following treatment with HA197 over time. Table shows the mean rate of biological triplicate data (n=3) along with the standard error of the replicates. Significance to the control data at each time point was calculated via a single tailed T test to produce a p value which is shown to 2 decimal places. Significance is \*p≤0.05 \*\*p≤0.005. All data is normalised to T0=0

		0	1	2	3	4
Control	Avg	0.00E+00	2.81E-05	3.97E-05	4.96E-05	9.35E-05
	SE	1.74E-06	6.70E-06	7.54E-06	1.06E-05	1.34E-07
	P=	N/A	N/A	N/A	N/A	N/A
10μΜ	Avg	0.00E+00	2.84E-05	4.11E-05	5.14E-05	6.99E-05
	SE	3.15E-06	4.12E-06	5.26E-06	4.42E-06	1.02E-05
	P=	0.06	0.45	0.30	0.40	0.39
50μΜ	Avg	0.00E+00	2.59E-05	4.37E-05	4.76E-05	7.46E-05
	SE	3.51E-06	3.57E-06	8.73E-06	4.03E-06	1.39E-05
	P=	0.06	0.28	0.23	0.39	0.16
100μΜ	Avg	0.00E+00	2.41E-05	4.00E-05	5.26E-05	5.98E-05
	SE	3.51E-06	5.11E-06	1.03E-05	1.22E-05	1.22E-05
	P=	0.04	0.06	0.11	0.10	0.06
250μΜ	Avg	0.00E+00	1.72E-05	2.41E-05	3.02E-05	3.54E-05
	SE	4.40E-06	1.44E-06	5.66E-06	8.05E-06	1.31E-05
	P=	0.15	0.09	0.13	0.01	0.02

**Table A2.2.** The average rate of reaction ( $\Delta A/s$ ) of HCT116 -/- culture media following treatment with HA197 over time. Table shows the mean rate of biological triplicate data (n=3) along with the standard error of the replicates. Significance to the control data at each time point was calculated via a single tailed T test to produce a p value which is shown to 2 decimal places. Significance is \*p≤0.05 \*\*p≤0.005. All data is normalised to T0=0

		0	1	2	3	4
Control	Avg	0.00E+00	2.90E-05	3.82E-05	4.38E-05	6.23E-05
	SE	3.63E-07	3.45E-07	2.97E-06	3.43E-06	1.72E-06
	P=	N/A	N/A	N/A	N/A	N/A
10μΜ	Avg	0.00E+00	3.18E-05	4.26E-05	5.70E-05	7.09E-05
	SE	2.06E-06	2.13E-06	3.80E-07	5.09E-07	2.14E-06
	P=	0.39	0.19	0.16	0.04	0.08
50μΜ	Avg	0.00E+00	2.92E-05	4.37E-05	4.89E-05	6.96E-05
	SE	6.03E-06	3.02E-07	4.02E-06	5.38E-06	5.37E-06
	P=	0.20	0.39	0.02	0.06	0.09
100μΜ	Avg	0.00E+00	2.39E-05	3.48E-05	4.81E-05	5.71E-05
	SE	3.02E-06	1.20E-06	5.91E-06	1.20E-05	1.43E-05
	P=	0.03	0.01	0.19	0.33	0.36
250μΜ	Avg	0.00E+00	1.40E-05	2.36E-05	2.43E-05	2.54E-05
	SE	7.06E-06	4.61E-06	4.22E-06	4.31E-06	2.55E-06
	P=	0.18	0.04	0.00	0.00	0.00

**Table A2.3.** The average rate of reaction ( $\Delta A/s$ ) of BxPc-3 culture media following treatment with HA197 over time. Table shows the mean rate of biological triplicate data (n=3) along with the standard error of the replicates. Significance to the control data at each time point was calculated via a single tailed T test to produce a p value which is shown to 2 decimal places. Significance is \*p≤0.05 \*\*p≤0.005. All data is normalised to T0=0

		0	1	2	3	4
Control	Avg	0.00E+00	9.53E-06	1.26E-05	1.57E-05	2.00E-05
	SE	1.43E-07	8.34E-07	1.45E-06	2.04E-06	8.39E-07
	P=	N/A	N/A	N/A	N/A	N/A
10μΜ	Avg	0.00E+00	8.78E-06	1.12E-05	1.63E-05	2.07E-05
	SE	6.93E-06	8.42E-07	1.76E-06	2.62E-06	1.92E-06
	P=	0.10	0.00	0.02	0.20	0.29
50μΜ	Avg	0.00E+00	7.69E-06	1.55E-05	1.39E-05	1.73E-05
	SE	1.19E-07	8.15E-07	2.35E-06	1.87E-06	2.68E-06
	P=	0.00	0.00	0.04	0.00	0.14
100μΜ	Avg	0.00E+00	5.89E-06	1.43E-05	1.27E-05	1.15E-05
	SE	2.68E-07	1.20E-06	4.73E-06	2.76E-06	4.27E-06
	P=	0.00	0.00	0.33	0.03	0.07
250μΜ	Avg	0.00E+00	4.67E-07	8.27E-06	7.88E-06	6.49E-06
	SE	5.46E-06	2.05E-06	2.12E-06	7.25E-07	1.56E-06
	P=	0.25	0.01	0.01	0.01	0.00

**Table A2.4.** The average rate of reaction ( $\Delta A/s$ ) of PSN-1 culture media following treatment with HA197 over time. Table shows the mean rate of biological triplicate data (n=3) along with the standard error of the replicates. Significance to the control data at each time point was calculated via a single tailed T test to produce a p value which is shown to 2 decimal places. Significance is \*p≤0.05 \*\*p≤0.005. All data is normalised to T0=0

		0	1	2	3	4
Control	Avg	0.00E+00	1.36E-05	2.54E-05	3.42E-05	4.16E-05
	SE					
	P=	N/A	N/A	N/A	N/A	N/A
10μΜ	Avg	0.00E+00	1.68E-05	2.88E-05	4.30E-05	5.40E-05
	SE					
	P=					
50μΜ	Avg	0.00E+00	1.35E-05	1.93E-05	2.91E-05	3.29E-05
	SE					
	P=					
100μΜ	Avg	0.00E+00	9.50E-06	1.53E-05	1.72E-05	2.06E-05
	SE					
	P=					
250μΜ	Avg	0.00E+00	2.64E-06	1.30E-05	1.10E-05	7.78E-06
	SE					
	P=					

**Table A3.1.** The average rate of reaction ( $\Delta A/s$ ) of HCT116 +/+ culture media following treatment with HA266 over time. Table shows the mean rate of biological triplicate data (n=3) along with the standard error of the replicates. Significance to the control data at each time point was calculated via a single tailed T test to produce a p value which is shown to 2 decimal places. Significance is \*p≤0.05 \*\*p≤0.005. All data is normalised to T0=0

		0	1	2	3	4
Control	Avg	0.00E+00	2.81E-05	3.97E-05	4.96E-05	9.35E-05
	SE	1.74E-06	6.70E-06	7.54E-06	1.06E-05	1.34E-07
	P=	N/A	N/A	N/A	N/A	N/A
10μΜ	Avg	0.00E+00	2.44E-05	3.69E-05	3.74E-05	4.53E-05
	SE	2.60E-06	4.69E-06	9.06E-06	8.25E-06	1.20E-05
	P=	0.01	0.11	0.10	0.02	0.03
50μΜ	Avg	0.00E+00	1.84E-05	2.63E-05	2.81E-05	3.80E-05
	SE	4.18E-06	4.56E-06	7.23E-06	6.40E-06	1.45E-05
	P=	0.19	0.02	0.00	0.02	0.03
100μΜ	Avg	0.00E+00	4.85E-06	1.94E-05	2.23E-05	2.79E-05
	SE	2.74E-06	4.32E-06	3.15E-06	4.81E-06	8.61E-06
	P=	0.10	0.08	0.02	0.02	0.01
250μΜ	Avg	0.00E+00	1.22E-05	1.74E-05	1.55E-05	1.42E-05
	SE	4.72E-06	3.87E-06	7.46E-06	6.58E-06	5.78E-06
	P=	0.10	0.02	0.00	0.01	0.00

**Table A3.2.** The average rate of reaction ( $\Delta A/s$ ) of HCT116 -/- culture media following treatment with HA266 over time. Table shows the mean rate of biological triplicate data (n=3) along with the standard error of the replicates. Significance to the control data at each time point was calculated via a single tailed T test to produce a p value which is shown to 2 decimal places. Significance is \*p≤0.05 \*\*p≤0.005. All data is normalised to T0=0

		0	1	2	3	4
Control	Avg	0.00E+00	2.90E-05	3.82E-05	4.38E-05	6.23E-05
	SE	3.63E-07	3.45E-07	2.97E-06	3.43E-06	1.72E-06
	P=	N/A	N/A	N/A	N/A	N/A
10μΜ	Avg	0.00E+00	2.77E-05	3.69E-05	4.12E-05	4.96E-05
	SE	2.93E-06	3.45E-07	2.07E-06	4.93E-06	6.72E-06
	P=	0.33	0.00	0.14	0.11	0.06
50μΜ	Avg	0.00E+00	1.87E-05	2.13E-05	2.50E-05	2.54E-05
	SE	6.83E-06	1.19E-06	3.07E-07	2.56E-06	1.81E-06
	P=	0.17	0.01	0.02	0.00	0.00
100μΜ	Avg	0.00E+00	1.48E-05	7.66E-06	1.39E-05	1.08E-05
	SE	4.75E-06	1.21E-06	5.87E-06	4.93E-06	6.32E-06
	P=	0.06	0.00	0.00	0.00	0.00
250μΜ	Avg	0.00E+00	4.01E-06	6.87E-06	2.01E-06	4.68E-06
	SE	5.03E-06	3.81E-06	4.73E-07	1.79E-06	2.33E-06
	P=	0.07	0.01	0.00	0.00	0.00

**Table A3.3.** The average rate of reaction ( $\Delta A/s$ ) of BxPc-3 culture media following treatment with HA266 over time. Table shows the mean rate of biological triplicate data (n=3) along with the standard error of the replicates. Significance to the control data at each time point was calculated via a single tailed T test to produce a p value which is shown to 2 decimal places. Significance is \*p  $\leq$  0.05 \*\*p $\leq$ 0.005. All data is normalised to T0=0

		0	1	2	3	4
Control	Avg	0.00E+00	9.53E-06	1.26E-05	1.57E-05	2.00E-05
	SE	1.43E-07	8.34E-07	1.45E-06	2.04E-06	8.39E-07
	P=	N/A	N/A	N/A	N/A	N/A
10μΜ	Avg	0.00E+00	5.51E-06	9.40E-06	1.41E-05	1.44E-05
	SE	1.98E-06	7.93E-07	2.34E-06	4.55E-06	6.77E-06
	P=	0.08	0.00	0.03	0.30	0.22
50μΜ	Avg	0.00E+00	5.94E-06	6.19E-06	7.60E-06	6.40E-06
	SE	1.77E-06	8.23E-07	8.23E-07	2.12E-06	2.62E-06
	P=	0.01	0.00	0.00	0.00	0.01
100μΜ	Avg	0.00E+00	1.10E-06	1.70E-06	6.16E-06	4.38E-06
	SE	1.99E-06	3.32E-06	3.47E-06	1.72E-06	2.83E-06
	P=	0.01	0.04	0.02	0.00	0.01
250μΜ	Avg	0.00E+00	0.00E+00	2.26E-06	3.68E-06	2.09E-06
	SE	2.38E-06	4.24E-08	8.57E-07	3.49E-07	7.36E-07
	P=	0.02	0.00	0.00	0.01	0.00

**Table A3.4.** The average rate of reaction ( $\Delta A/s$ ) of PSN-1 culture media following treatment with HA266 over time. Table shows the mean rate of biological triplicate data (n=3) along with the standard error of the replicates. Significance to the control data at each time point was calculated via a single tailed T test to produce a p value which is shown to 2 decimal places. Significance is \*p≤0.05 \*\*p≤0.005. All data is normalised to T0=0

		0	1	2	3	4
Control	Avg	0.00E+00	1.36E-05	2.54E-05	3.42E-05	4.16E-05
	SE	1.52E-06	1.10E-06	1.14E-06	1.82E-06	1.54E-06
	P=	N/A	N/A	N/A	N/A	N/A
10μΜ	Avg	0.00E+00	1.61E-05	2.41E-05	3.30E-05	3.49E-05
	SE	1.08E-06	9.93E-07	1.13E-06	2.04E-06	5.57E-07
	P=	0.01	0.00	0.00	0.02	0.04
50μΜ	Avg	0.00E+00	1.26E-05	1.40E-05	1.82E-05	1.60E-05
	SE	1.92E-06	2.34E-06	2.18E-06	3.48E-06	2.36E-06
	P=	0.09	0.25	0.04	0.05	0.00
100μΜ	Avg	0.00E+00	8.25E-06	1.05E-05	1.07E-05	1.08E-05
	SE	7.41E-06	1.30E-06	1.48E-06	4.47E-07	1.10E-06
	P=	0.07	0.08	0.01	0.00	0.00
250μΜ	Avg	0.00E+00	1.93E-06	8.35E-06	7.01E-06	3.02E-06
	SE	3.66E-06	2.13E-06	2.06E-06	2.61E-06	5.88E-07
	P=	0.12	0.00	0.02	0.01	0.00

**Table A4.1.** The average rate of reaction ( $\Delta A/s$ ) of HCT116 +/+ culture media following treatment with silibinin over time. Table shows the mean rate of biological triplicate data (n=3) along with the standard error of the replicates. Significance to the control data at each time point was calculated via a single tailed T test to produce a p value which is shown to 2 decimal places. Significance is \*p≤0.05 \*\*p≤0.005. All data is normalised to T0=0

		0	1	2	3	4
Control	Avg	0.00E+00	2.81E-05	3.97E-05	4.96E-05	9.35E-05
	SE	1.74E-06	6.70E-06	7.54E-06	1.06E-05	1.34E-07
	P=	N/A	N/A	N/A	N/A	N/A
10μΜ	Avg	0.00E+00	2.69E-05	3.63E-05	4.19E-05	5.62E-05
	SE	1.60E-06	5.76E-06	7.60E-06	5.53E-06	1.12E-05
	P=	0.39	0.17	0.00	0.14	0.04
50μΜ	Avg	0.00E+00	2.55E-05	3.28E-05	4.29E-05	5.72E-05
	SE	1.93E-06	4.25E-06	6.21E-06	6.33E-06	9.87E-06
	P=	0.00	0.20	#DIV/0!	0.13	0.03
100μΜ	Avg	0.00E+00	2.60E-05	3.69E-05	3.96E-05	5.30E-05
	SE	1.48E-06	5.25E-06	6.83E-06	6.15E-06	9.82E-06
	P=	0.01	0.14	0.11	0.08	0.03
250μΜ	Avg	0.00E+00	2.07E-05	3.18E-05	3.47E-05	4.33E-05
	SE	3.02E-06	4.08E-06	7.46E-06	7.50E-06	9.91E-06
	P=	0.24	0.05	0.05	0.02	0.02

**Table A4.2.** The average rate of reaction ( $\Delta A/s$ ) of HCT116 -/- culture media following treatment with silibinin over time. Table shows the mean rate of biological triplicate data (n=3) along with the standard error of the replicates. Significance to the control data at each time point was calculated via a single tailed T test to produce a p value which is shown to 2 decimal places. Significance is \*p≤0.05 \*\*p≤0.005. All data is normalised to T0=0

		0	1	2	3	4
Control	Avg	0.00E+00	2.90E-05	3.82E-05	4.38E-05	6.23E-05
	SE	3.63E-07	3.45E-07	2.97E-06	3.43E-06	1.72E-06
	P=	N/A	N/A	N/A	N/A	N/A
10μΜ	Avg	0.00E+00	2.39E-05	3.39E-05	4.36E-05	5.33E-05
	SE	2.22E-07	4.39E-07	9.90E-07	5.43E-06	2.04E-06
	P=	0.09	0.00	0.08	0.46	0.00
50μΜ	Avg	0.00E+00	2.45E-05	3.57E-05	4.67E-05	5.71E-05
	SE	1.55E-07	9.99E-07	5.79E-09	5.44E-06	3.19E-06
	P=	0.06	0.01	0.25	0.14	0.04
100μΜ	Avg	0.00E+00	2.71E-05	3.81E-05	4.95E-05	6.28E-05
	SE	1.93E-07	9.81E-07	1.13E-06	6.33E-06	4.78E-06
	P=	0.21	0.05	0.49	0.09	0.45
250μΜ	Avg	0.00E+00	2.82E-05	3.68E-05	4.24E-05	5.38E-05
	SE	2.08E-06	5.13E-07	4.53E-07	1.56E-06	3.58E-07
	P=	0.37	0.22	0.36	0.26	0.01

**Table A4.3.** The average rate of reaction ( $\Delta A/s$ ) of BxPc-3 culture media following treatment with silibinin over time. Table shows the mean rate of biological triplicate data (n=3) along with the standard error of the replicates. Significance to the control data at each time point was calculated via a single tailed T test to produce a p value which is shown to 2 decimal places. Significance is \*p≤0.05 \*\*p≤0.005. All data is normalised to T0=0

		0	1	2	3	4
Control	Avg	0.00E+00	9.53E-06	1.26E-05	1.57E-05	2.00E-05
	SE	1.43E-07	8.34E-07	1.45E-06	2.04E-06	8.39E-07
	P=	N/A	N/A	N/A	N/A	N/A
10μΜ	Avg	0.00E+00	7.61E-06	1.06E-05	1.42E-05	1.70E-05
	SE	4.89E-07	1.20E-06	2.47E-07	1.45E-06	1.93E-06
	P=	0.00	0.02	0.11	0.06	0.05
50μΜ	Avg	0.00E+00	3.92E-06	1.12E-05	1.36E-05	1.80E-05
	SE	1.90E-07	2.82E-06	1.79E-07	1.31E-06	2.13E-06
	P=	0.00	0.05	0.18	0.05	0.13
100μΜ	Avg	0.00E+00	4.95E-06	1.14E-05	1.26E-05	1.40E-05
	SE	1.41E-06	1.43E-06	5.40E-07	1.28E-06	9.84E-07
	P=	0.01	0.01	0.15	0.03	0.00
250μΜ	Avg	0.00E+00	5.58E-06	1.00E-05	1.30E-05	1.35E-05
	SE	9.72E-07	6.62E-08	1.97E-08	1.48E-07	3.40E-08
	P=	0.00	0.02	0.11	0.17	0.01

**Table A4.4.** The average rate of reaction ( $\Delta A/s$ ) of PSN-1 culture media following treatment with silibinin over time. Table shows the mean rate of biological triplicate data (n=3) along with the standard error of the replicates. Significance to the control data at each time point was calculated via a single tailed T test to produce a p value which is shown to 2 decimal places. Significance is \*p $\leq$ 0.05 \*\*p $\leq$ 0.005. All data is normalised to T0=0

		0	1	2	3	4
Control	Avg	0.00E+00	1.36E-05	2.54E-05	3.42E-05	4.16E-05
	SE	1.52E-06	1.10E-06	1.14E-06	1.82E-06	1.54E-06
	P=	N/A	N/A	N/A	N/A	N/A
10μΜ	Avg	0.00E+00	1.55E-05	2.38E-05	3.16E-05	3.66E-05
	SE	1.08E-06	9.99E-07	2.37E-06	1.44E-06	2.32E-06
	P=	0.06	0.00	0.35	0.25	0.01
50μM	Avg	0.00E+00	1.38E-05	2.36E-05	3.39E-05	3.89E-05
	SE	7.83E-07	6.88E-07	3.49E-06	4.02E-07	1.22E-07
	P=	0.09	0.34	0.37	0.43	0.12
100μΜ	Avg	0.00E+00	1.68E-05	3.03E-05	3.44E-05	4.49E-05
	SE	1.55E-06	1.93E-06	4.45E-07	1.11E-06	6.80E-07
	P=	0.00	0.03	0.01	0.38	0.03
250μΜ	Avg	0.00E+00	1.62E-05	2.17E-05	2.85E-05	3.49E-05
	SE	5.05E-07	1.72E-06	5.61E-07	4.34E-07	2.04E-06
	P=	0.11	0.03	0.08	0.06	0.00

**Table A5.1.** The average rate of reaction ( $\Delta A/s$ ) of HCT116 +/+ culture media following treatment with sodium oxamate over time. Table shows the mean rate of biological triplicate data (n=3) along with the standard error of the replicates. Significance to the control data at each time point was calculated via a single tailed T test to produce a p value which is shown to 2 decimal places. Significance is \*p $\leq$ 0.005 \*\*p $\leq$ 0.005. All data is normalised to T0=0

		0	1	2	3	4
Control	Avg	0.00E+00	2.81E-05	3.97E-05	4.96E-05	9.35E-05
	SE	1.74E-06	6.70E-06	7.54E-06	1.06E-05	1.34E-07
	P=	N/A	N/A	N/A	N/A	N/A
10μΜ	Avg	0.00E+00	2.20E-05	3.92E-05	4.57E-05	6.33E-05
	SE	2.17E-06	1.77E-06	5.10E-06	1.55E-06	1.02E-05
	P=	0.00	0.17	0.42	0.35	0.05
50μΜ	Avg	0.00E+00	2.62E-05	4.33E-05	4.89E-05	6.70E-05
	SE	7.44E-07	4.25E-06	9.90E-06	7.07E-06	1.20E-05
	P=	0.22	0.27	0.31	0.43	0.08
100μΜ	Avg	0.00E+00	2.64E-05	4.26E-05	4.81E-05	6.76E-05
	SE	2.97E-06	4.84E-06	1.08E-05	6.37E-06	1.51E-05
	P=	0.04	0.24	0.11	0.38	0.12
250μΜ	Avg	0.00E+00	2.39E-05	3.80E-05	4.96E-05	6.42E-05
	SE	4.18E-06	3.80E-06	1.01E-05	9.59E-06	1.67E-05
	P=	0.18	0.14	0.18	0.48	0.11

**Table A5.2.** The average rate of reaction ( $\Delta A/s$ ) of HCT116 -/- culture media following treatment with sodium oxamate over time. Table shows the mean rate of biological triplicate data (n=3) along with the standard error of the replicates. Significance to the control data at each time point was calculated via a single tailed T test to produce a p value which is shown to 2 decimal places. Significance is \*p $\leq$ 0.005 \*\*p $\leq$ 0.005. All data is normalised to T0=0

		0	1	2	3	4
Control	Avg	0.00E+00	2.90E-05	3.82E-05	4.38E-05	6.23E-05
	SE	3.63E-07	3.45E-07	2.97E-06	3.43E-06	1.72E-06
	P=	N/A	N/A	N/A	N/A	N/A
10μΜ	Avg	0.00E+00	2.36E-05	4.02E-05	4.48E-05	6.04E-05
	SE	2.90E-06	1.41E-06	5.12E-06	8.06E-06	2.79E-06
	P=	0.48	0.05	0.22	0.42	0.11
50μΜ	Avg	0.00E+00	2.60E-05	3.31E-05	4.12E-05	5.93E-05
	SE	3.12E-07	1.34E-06	2.77E-06	5.33E-06	3.46E-06
	P=	0.00	0.05	0.00	0.15	0.11
100μΜ	Avg	0.00E+00	2.52E-05	3.79E-05	4.55E-05	5.95E-05
	SE	4.02E-06	1.25E-06	1.78E-06	1.65E-06	2.01E-06
	P=	0.39	0.03	0.48	0.23	0.01
250μΜ	Avg	0.00E+00	2.69E-05	3.84E-05	4.80E-05	5.48E-05
	SE	3.40E-06	2.10E-06	2.70E-06	2.57E-06	3.03E-06
	P=	0.44	0.24	0.49	0.02	0.01

**Table A5.3.** The average rate of reaction ( $\Delta A/s$ ) of BxPc-3 culture media following treatment with sodium oxamate over time. Table shows the mean rate of biological triplicate data (n=3) along with the standard error of the replicates. Significance to the control data at each time point was calculated via a single tailed T test to produce a p value which is shown to 2 decimal places. Significance is \*p $\leq$ 0.005 \*\*p $\leq$ 0.005. All data is normalised to T0=0

		0	1	2	3	4
Control	Avg	0.00E+00	9.53E-06	1.26E-05	1.57E-05	2.00E-05
	SE	1.43E-07	8.34E-07	1.45E-06	2.04E-06	8.39E-07
	P=	N/A	N/A	N/A	N/A	N/A
10μΜ	Avg	0.00E+00	6.00E-06	1.05E-05	1.51E-05	1.90E-05
	SE	7.38E-06	9.71E-07	2.12E-06	3.21E-06	3.19E-06
	P=	0.03	0.00	0.04	0.34	0.35
50μΜ	Avg	0.00E+00	6.92E-06	9.27E-06	1.46E-05	1.88E-05
	SE	1.48E-08	1.27E-06	8.39E-07	2.86E-06	1.20E-06
	P=	0.00	0.01	0.02	0.16	0.04
100μΜ	Avg	0.00E+00	5.98E-06	1.18E-05	1.38E-05	1.77E-05
	SE	1.76E-06	4.29E-07	4.03E-08	1.00E-06	2.25E-06
	P=	0.01	0.01	0.31	0.11	0.12
250μΜ	Avg	0.00E+00	7.15E-06	1.29E-05	1.39E-05	1.68E-05
	SE	8.18E-06	2.49E-07	7.65E-07	1.61E-06	8.67E-07
	P=	0.11	0.03	0.37	0.03	0.00

**Table A5.4.** The average rate of reaction ( $\Delta A/s$ ) of PSN-1 culture media following treatment with sodium oxamate over time. Table shows the mean rate of biological triplicate data (n=3) along with the standard error of the replicates. Significance to the control data at each time point was calculated via a single tailed T test to produce a p value which is shown to 2 decimal places. Significance is \*p $\leq$ 0.005 \*\*p $\leq$ 0.005. All data is normalised to T0=0

		0	1	2	3	4
Control	Avg	0.00E+00	1.36E-05	2.54E-05	3.42E-05	4.16E-05
	SE	1.52E-06	1.10E-06	1.14E-06	1.82E-06	1.54E-06
	P=	N/A	N/A	N/A	N/A	N/A
10μΜ	Avg	0.00E+00	1.34E-05	2.43E-05	2.93E-05	3.83E-05
	SE	3.68E-07	7.56E-07	2.11E-06	2.68E-06	4.48E-07
	P=	0.17	0.29	0.20	0.01	0.05
50μΜ	Avg	0.00E+00	1.70E-05	2.37E-05	3.81E-05	4.90E-05
	SE	6.68E-07	1.26E-06	1.37E-06	2.46E-06	6.18E-06
	P=	0.11	0.00	0.29	0.23	0.13
100μΜ	Avg	0.00E+00	1.55E-05	2.65E-05	3.02E-05	3.94E-05
	SE	1.09E-06	1.04E-06	9.48E-07	3.25E-06	9.45E-07
	P=	0.02	0.00	0.01	0.05	0.24
250μΜ	Avg	0.00E+00	1.53E-05	2.22E-05	3.26E-05	3.99E-05
	SE	1.74E-06	8.08E-07	9.58E-07	1.25E-06	1.09E-06
	P=	0.05	0.01	0.13	0.05	0.30